PNNL-23620

Pacific Northwest
NATIONAL LABORATORY
Proudly Operated by Battelle Since 1965

LEU-Mo Fuel Out-of-Pile Characterization for TUM: Final Report

PNNL Project Number 65897

September 2014

DE Burkes
AJ Casella
EC Buck
AM Casella
MK Edwards
PJ MacFarlan
KN Pool
FN Smith
FH Steen

U.S. DEPARTMENT OF ENERGY

Prepared for the U.S. Department of Energy
under Contract DE-AC05-76RL01830

PACIFIC NORTHWEST NATIONAL LABORATORY
operated by
BATTELLE
for the
UNITED STATES DEPARTMENT OF ENERGY
under Contract DE-AC05-76RL01830

Printed in the United States of America

Available to DOE and DOE contractors from the
Office of Scientific and Technical Information,
P.O. Box 62, Oak Ridge, TN 37831-0062;
ph: (865) 576-8401
fax: (865) 576-5728
email: reports@adonis.osti.gov

Available to the public from the National Technical Information Service
5301 Shawnee Rd., Alexandria, VA 22312
ph: (800) 553-NTIS (6847)
email: orders@ntis.gov <http://www.ntis.gov/about/form.aspx>
Online ordering: http://www.ntis.gov

This document was printed on recycled paper.

(8/2010)

PNNL-23620

LEU-Mo Fuel Out-of-Pile Characterization for TUM: Final Report

PNNL Project Number 65897

DE Burkes
AJ Casella
EC Buck
AM Casella
MK Edwards
PJ MacFarlan
KN Pool
FN Smith
FH Steen

September 2014

Prepared for
the Technische Universität München
under Agreement No. 65897

Pacific Northwest National Laboratory
Richland, Washington 99352

Summary

The Technische Universität München (TUM) located in Germany requested that Pacific Northwest National Laboratory (PNNL) perform thermal-physical property measurement services for determining the thermal conductivities of irradiated U-Mo dispersion fuel samples. Two dispersion fuel segments containing U-7Mo dispersion fuel in an Al-2wt% Si matrix harvested from the AFIP-1 irradiation experiment were provided to PNNL for this effort. The segments were sectioned into samples for pycnometry (density) and laser flash analysis (thermal diffusivity), differential scanning calorimetry (specific heat capacity), and optical metallography (thickness, image analysis). This report summarizes the findings of the analysis performed at TUM's request.

Acknowledgments

The authors wish to acknowledge Mr. Jason Schulthess, Mr. Adam Robinson, Dr. Dan Wachs, and Mrs. Susan Case from Idaho National Laboratory for the delivery of the fuel segments to PNNL. Operations conducted in hot cells comprise a large undertaking and the authors wish to acknowledge those at Pacific Northwest National Laboratory who were involved in the preparation of samples and performance of measurements, specifically Ms. Nicole Green, Mr. Jake Bohlke, Mr. Jamin Trevino, Mr. Eric Hanson, and Mr. Robert Orton. The authors wish to acknowledge Meghan Chalk and Sharon Eaton for their assistance with formatting and copyediting of this report. The authors wish to acknowledge the support of the Global Threat Reduction Initiative (NA-21) for the opportunity to use samples obtained from the AFIP-1 experiment for this work and also for providing support to dispose of waste generated as a result of this work. Finally, the authors are grateful to the Technische Universität München, specifcally Ms. Tanja Huber, Dr. Harald Breitkreutz, and Prof. Dr. Winfried Petry, for the opportunity to conduct this work under Agreement No. 65897.

Acronyms and Abbreviations

AFIP	Advanced Test Reactor Full-size Plate In Center Flux Trap Position
DSC	differential scanning calorimeter / calorimetry
EDF	extended depth-of-focus
LEU	low-enriched uranium
LEU-Mo	low-enriched uranium-molybdenum
LFA	laser flash apparatus / analysis
NIST	National Institute of Standards and Technology
OM	optical microscopy
PNNL	Pacific Northwest National Laboratory
STDM	scanning thermal diffusivity microscope
TUM	Technische Universität München
U-Mo	uranium-molybdenum alloy

Contents

Figures

Tables

1.0 Introduction

The evolution of the thermal conductivity during irradiation of research-reactor fuel plays a significant role in fuel element performance. It is crucial to investigate the change in thermal conductivity as a function of fission density / ^{235}U burnup, as well as temperature, in order to correctly simulate the heat fluxes and temperatures in the fuel meat[1] during both normal reactor operation and potential accident scenarios. Accordingly, such data is needed during the qualification process of a new fuel type. In addition, the thermal conductivity of the spent fuel might include information needed to identify and assess the mechanisms that lead to the accelerated swelling of uranium-molybdenum (U-Mo) dispersion fuel designs beyond fission densities of 4.5×10^{21} fissions•cm^{-3}. Consequently, these measurements are included in the comprehension phase of the current HERACLES roadmap.

Thermal conductivity cannot be accessed directly; rather it is a composition of the material's density, thermal diffusivity, and specific heat. Each of these parameters can be measured separately. It is known that the density of the dispersion fuel plate decreases with burnup from immersion density measurements (Robinson *et al.* 2012). Mainly, the gaseous fission products that agglomerate in the fuel meat during irradiation cause the decrease in density.

Recently, the Idaho National Laboratory developed a Scanning Thermal Diffusivity Microscope (STDM) (Huber *et al.* 2012) to measure the thermal diffusivity on a micrometer scale of irradiated reactor fuel at room temperature. Initial measurements showed that the thermal diffusivity of irradiated monolithic U-10Mo (nominal wt%) fuel with 20 nominal wt% ^{235}U burnup is about 30% lower than the thermal diffusivity of fresh U-10Mo fuel. One irradiated U-7Mo dispersion fuel sample has also been investigated with this method, but due to the complex structure of the fuel meat, it was not possible to assign a definite thermal conductivity on either the single fuel components or the entire composite. To obtain more precise information on the thermal diffusivity of the composite, another technique—namely laser flash analysis (LFA)—is more appropriate. With this technique, a larger surface area of about 100 mm^2 can be covered, compared to the STDM with roughly 0.2 mm^2 of surface area, which is about the surface area of a single fuel particle. This way, information of the entire dispersion fuel composite can be obtained. Another important issue, especially regarding temperature excursions in the fuel during reactor operation, is the temperature dependence, which can be examined with the LFA but not with the STDM in its current configuration.

The third fundamental parameter of the thermal conductivity is the specific heat capacity. The specific heat capacity can be obtained with a Differential Scanning Calorimeter (DSC), which is sensitive to changes in the material composition that occur during irradiation of dispersion fuel.

The Pacific Northwest National Laboratory (PNNL) has installed a suite of thermal analysis instruments in hot cells for the examination of irradiated reactor fuel. This set-up provides a unique environment to investigate all three parameters (density, thermal diffusivity, and specific heat capacity) that are mandatory for the calculation of the thermal conductivity of irradiated U-Mo dispersion fuel. Additionally, an optical microscope has been installed in a hot cell to quantify the structural changes in the fuel, which lead to a change in the thermal properties. This capability was initially established in support of the Global Threat Reduction Initiative's Domestic Research Reactor Conversion efforts. As a

[1] "Fuel meat" is a combination of fuel materials with a nonfissionable, heat-conducting (matrix) material, confined inside a fuel plate.

result of this capability, the Technische Universität München (TUM) located in Germany has requested that PNNL perform thermal-physical property measurement services for determining thermal conductivity of irradiated U-Mo dispersion fuel samples (Petry 2013). This effort will, in turn, support global research reactor conversion efforts in collaboration with the Global Threat Reduction Initiative.

2.0 Experimental Processes, Methods, and Materials

2.1 Fuel System Description

The Advanced Test Reactor Full-size Plate In Center Flux Trap Position (AFIP)-1 experiment was designed to demonstrate the performance of second-generation U-Mo dispersion fuel at a scale prototypic of research reactor fuel plates. The experiment was fabricated using commercially standard practices at Babcock & Wilcox Nuclear Operations Group in Lynchburg, VA. The U-7wt% Mo (nominal composition) fuel particles were supplied by the Korean Atomic Energy Research Institute using equipment intended for commercial supply. Two fuel plates were irradiated as part of the experiment that incorporated two different matrix compositions: Al-2wt% Si and Al-4043 (~5wt% Si). The resultant fuel plates were nominally 57.2 cm long × 5.60 cm wide × 0.127 cm thick. The nominal fuel meat zone was 52.4 cm long × 3.68 cm wide. The fuel meat was clad in aluminum alloy 6061 (AA6061) and contained typical Mg and Si impurities. The fuel plate was irradiated in the Advanced Test Reactor for 158.2 effective full-power days. Additional details on the AFIP-1 experiment can be found in Perez et al. (2011).

2.2 Fuel Segment Preparation

Two square segments were prepared from the AFIP-1 fuel plate at Idaho National Laboratory containing an aluminum matrix with 2 wt% Si. The requested dimensions of the segments were 12.5 mm in length × 12.5 mm wide. The midplane of the low burnup sample was located 23 cm from the top of the fuel plate (edge with the plate identification stamp). The approximate fuel meat fission density of this segment was 2.78×10^{21} fissions•cm^{-3} and the beginning of life heat flux was 210 W•cm^{-2}. This sample was placed into KGT container #1687 for shipment to PNNL. The midplane of the high burnup sample was located 4.5 cm from the bottom of the fuel plate (the edge opposite that with the plate identification stamp). The approximate fuel meat fission density of this segment was 3.5×10^{21} fissions•cm^{-3} and the beginning of life heat flux was 315 W•cm^{-2}. This sample was placed into KGT container #1675 for shipment to PNNL. The segments consisted of only the fueled region of the fuel plate, i.e., the AA6061 edges of the fuel plate were trimmed away from the segment.

2.3 As-received Fuel Segment Conditions

The two fuel segments were received at the PNNL Radiochemical Processing Laboratory on April 22, 2014. The aluminum containers, referred to as KGT, in which the fuel segments were shipped were removed from the shipping cask and an initial inspection of the segments was performed. The segments were in acceptable condition visually and no observable delamination or other damage had occurred. The fuel segments were given unique alphabetic identifiers by PNNL. The sample shipped in KGT container #1675 was labeled as TUM Segment K, while the sample shipped in KGT container #1687 was labeled as TUM Segment L. Photographs of the as-received fuel segments are provided in Figure 2.1. Table 2.1 summarizes the physical dimensions of segments K and L. Note that samples are typically bowed. Bowing is not delamination or damage but does affect the ability to perform accurate thickness measurements on larger segments.

Figure 2.1. In-cell Photographs of As-received Fuel Segments K (left) and L (right)

Table 2.1. Summary of Physical Dimensions[a] of As-Received Fuel Segments from Idaho National Laboratory

Fuel Segment	Measured Length	Measured Width	Measured Thickness[b]	Measured Mass (g)
K	13.5	12.5	1.362	1.241
L	13.0	12.5	1.328	1.228

(a) All dimensions are in mm, unless noted otherwise.
(b) Because of the bowing of the fuel segments, the measured thickness reported was obtained in approximately the middle of the fuel segment.

Fuel segments were stored under argon in a desiccator until distributed for further segmentation. Similarly, fuel samples obtained after segmentation were stored under argon before the various property measurements. At PNNL, fuel segments for thermo-physical property analysis are denoted by a "T" followed by the segment identification letter: e.g., "TK" is fuel segment K allocated for thermo-physical property measurement. This notation is used throughout the remainder of this report.

2.4 Fuel Sample Preparation

The fuel segments were sectioned further to produce samples for various thermal and physical measurements. The sectioning was accomplished with a specialized low-speed saw with a Buehler diamond-wafering blade. Multiple cuts made under an inert argon environment were performed to transform the as-received fuel segment into samples for laser flash analysis and gas pycnometry, DSC, and optical microscopy. Each cut was performed twice to make sure the wafering blade penetrated the full thickness of the segment. Additional samples were produced as a result of cutting efficiency and were held in reserve for use in additional DSC, fission gas analysis, or other measurements (e.g., analytical chemistry).

Final sectioning diagrams used to produce the various samples from the fuel segments are provided in Figure 2.2 for Segment K and Figure 2.3 for Segment L. Included on the final sectioning diagrams are the approximate length and width dimensions (in mm) for each sample. The nomenclature identified in these final sectioning diagrams will be used to identify samples throughout this report. Note that the laser flash apparatus (LFA) and pycnometry samples are the same, although labeled in the diagrams solely as LFA. Also note that the TK-TRIM and TK-Spare 2 samples delaminated upon retrieval from the segmentation jig and could not be recovered as whole samples.

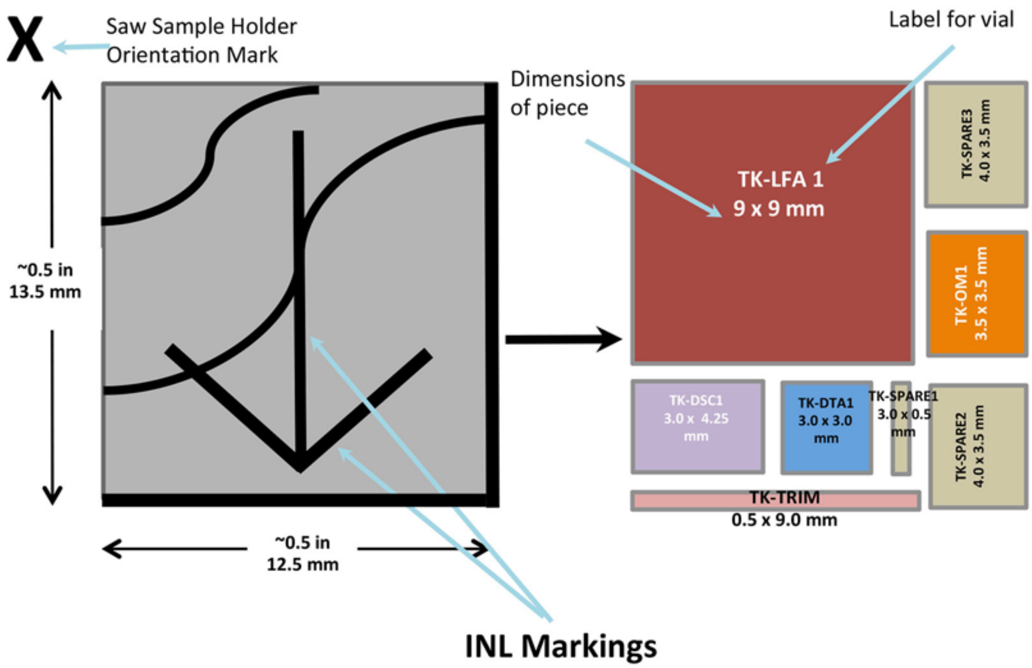

Figure 2.2. Final Sectioning Diagram Used to Produce Multiple Samples from the TK Fuel Segment

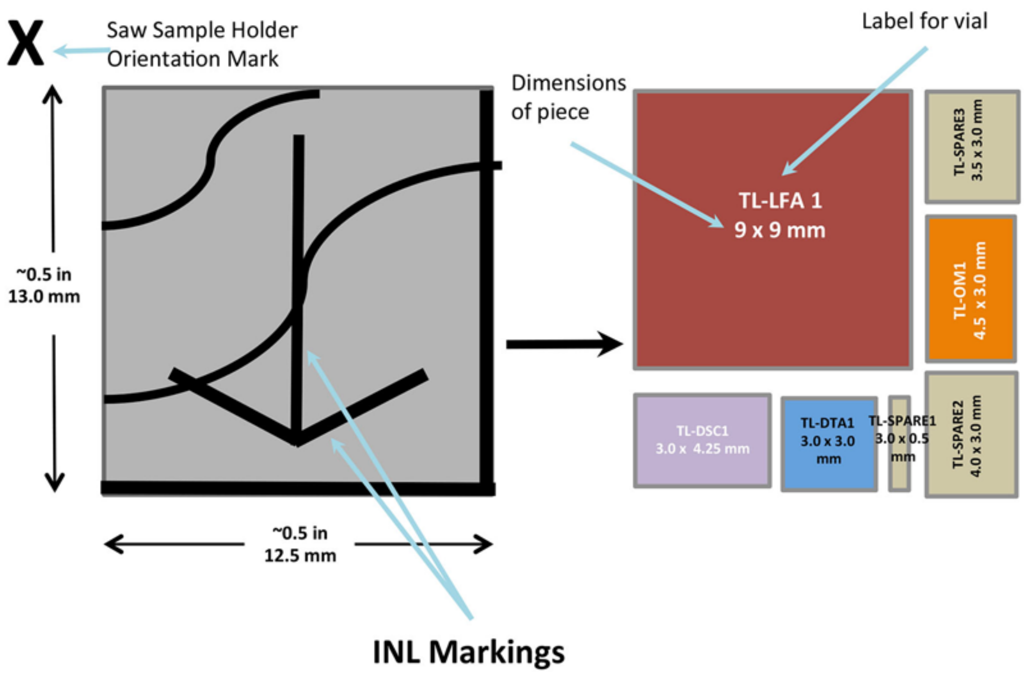

Figure 2.3. Final Sectioning Diagram Used to Produce Multiple Samples from the TL Fuel Segment

2.5 Optical Microscopy

Optical microscopy (OM) analysis was conducted to provide values for the internal dimensions of the fuel samples, including component layer thicknesses and variability across the sample. Samples were prepared by mounting in epoxy (VariDur Acrylic from Buehler), segmented using an Isomet low-speed saw to obtain the desired edge, and then polished. All polishing operations were conducted with a Buehler Minimet polisher using exchangeable pads starting with 400 grit abrasive discs increasing to 1200 grit over various steps. After the abrasive discs, polishing clothes were used with diamond suspension solutions starting at 9 µm and polishing stepwise down to 0.02 µm.

Samples were examined with a Nikon MA200 inverted optical microscope using polarized light, cross-polars, and a ¼ wave-plate compensator to improve the visibility of features when necessary. The Nikon MA200 was installed in a hot cell equipped with remote control of *x*-*y* translation, *z*-focus, illumination intensity, and the objective lens turret. An extended depth-of-focus (EDF) module in the microscope software enabled the automatic acquisition of images at different focal planes (*z*-stack) to produce an image that had all regions of the specimen in focus. The images were recorded using a Nikon Digital Camera and Elements software package. The microscope images were calibrated using a length standard, SRM-2400, purchased from the National Institute of Standards and Technology (NIST). After the analysis was completed, the specimen was removed from the hot cell and placed into storage as quickly as possible to minimize potential damage to the digital camera.

2.6 Density

An AccuPyc 1300 gas expansion pycnometer was used for density determination. The instrument consists of a sample chamber and an expansion chamber separated by an expansion valve. After inserting a sample into the sample chamber, the sample chamber is filled with helium. The helium is discharged into an expansion chamber having a known internal volume. The pressure difference between the isolated sample chamber and that of the sample chamber and expansion chamber combined is used to calculate volume displacement using Boyle's Law:

$$pV = k \tag{1}$$

where p denotes the pressure of the system, V is the volume of the gas, and k is a constant value representative of the pressure and volume of the system. Rearranging Equation 1 to fit the current system gives (Lowell *et al.* 2004):

$$V_S = V_C + \frac{V_R}{1 - \frac{p_1}{p_2}} \tag{2}$$

where V_S is the sample volume, V_C is the volume of the empty sample chamber, V_R is the reference volume, p_1 is the first pressure (in the sample chamber only), and p_2 is the second pressure after expansion of the gas into the combined volumes of sample chamber and reference chamber. V_S is then used with the pre-determined mass of the sample (m) to obtain the sample density (ρ):

$$\rho = \frac{m}{V_S} \tag{3}$$

The samples were weighed (m) using a calibrated balance in the hot cell. The AccuPyc 1330 was calibrated per the manufacturer's instructions and confirmed before and after sample analysis with a verified standard. The gas pycnometer calibration standard was run multiple times during instrument operation and was considered acceptable if the measured volume was within ±0.5% of the certified value. The samples were placed in a tared 1-cm^3 pycnometer sample cup and weighed. The pycnometer cup and sample were placed in the AccuPyc 1330 sample chamber and the chamber cap was fastened securely. Each sample was analyzed 10 times using ultra-high purity helium (V_S); the results were averaged and the density with standard deviation was recorded.

2.7 Differential Scanning Calorimetry

A Perkin Elmer Pyris 1 power-compensated DSC was used to perform specific heat capacity measurements on the fuel samples as a function of temperature. A constant flow of inert ultra-high purity argon gas was purged through the system during operation to minimize sample oxidation and provide a consistent sampling environment. Flow rate through the instrument was verified by a flow meter attached to the argon source external to the hot cell and a flow meter attached to the purge-gas exit line from the DSC interior to the hot cell. A chiller unit was housed outside the hot cell that used a mixture of 80/20 propylene glycol/water and was set to 5^{o}C to provide cooling capacity to the instrument.

Prior to testing, the DSC was balance- and slope-corrected, and then temperature was calibrated over the range of 156.6 ^{o}C (In) to 419.5 ^{o}C (Zn) using In, Sn, Pb, and Zn standard materials. Melt checks using two or more of the standard materials were performed before the actual sample run and after the sample run was complete. Melt onset temperatures were determined by calculating the intersection of two slopes that compose the melt curve. Measurements were performed on each thermogram, and the instrument was considered to be within tolerance if the smoothed melt onset temperature was within ±0.5 ^{o}C of the reported standard values. On the same thermogram, an average of two separate area-under-the-peak measurements was calculated to determine the enthalpy of fusion. The instrument was considered to be within tolerance if the average enthalpy of fusion of the smoothed data was within ±5% of the reported standard values.

Five separate runs using the same sample and reference pans with identical temperature profiles were performed: a baseline run with two empty Al pans, a reference run with a sapphire standard placed in the sample Al pan, a sample run with the fuel sample placed in the sample Al pan, and an additional baseline run and sapphire run after the sample run to check for instrument stability (at the request of the customer). The same series of five runs was made for each fuel sample investigated. The thermal profile used to conduct the DSC measurements is provided in Table 2.2. Note that only a single cycle through the temperature profile was performed for the baseline and reference runs, while the sample was subjected to five cycles of the temperature profile. To guarantee maximum contact with the heating stage, the flattest of the two large sample faces was selected for face-down placement in the Al sample pan (i.e., the four edges were not considered). Samples were loaded and centered in the aluminum sample pan that was subsequently centered in the platinum crucible (i.e., DSC sample holder).

Table 2.2. Thermal Profile Used to Conduct the DSC Measurements

Step	Temperature (^oC)	Function	Ramp Rate ($^oC\bullet min^{-1}$)	Time (min)
1	40	Isotherm	0	10.0
2	130	Heat	40	2.25
3	130	Isotherm	0	10.0
4	70	Cool	40	1.50
5	70	Isotherm	0	10.0
6	170	Heat	40	2.50
7	170	Isotherm	0	10.0
8	110	Cool	40	1.50
9	110	Isotherm	0	10.0
10	210	Heat	40	2.50
11	210	Isotherm	0	10.0
12	40	Cool	40	4.25
13	40	Isotherm	0	10.0
14	150	Heat	40	2.75
15	150	Isotherm	0	10.0
16	250	Heat	40	2.50
17	250	Isotherm	0	10.0
18	190	Cool	40	1.50
19	190	Isotherm	0	10.0
20	290	Heat	40	2.50
21	290	Isotherm	0	10.0
22	230	Cool	40	1.50
23	230	Isotherm	0	10.0
24	310	Heat	40	2.00
25	310	Isotherm	0	10.0
26	40	Cool	40	6.75

2.8 Laser Flash Analysis

Thermal diffusivity measurements were performed using a Netzsch LFA 457 MicroFlash® Laser Flash Apparatus. The same samples used for density measurements were also subjected to laser flash analysis. A sapphire support was specially fabricated to accommodate the precise sample orientation necessary for proper laser flash analysis. The support was required in order to configure the sample in an orientation that allowed full laser irradiation of the sample side facing the laser, while also preventing any fine fuel fragments that may have separated from the sample during analysis from falling down into the instrument. Sapphire was specifically selected because of its transparency to laser light in the energy range of the laser used and also based on reports of successful use (Sheindlin *et al.* 1998). A vacuum of approximately 250 mtorr was applied to the closed sample chamber after the sample was loaded. Once under vacuum, a helium purge was initiated and the vacuum pump shut off to allow for a helium environment in the chamber. To minimize sample oxidation and guarantee a consistent sampling environment, this process was repeated a second time. Once the chamber was refilled with helium at approximately atmospheric pressure, the chamber was sealed and the purge gas shut off. Helium gas was selected because this allowed for better temperature control in the instrument at lower temperatures.

Before and after sample measurements, thermal diffusivity of a NIST-traceable iron standard was measured over the temperature range of interest. The instrument was considered in calibration if the iron standard measurements were within ±5% of the expected values. Prior to laser flash measurements, the samples were coated with a thin layer of graphite (Graphit 33 from CRC Industries Deutschland). The thermal profile used to conduct the LFA measurements is provided in Table 2.3.

Table 2.3. Thermal Profile Used to Conduct the LFA Measurements

Step	Temperature (^{o}C)	Heating Rate (K•min^{-1})	Pos.2 Shots (number of shots)	Time Dist. (min)
0	25	--	--	--
1	25	0	5	1
2	50	3	5	1
3	75	3	5	1
4	100	3	5	1
5	125	3	10	1
6	100	3	6	1
7	75	3	6	1
8	50	3	6	1
9	25	3	6	1
10	150	10	5	1
11	200	10	5	1
12	250	10	5	1
13	300	10	10	1
14	250	10	5	1
15	200	10	5	1
16	150	10	5	1

ASTM E1461 (ASTM 2011) was used as a reference to perform the thermal diffusivity measurements. Measurements were originally acquired using the Cowan + Pulse Correction model (Cowan 1963) as it allowed for more data points to be recorded. NETZSCH Proteus software[2] was used to calculate thermal diffusivity using the Cape-Lehman + pulse correction model (Cape and Lehman 1963) that accounts for any heat transfer from the sample to the environment and for finite pulse width effects (given the relative thinness of the samples) using the measured data. The Cape-Lehman model was selected based on equipment manufacture recommendations and because thermal diffusivity values reported for the Fe standard were also calculated using this model. The raw LFA data can be used to calculate thermal diffusivity using alternative methods (e.g., Cowan) and/or thickness values (e.g., measured by OM) upon request.

[2] Netzsch Proteus LFA Analysis, Version 6.0.0, May 7, 2012.

3.0 Results

The results presented in this section are organized according to optical metallography, density, differential scanning calorimetry, and laser flash analysis.

3.1 Optical Metallography

The optical metallography results presented in this section are organized according to fuel segment identification.

3.1.1 Segment K

The OM sample obtained from Segment K measured approximately 3.5 mm long by 3.5 mm wide, 1.513 mm thick, and weighed 102.1 mg. The optical microscopy montage of TK-OM is provided in Figure 3.1. This montage was used to obtain thickness measurements over the sample length. The fuel meat sandwiched between AA6061 clad can be clearly observed in Figure 3.1.

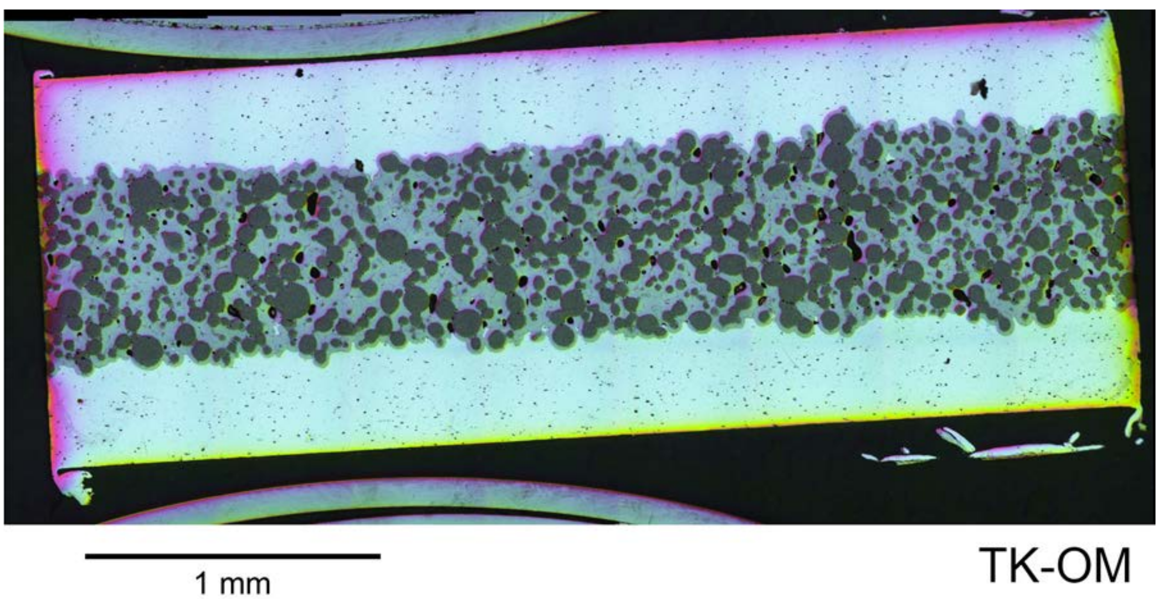

Figure 3.1. Low Magnification Optical Microscopy Montage of the TK-OM Sample

Optical microscopy thickness measurements of the fuel meat obtained from the TK-OM sample are provided in Table 3.1. The average fuel meat thickness determined from the 188 measurements was 666.5 ± 33.2 μm. Four measurements made over the entire thickness of the TK-OM sample yielded an average of 1320.7 ± 5.5 μm. Image analysis revealed an average fuel particle diameter of 46.4 ± 19.3 μm with a distribution shown in Figure 3.2 obtained from 355 measurements. Furthermore, the proportions of different regions were determined by image analysis, with the AA6061 cladding representing 47% of the sample, the fuel particles representing 26% of the sample, and the interaction layer phase representing the remaining 27% of the sample, i.e., there was no original matrix remaining in the sample.

Table 3.1. Fuel Meat Thickness Measurements Obtained from the TK-OM Sample as a Function of Distance Across the Length of the Sample Starting at One End

Distance (μm)	Layer Thickness (μm)	Distance (μm)	Layer Thickness (μm)	Distance (μm)	Layer Thickness (μm)	Distance (μm)	Layer Thickness (μm)	Distance (μm)	Layer Thickness (μm)
0	711.4	759.6	631.1	1519.2	695.6	2278.8	669.8	3038.4	625.5
20.0	675.9	779.6	644.6	1539.2	674.5	2298.8	682.3	3058.4	680.7
40.0	661.4	799.6	667.5	1559.2	633.9	2318.8	678.3	3078.4	669.6
60.0	674.7	819.6	684.0	1579.2	668.2	2338.7	634.8	3098.3	672.2
80.0	680.9	839.6	702.7	1599.1	660.2	2358.7	604.8	3118.3	641.9
99.9	645.9	859.5	685.2	1619.1	634.1	2378.7	565.8	3138.3	667.0
119.9	656.1	879.5	628.8	1639.1	666.9	2398.7	589.9	3158.3	688.3
139.9	693.4	899.5	638.3	1659.1	695.6	2418.7	659.9	3178.3	700.8
159.9	691.4	919.5	631.2	1679.1	691.0	2438.7	668.6	3198.3	661.0
179.9	668.3	939.5	625.7	1699.1	681.6	2458.7	648.5	3218.3	627.1
199.9	617.6	959.5	613.2	1719.1	647.2	2478.7	612.1	3238.3	666.9
219.9	635.1	979.5	642.8	1739.1	671.5	2498.7	645.4	3258.3	681.0
239.9	670.6	999.5	605.2	1759.1	699.2	2518.7	668.1	3278.2	692.0
259.9	682.0	1019.5	578.0	1779.0	699.1	2538.6	671.2	3298.2	724.6
279.9	693.6	1039.4	573.9	1799.0	697.2	2558.6	658.9	3318.2	724.8
299.8	704.7	1059.4	643.4	1819.0	669.5	2578.6	673.6	3338.2	715.9
319.8	685.1	1079.4	649.5	1839.0	621.1	2598.6	730.5	3358.2	748.6
339.8	647.7	1099.4	672.4	1859.0	643.6	2618.6	713.0	3378.2	742.3
359.8	655.9	1119.4	677.6	1879.0	644.3	2638.6	635.1	3398.2	680.9
379.8	675.8	1139.4	647.6	1899.0	640.9	2658.6	662.2	3418.2	670.8
399.8	682.9	1159.4	618.3	1919.0	660.8	2678.6	736.4	3438.2	655.2
419.8	680.9	1179.4	643.4	1939.0	683.2	2698.6	761.9	3458.1	676.8
439.8	638.2	1199.4	643.8	1959.0	672.8	2718.5	762.9	3478.1	682.9
459.8	656.8	1219.3	621.1	1978.9	661.7	2738.5	770.3	3498.1	668.2
479.7	676.6	1239.3	643.8	1998.9	652.3	2758.5	759.2	3518.1	648.3
499.7	676.6	1259.3	666.2	2018.9	658.4	2778.5	710.0	3538.1	656.0
519.7	679.9	1279.3	659.9	2038.9	659.1	2798.5	687.1	3558.1	662.1
539.7	695.3	1299.3	625.4	2058.9	656.5	2818.5	673.7	3578.1	668.6
559.7	700.5	1319.3	628.0	2078.9	632.2	2838.5	666.4	3598.1	665.8
579.7	691.3	1339.3	647.8	2098.9	669.6	2858.5	676.9	3618.1	673.3
599.7	659.8	1359.3	697.3	2118.9	658.5	2878.5	656.4	3638.1	679.5
619.7	629.9	1379.3	710.2	2138.9	658.4	2898.4	667.4	3658.0	691.7
639.7	630.8	1399.3	722.5	2158.8	649.8	2918.4	655.9	3678.0	610.0
659.6	639.3	1419.2	686.9	2178.8	679.6	2938.4	603.2	3698.0	671.6
679.6	623.7	1439.2	687.7	2198.8	692.1	2958.4	650.6	3718.0	673.7
699.6	653.8	1459.2	689.4	2218.8	668.7	2978.4	648.9	3738.0	650.1
719.6	620.6	1479.2	670.3	2238.8	652.5	2998.4	645.2		
739.6	628.9	1499.2	673.1	2258.8	662.4	3018.4	663.5		

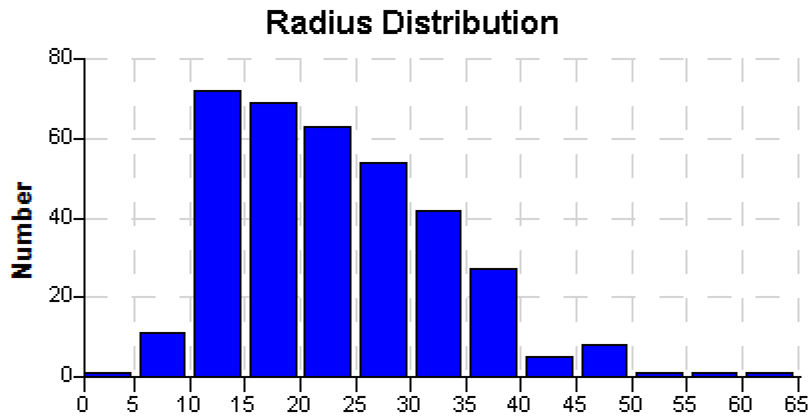

Figure 3.2. Fuel Particle Radius Distribution Obtained Using Image Analysis on Sample TK-OM

Higher magnification optical images of the fuel-matrix interaction are provided in Figure 3.3. The metallographs provided in Figure 3.3 were obtained across the length of the sample (which was oriented from top to bottom on the microscope). Observation of the metallographs clearly shows that a majority of the original Al-2 wt% Si matrix has been consumed and the resultant interaction product separates the original fuel particles. There are a few regions of porosity that may be observed in the metallographs, but it is not possible to discern from these images whether this is remnant porosity from the fabrication process or if it is the result of irradiation.

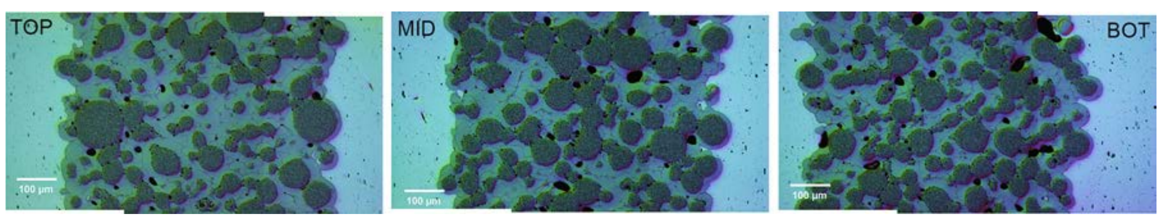

Figure 3.3. Extended Depth of Focus Optical Microscopy Images of the Fuel-Matrix Interaction for the TK-OM Sample Taken at the Top, Middle (MID), and Bottom (BOT)

Higher magnification EDF images of the fuel and matrix are provided in Figure 3.4 for the TK-OM sample. Observation of these metallographs again clearly shows consumption of the matrix and resultant interaction product. Furthermore, small, uniform fission gas bubbles have consumed the original fuel particle grain structure, indicating that recrystallization has occurred. Coarser fission gas bubbles that are less uniform in size and distribution are also present in the metallographs, particularly at the intersection of adjacent fuel particles.

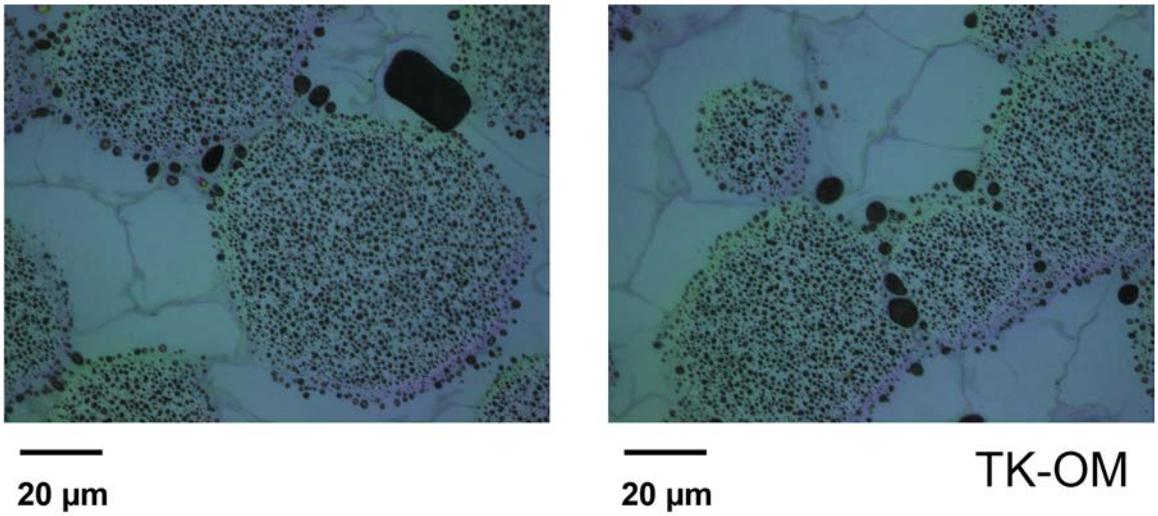

Figure 3.4. Higher Magnification EDF Images of the Irradiated Fuel and Surrounding Matrix for the TK-OM Sample

3.1.2 Segment L

The OM sample obtained from Segment L measured approximately 4.25 mm long by 3.0 mm wide, 1.417 mm thick, and weighed 108.8 mg. The optical microscopy montage of the TL-OM sample is provided in Figure 3.5. This montage was used to obtain thickness measurements over the sample length. The fuel meat can clearly be observed within the AA6061 cladding in Figure 3.5.

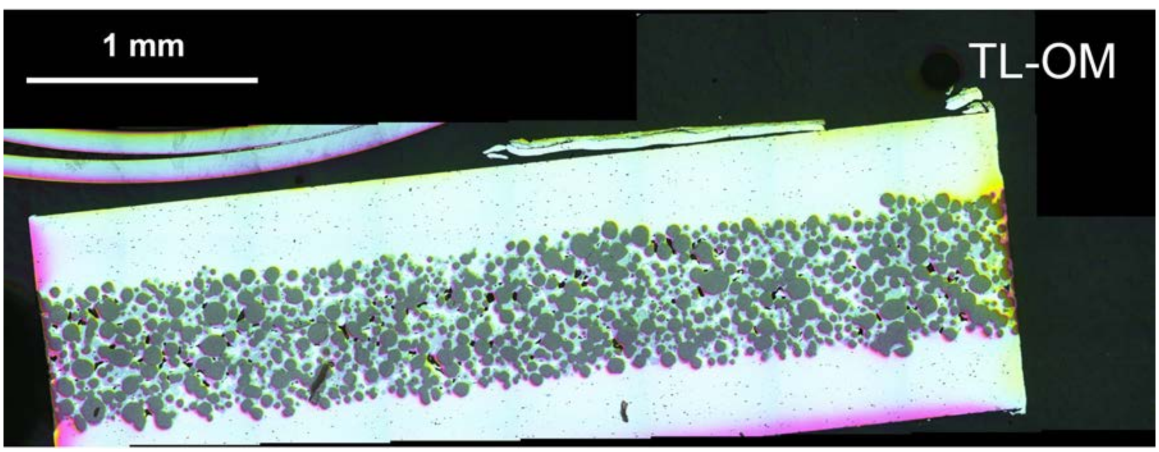

Figure 3.5. Low Magnification Optical Microscopy Montage of the TL-OM Sample

Optical microscopy thickness measurements of the fuel meat obtained from the TL-OM sample are provided in Table 3.2. The average fuel meat thickness determined from the 77 measurements was 595.4 ± 33.3 µm. Four measurements made over the entire thickness of the TK-OM sample yielded an average of 1306.2 ± 2.2 µm. Image analysis revealed an average fuel particle diameter of 47.5 ± 20.7 µm with a distribution shown in Figure 3.6 obtained from 246 measurements. Furthermore, the proportions of different regions were determined by image analysis, with the AA6061 cladding representing 47% of the sample, the fuel particles representing 27% of the sample, the interaction layer phase representing the remaining 19% of the sample, and the original Al-2 wt% Si matrix representing 7-8% of the sample.

Table 3.2. Fuel Meat Thickness Measurements Obtained from the TL-OM Optical Microscopy Sample as a Function of Distance Across the Length of the Sample Starting at One End

Distance (μm)	Layer Thickness (μm)	Distance (μm)	Layer Thickness (μm)	Distance (μm)	Layer Thickness (μm)
0	602.3	1461.5	619.0	2922.9	627.2
56.2	545.8	1517.7	606.1	2979.2	610.7
112.4	647.3	1573.9	591.8	3035.4	610.7
168.6	557.6	1630.1	569.0	3091.6	601.2
224.8	556.8	1686.3	627.2	3147.8	547.0
281.1	580.8	1742.5	672.8	3204.0	593.4
337.3	582.7	1798.7	569.0	3260.2	593.4
393.5	665.2	1854.9	590.3	3316.4	605.1
449.7	566.0	1911.2	588.1	3372.6	568.3
505.9	637.5	1967.4	560.0	3428.8	594.3
562.1	552.1	2023.6	594.8	3485.1	610.7
618.3	581.5	2079.8	573.1	3541.3	522.9
674.5	566.4	2136.0	563.3	3597.5	562.1
730.7	578.0	2192.2	637.6	3653.7	531.6
786.9	623.7	2248.4	607.9	3709.9	597.4
843.2	564.7	2304.6	587.5	3766.1	599.6
899.4	531.5	2360.8	600.0	3822.3	618.5
955.6	581.9	2417.1	552.5	3878.5	573.1
1011.8	583.8	2473.3	620.9	3934.7	622.2
1068.0	661.1	2529.5	563.4	3990.9	582.4
1124.2	693.3	2585.7	620.6	4047.2	615.3
1180.4	603.8	2641.9	569.0	4103.4	586.3
1236.6	616.4	2698.1	656.9	4159.6	600.7
1292.8	620.3	2754.3	591.4	4215.8	612.5
1349.1	624.2	2810.5	631.9	4272.0	628.3
1405.3	565.3	2866.7	578.3		

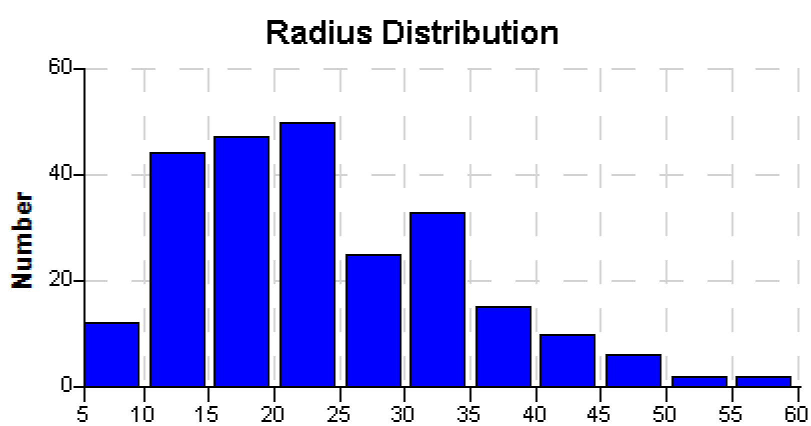

Figure 3.6. Fuel Particle Radius Distribution Obtained Using Image Analysis on Sample TL-OM

Higher magnification optical images of the fuel-matrix interaction are provided in Figure 3.7. The metallographs provided in Figure 3.7 were obtained across the length of the sample (which was oriented from top to bottom on the microscope). Observation of the metallographs shows that contrary to sample TK-OM, only a fraction of the original Al-2 wt% Si matrix has been consumed. The reaction product appears to be more prominent around finer fuel particles compared to coarser fuel particles. As with sample TK-OM, a few regions of porosity may be observed in the metallographs, but it is not possible to discern from these images whether this is remnant porosity from the fabrication process or if it is the result of irradiation.

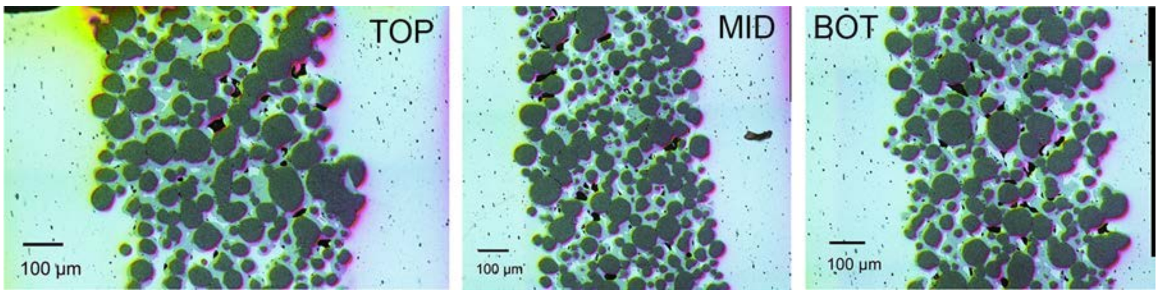

Figure 3.7. Extended Depth of Focus Optical Microscopy Images of the Fuel-Matrix Interaction for the TL-OM Sample Taken at the Top, Middle (MID), and Bottom (BOT)

Higher magnification EDF images of the fuel and matrix are provided in Figure 3.8 for the TL-OM sample. Observation of these metallographs clearly shows the fuel particles (dark spheres) surrounded by an interaction layer product (dark gray) and some regions of the original Al-2wt% Si matrix (light gray) still present in the fuel meat. As with sample TK-OM, small, uniform fission gas bubbles are present throughout the fuel particles, although the bubbles do not appear to have completely consumed the original grain structure yet. Coarser fission gas bubbles that are less uniform in size and distribution are also present in the metallographs, again particularly at the intersection of adjacent fuel particles, although the density and size of these bubbles are not as great as those observed in the TK-OM sample.

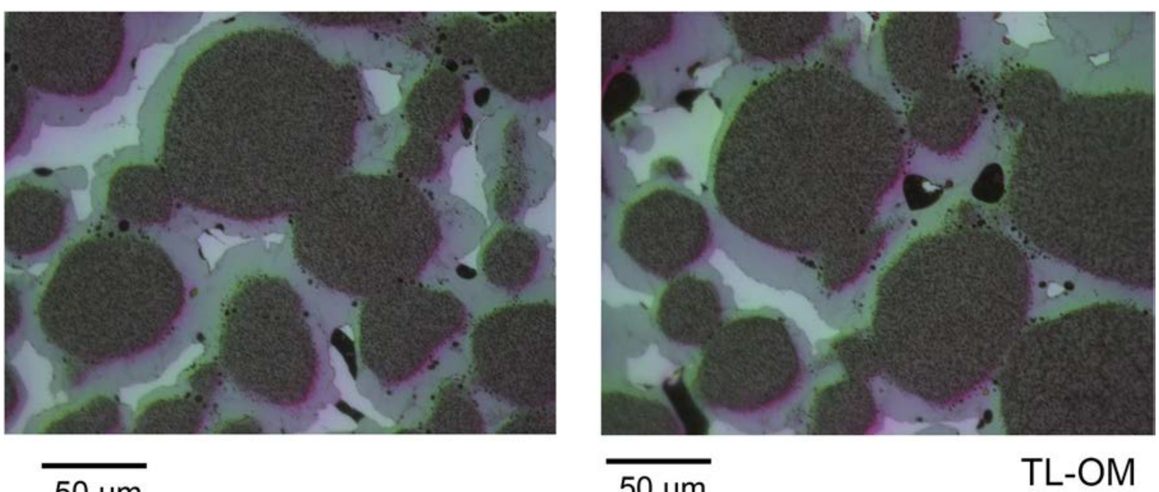

Figure 3.8. Higher Magnification EDF Images of the Irradiated Fuel and Surrounding Matrix for the TL-OM Sample

3.2 Density

Density measurements obtained on the two laser flash analysis samples are provided in Table 3.3. Based on the 10 measurements performed, the average room temperature composite density was 5.6215 ± 0.0084 g•cm^{-3} for the TK-LFA sample and 5.7839 ± 0.0113 g•cm^{-3} for the TL-LFA sample. As expected, the composite density was lower for the sample with higher expected burnup, TK-LFA.

Table 3.3. Room Temperature Composite Density of the Two LFA Samples Measured by Pycnometry

Segment TK		Segment TL	
Density (g•cm^{-3})	Density Deviation (g•cm^{-3})	Density (g•cm^{-3})	Density Deviation (g•cm^{-3})
5.6082	-0.0133	5.7701	-0.0138
5.6142	-0.0073	5.7703	-0.0136
5.6163	-0.0051	5.7710	-0.0129
5.6187	-0.0027	5.8067	0.0228
5.6155	-0.0060	5.7946	0.0107
5.6239	0.0025	5.7862	0.0023
5.6356	0.0141	5.7848	0.0009
5.6196	-0.0019	5.7827	-0.0012
5.6316	0.0101	5.7798	-0.0041
5.6311	0.0096	5.7927	0.0088

3.3 Differential Scanning Calorimetry

The differential scanning calorimety results presented in this section are organized according to fuel segment identification.

3.3.1 Segment K

The DSC sample obtained from Segment K measured approximately 3.0 mm long by 4.25 mm wide, 1.458 mm thick, and weighed 94.3 mg. A baseline of the DSC instrument was obtained by running both the sample and reference pans empty over a single thermal cycle defined in Table 2.2 both before and after the sample measurement. A graphical representation of the baseline run as a function of temperature for both the pre-sample and post-sample measurement is provided in Figure 3.9. A reduced data set of the DSC signal as a function of time and temperature for the pre-sample measurement is provided in Table 3.4. The reference run was obtained by placing a 96.59 mg NIST traceable sapphire into the sample pan of the instrument over a single thermal cycle defined in Table 2.2 both before and after the sample measurement. A graphical representation of the DSC signal as a function of temperature is provided in Figure 3.10 for both the pre-sample and post-sample measurement. A reduced data set of the DSC signal as a function of time and temperature is provided in Table 3.5 for the pre-sample measurement. Finally, the sample runs were obtained by placing the DSC sample into the sample pan of the instrument. The sample was subjected to five thermal cycles, as defined in Table 2.2, run in series. A graphical representation of the DSC signal as a function of temperature is provided in Figure 3.11, and a reduced data set of the DSC signal as a function of time and temperature is provided in Table 3.6 through Table 3.10 for each measurement cycle. Observation of Figure 3.11 shows the very repeatable behavior of the segment K sample over each measurement cycle.

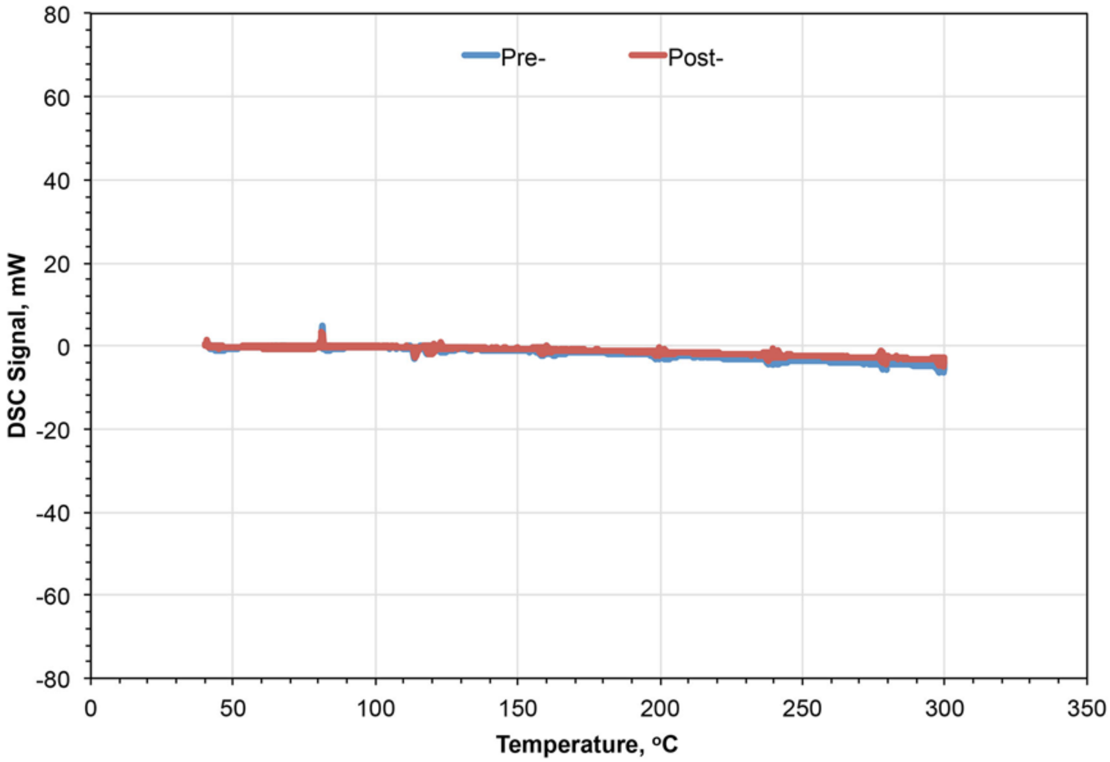

Figure 3.9. DSC Signal as a Function of Temperature for the Baseline Run of Segment K Before and After the Sample Measurement

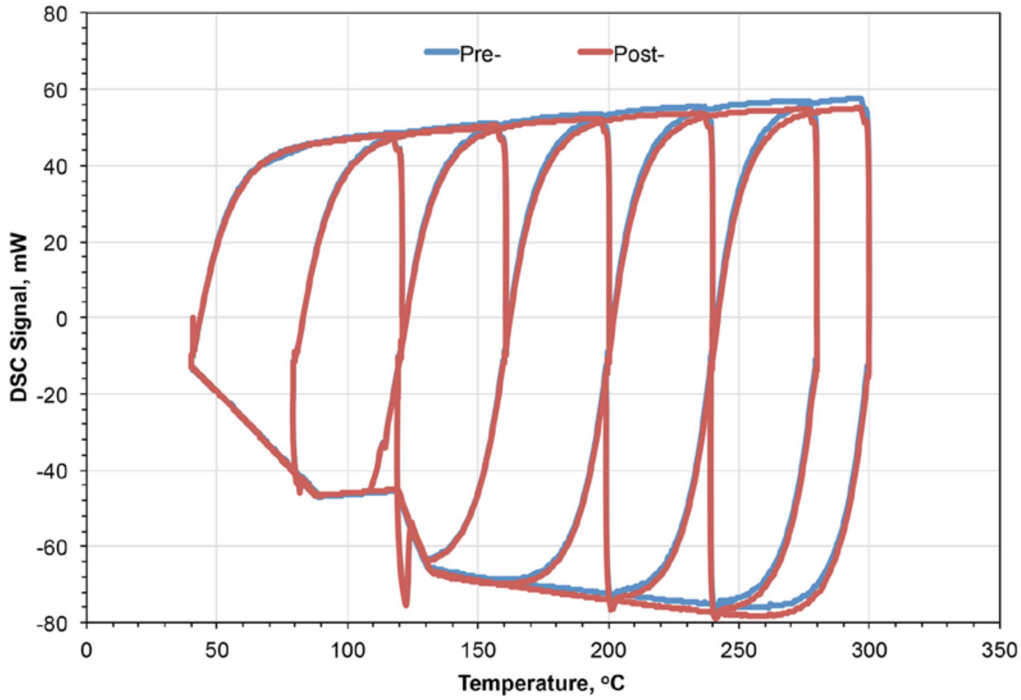

Figure 3.10. DSC Signal as a Function of Temperature for the Reference Run of Segment K Before and After the Sample Measurement

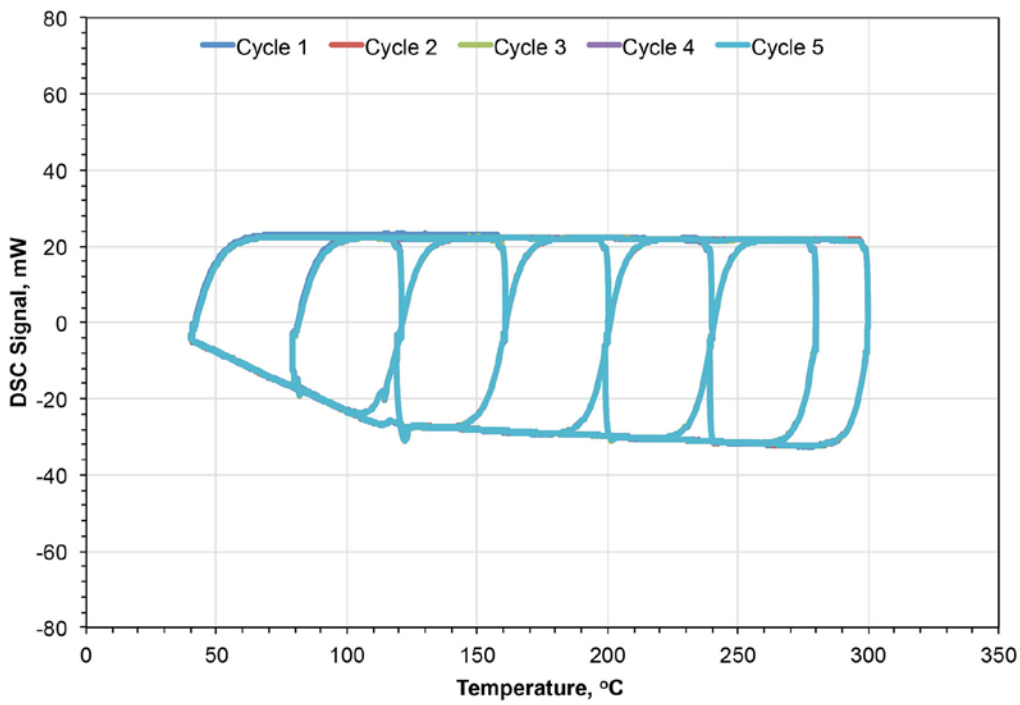

Figure 3.11. DSC Signal as a Function of Temperature for the Sample Run of Segment K for Each Thermal Cycle

Table 3.4. Reduced Dataset of DSC Signal as a Function of Time and Temperature for Segment K Baseline Run (Pre-Sample)

Time (min)	T_s (°C)	DSC (mW)	Time (min)	T_s (°C)	DSC (mW)	Time (min)	T_s (°C)	DSC (mW)	Time (min)	T_s (°C)	DSC (mW)	Time (min)	T_s (°C)	DSC (mW)	Time (min)	T_s (°C)	DSC (mW)	Time (min)	T_s (°C)	DSC (mW)
0.0	41	0.00	33.6	101	-0.42	57.7	185	-1.78	78.0	41	-0.01	96.4	213	-2.57	130.0	280	-4.45	154.1	239	-2.92
2.0	41	-0.03	33.7	105	-0.42	57.8	189	-1.94	80.0	41	-0.02	96.5	217	-2.68	130.1	278	-3.37	154.2	235	-2.76
4.0	41	-0.03	33.8	109	-0.52	57.9	193	-2.01	82.0	41	0.06	96.6	221	-2.82	130.2	275	-3.08	154.3	231	-2.68
6.0	41	-0.02	33.9	113	-0.60	58.0	197	-2.22	82.1	41	-0.06	96.7	225	-3.21	130.3	271	-3.62	154.4	227	-2.59
8.0	41	-0.03	34.0	117	-0.62	60.0	200	-2.17	82.2	44	-1.07	96.8	229	-2.89	130.4	267	-3.74	154.5	223	-2.42
10.0	41	0.04	34.1	121	-0.64	62.0	200	-2.17	82.3	48	-0.76	96.9	233	-3.11	130.5	263	-3.32	154.6	219	-2.29
10.1	41	0.03	34.2	125	-0.66	64.0	200	-2.13	82.4	52	-0.48	97.0	237	-3.23	130.6	259	-3.38	154.7	215	-2.28
10.2	44	-1.02	34.3	129	-0.73	66.0	200	-2.12	82.5	56	-0.30	99.0	240	-3.22	130.7	255	-3.38	154.8	211	-2.15
10.3	48	-0.82	34.4	133	-0.79	68.0	200	-2.28	82.6	61	-0.20	101.0	240	-3.19	130.8	251	-3.32	154.9	207	-2.04
10.4	52	-0.49	34.5	137	-0.78	68.1	199	-1.33	82.7	65	-0.05	103.0	240	-3.19	130.9	247	-3.10	155.0	203	-1.97
10.5	56	-0.27	34.6	141	-0.93	68.2	195	-1.32	82.8	69	-0.13	105.0	240	-3.21	131.0	243	-2.90	155.1	199	-1.89
10.6	61	-0.14	34.7	145	-1.05	68.3	191	-1.62	82.9	73	-0.15	107.0	240	-3.30	133.0	239	-2.99	155.2	195	-1.76
10.7	65	-0.18	34.8	149	-1.18	68.4	187	-1.70	83.0	77	-0.24	107.1	238	-2.28	135.0	240	-3.15	155.3	191	-1.69
10.8	69	-0.21	34.9	153	-1.16	68.5	183	-1.56	83.1	81	-0.26	107.2	235	-2.37	137.0	240	-3.04	155.4	187	-1.61
10.9	73	-0.21	35.0	157	-1.32	68.6	179	-1.44	83.2	85	-0.29	107.3	231	-2.55	139.0	240	-3.23	155.5	183	-1.53
11.0	77	-0.24	37.0	160	-1.25	68.7	175	-1.41	83.3	89	-0.33	107.4	227	-2.55	141.0	240	-2.95	155.6	179	-1.38
11.1	81	-0.27	39.0	160	-1.26	68.8	171	-1.29	83.4	93	-0.40	107.5	223	-2.50	141.1	241	-4.02	155.7	175	-1.34
11.2	85	-0.31	41.0	160	-1.22	68.9	167	-1.29	83.5	97	-0.44	107.6	219	-2.39	141.2	244	-3.86	155.8	171	-1.24
11.3	89	-0.33	43.0	160	-1.27	69.0	163	-1.09	83.6	101	-0.46	107.7	215	-2.28	141.3	248	-3.61	155.9	167	-1.13
11.4	93	-0.36	45.0	160	-1.35	69.1	159	-1.05	83.7	105	-0.53	107.8	211	-2.25	141.4	252	-3.61	156.0	163	-1.10
11.5	97	-0.39	45.1	159	-0.63	69.2	155	-0.91	83.8	109	-0.56	107.9	207	-2.14	141.5	257	-3.75	156.1	159	-1.04
11.6	101	-0.39	45.2	156	-0.59	69.3	151	-0.90	83.9	113	-0.59	108.0	203	-1.96	141.6	261	-3.83	156.2	155	-0.90
11.7	105	-0.48	45.3	152	-0.81	69.4	147	-0.80	84.0	117	-0.58	110.0	200	-1.99	141.7	265	-4.01	156.3	151	-0.83
11.8	109	-0.54	45.4	148	-0.81	69.5	143	-0.74	84.1	121	-0.68	112.0	200	-2.07	141.8	269	-4.06	156.4	147	-0.76
11.9	113	-0.53	45.5	144	-0.77	69.6	139	-0.67	84.2	125	-0.75	114.0	200	-2.05	141.9	273	-4.21	156.5	143	-0.69
12.0	117	-0.66	45.6	140	-0.69	69.7	136	-0.58	84.3	129	-0.80	116.0	200	-2.04	142.0	277	-4.34	156.6	139	-0.64
14.0	120	-0.52	45.7	136	-0.66	69.8	132	-0.59	84.4	133	-0.96	118.0	200	-1.95	142.1	281	-4.49	156.7	135	-0.52
16.0	120	-0.61	45.8	132	-0.61	69.9	128	-0.55	84.5	137	-0.99	118.1	201	-2.90	142.2	285	-4.47	156.8	131	-0.52
18.0	120	-0.55	45.9	128	-0.53	70.0	124	-0.50	84.6	141	-0.96	118.2	204	-2.87	142.3	289	-4.65	156.9	128	-0.46
20.0	120	-0.57	46.0	124	-0.48	70.1	120	-1.15	84.7	145	-1.02	118.3	208	-2.53	142.4	293	-4.79	157.0	124	-0.52
22.0	120	-0.66	48.0	120	-0.52	70.2	116	-0.34	84.8	149	-1.12	118.4	212	-2.64	142.5	297	-5.05	157.1	120	-1.63
22.1	119	-0.09	50.0	120	-0.56	70.3	112	-0.26	84.9	153	-1.35	118.5	217	-2.57	144.5	300	-4.98	157.2	116	-0.30

Time (min)	T_s (°C)	DSC (mW)	Time (min)	T_s (°C)	DSC (mW)	Time (min)	T_s (°C)	DSC (mW)	Time (min)	T_s (°C)	DSC (mW)	Time (min)	T_s (°C)	DSC (mW)	Time (min)	T_s (°C)	DSC (mW)	Time (min)	T_s (°C)	DSC (mW)
22.2	117	0.01	52.0	120	-0.54	70.4	108	-0.29	85.0	157	-1.23	118.6	221	-2.72	146.5	300	-4.98	157.3	112	-0.23
22.3	113	-1.29	54.0	120	-0.54	70.5	105	-0.31	87.0	160	-1.31	118.7	225	-3.19	148.5	300	-5.02	157.4	108	-0.28
22.4	109	-0.20	56.0	120	-0.43	70.6	101	-0.31	89.0	160	-1.37	118.8	229	-3.26	150.5	300	-4.97	157.5	105	-0.30
22.5	106	-0.29	56.1	121	-1.07	70.7	98	-0.29	91.0	160	-1.41	118.9	233	-3.11	152.5	300	-5.02	157.6	101	-0.27
22.6	102	-0.35	56.2	125	-1.35	70.8	95	-0.29	93.0	160	-1.21	119.0	237	-3.15	152.6	298	-3.98	157.7	98	-0.26
22.7	99	-0.34	56.3	129	-0.93	70.9	92	-0.34	95.0	160	-1.24	119.1	241	-3.29	152.7	295	-4.15	157.8	95	-0.28
22.8	96	-0.33	56.4	133	-0.88	71.0	89	-0.35	95.1	161	-1.94	119.2	245	-3.38	152.8	291	-4.39	157.9	92	-0.31
22.9	93	-0.36	56.5	137	-0.89	71.1	87	-0.37	95.2	165	-2.06	119.3	249	-3.40	152.9	287	-4.30	158.0	90	-0.30
23.0	90	-0.32	56.6	141	-0.87	71.2	84	-0.40	95.3	169	-1.72	119.4	253	-3.65	153.0	283	-4.29	158.1	87	-0.35
25.0	80	-0.11	56.7	145	-1.00	71.3	82	-0.45	95.4	173	-1.56	119.5	257	-3.67	153.1	279	-3.72	158.2	85	-0.38
27.0	80	-0.10	56.8	149	-1.22	71.4	80	-0.50	95.5	177	-1.67	119.6	261	-3.83	153.2	275	-3.74	158.3	82	-0.42
29.0	80	-0.15	56.9	153	-1.09	71.5	78	-0.53	95.6	181	-1.71	119.7	265	-3.94	153.3	271	-3.91	158.4	80	-0.45
31.0	80	-0.11	57.0	157	-1.24	71.6	76	-0.59	95.7	185	-1.86	119.8	269	-4.07	153.4	267	-3.75	158.5	78	-0.52
33.0	80	-0.03	57.1	161	-1.44	71.7	74	-0.65	95.8	189	-1.92	119.9	273	-4.14	153.5	263	-3.48	158.6	76	-0.57
33.1	81	-0.36	57.2	165	-1.50	71.8	72	-0.70	95.9	193	-2.01	120.0	277	-4.37	153.6	259	-3.42	158.7	74	-0.62
33.2	85	-0.91	57.3	169	-1.56	71.9	70	-0.76	96.0	197	-2.18	122.0	280	-4.38	153.7	255	-3.36	158.8	72	-0.68
33.3	89	-0.54	57.4	173	-1.52	72.0	68	-0.74	96.1	201	-2.23	124.0	280	-4.37	153.8	251	-3.20	158.9	70	-0.74
33.4	93	-0.40	57.5	177	-1.66	74.0	48	-0.17	96.2	205	-2.34	126.0	280	-4.41	153.9	247	-3.06			
33.5	97	-0.39	57.6	181	-1.76	76.0	40	0.07	96.3	209	-2.37	128.0	280	-4.31	154.0	243	-3.03			

Table 3.5. Reduced Dataset of DSC Signal as a Function of Time and Temperature for Segment K Reference Run (Pre-Sample)

Time (min)	T_s (°C)	DSC (mW)	Time (min)	T_s (°C)	DSC (mW)	Time (min)	T_s (°C)	DSC (mW)	Time (min)	T_s (°C)	DSC (mW)	Time (min)	T_s (°C)	DSC (mW)	Time (min)	T_s (°C)	DSC (mW)	Time (min)	T_s (°C)	DSC (mW)
0.0	41	-0.31	33.6	101	39.70	57.7	185	53.08	78.0	41	-9.70	96.4	213	54.52	130.0	280	-11.30	154.1	239	-75.20
2.0	41	-9.94	33.7	105	42.75	57.8	189	53.21	80.0	41	-9.87	96.5	217	54.76	130.1	278	-17.19	154.2	235	-74.88
4.0	41	-9.85	33.8	109	44.94	57.9	193	53.45	82.0	41	-9.81	96.6	221	54.91	130.2	275	-35.76	154.3	231	-74.61
6.0	41	-9.84	33.9	113	46.39	58.0	197	53.57	82.1	41	-7.84	96.7	225	55.06	130.3	271	-50.20	154.4	227	-74.34
8.0	41	-9.85	34.0	117	47.41	60.0	200	-10.66	82.2	44	1.78	96.8	229	55.25	130.4	267	-59.87	154.5	223	-74.10
10.0	41	-9.79	34.1	121	48.22	62.0	200	-10.45	82.3	48	14.12	96.9	233	55.43	130.5	263	-65.93	154.6	219	-73.77
10.1	41	-7.67	34.2	125	48.77	64.0	200	-10.42	82.4	52	23.94	97.0	237	55.33	130.6	259	-69.60	154.7	215	-73.47
10.2	44	1.88	34.3	129	49.22	66.0	200	-10.39	82.5	56	30.97	99.0	240	-10.97	130.7	255	-71.89	154.8	211	-73.10
10.3	48	14.26	34.4	133	49.60	68.0	200	-10.47	82.6	60	35.77	101.0	240	-10.86	130.8	251	-73.24	154.9	207	-72.84
10.4	52	24.18	34.5	137	49.93	68.1	199	-14.85	82.7	65	39.06	103.0	240	-10.92	130.9	247	-73.92	155.0	203	-72.54

Time (min)	T_s (°C)	DSC (mW)	Time (min)	T_s (°C)	DSC (mW)	Time (min)	T_s (°C)	DSC (mW)	Time (min)	T_s (°C)	DSC (mW)	Time (min)	T_s (°C)	DSC (mW)	Time (min)	T_s (°C)	DSC (mW)	Time (min)	T_s (°C)	DSC (mW)
10.5	56	31.17	34.6	141	50.27	68.2	195	-30.62	82.8	69	41.36	105.0	240	-10.98	131.0	243	-74.30	155.1	199	-72.30
10.6	60	35.94	34.7	145	50.49	68.3	192	-44.26	82.9	73	42.94	107.0	240	-10.65	133.0	239	-10.45	155.2	195	-72.00
10.7	65	38.95	34.8	149	50.72	68.4	188	-53.56	83.0	77	44.09	107.1	238	-15.92	135.0	240	-10.71	155.3	191	-71.68
10.8	69	40.64	34.9	153	50.98	68.5	184	-59.65	83.1	81	44.90	107.2	235	-33.22	137.0	240	-10.61	155.4	187	-71.37
10.9	73	41.92	35.0	157	51.15	68.6	180	-63.58	83.2	85	45.53	107.3	231	-47.42	139.0	240	-10.58	155.5	183	-71.02
11.0	77	43.04	37.0	160	-10.53	68.7	176	-65.99	83.3	89	46.06	107.4	227	-56.80	141.0	240	-10.62	155.6	179	-70.65
11.1	81	44.18	39.0	160	-10.13	68.8	172	-67.44	83.4	93	46.49	107.5	223	-62.68	141.1	241	-4.97	155.7	175	-70.51
11.2	85	45.23	41.0	160	-10.13	68.9	168	-68.22	83.5	97	46.85	107.6	219	-67.00	141.2	244	14.22	155.8	171	-70.11
11.3	89	46.04	43.0	160	-10.23	69.0	164	-68.59	83.6	101	47.21	107.7	215	-69.16	141.3	248	29.14	155.9	167	-69.73
11.4	93	46.63	45.0	160	-10.26	69.1	160	-68.70	83.7	105	47.50	107.8	211	-70.91	141.4	252	38.85	156.0	163	-69.26
11.5	97	47.03	45.1	159	-13.85	69.2	156	-68.56	83.8	109	47.81	107.9	207	-71.53	141.5	256	45.21	156.1	159	-68.90
11.6	101	47.33	45.2	156	-27.58	69.3	152	-68.32	83.9	113	48.08	108.0	203	-71.77	141.6	260	49.39	156.2	155	-68.51
11.7	105	47.72	45.3	152	-40.30	69.4	148	-67.95	84.0	117	48.37	110.0	200	-10.11	141.7	265	52.14	156.3	151	-68.11
11.8	109	48.00	45.4	148	-49.34	69.5	144	-67.60	84.1	121	48.66	112.0	200	-10.31	141.8	269	53.97	156.4	147	-67.72
11.9	113	48.26	45.5	144	-55.57	69.6	140	-67.08	84.2	125	48.89	114.0	200	-10.34	141.9	273	55.15	156.5	143	-67.21
12.0	117	48.46	45.6	140	-59.30	69.7	136	-66.51	84.3	129	49.16	116.0	200	-10.36	142.0	277	55.97	156.6	139	-66.65
14.0	120	-10.14	45.7	136	-61.70	69.8	132	-65.98	84.4	133	49.46	118.0	200	-10.28	142.1	281	56.52	156.7	136	-66.30
16.0	120	-9.90	45.8	132	-63.00	69.9	128	-61.30	84.5	137	49.69	118.1	201	-5.11	142.2	285	56.96	156.8	132	-65.69
18.0	120	-9.85	45.9	128	-61.06	70.0	124	-54.82	84.6	141	49.95	118.2	204	12.83	142.3	289	57.29	156.9	128	-60.87
20.0	120	-9.80	46.0	124	-54.33	70.1	120	-47.52	84.7	145	50.29	118.3	208	27.43	142.4	293	57.45	157.0	124	-54.32
22.0	120	-9.88	48.0	120	-9.45	70.2	116	-45.63	84.8	149	50.47	118.4	212	37.07	142.5	297	57.49	157.1	120	-46.92
22.1	119	-12.69	50.0	120	-9.84	70.3	113	-45.79	84.9	153	50.75	118.5	216	43.48	144.5	300	-11.60	157.2	116	-45.63
22.2	117	-23.56	52.0	120	-9.88	70.4	109	-45.95	85.0	157	50.92	118.6	220	47.75	146.5	300	-11.47	157.3	113	-45.79
22.3	113	-33.54	54.0	120	-9.89	70.5	106	-46.10	87.0	160	-10.34	118.7	224	50.50	148.5	300	-11.59	157.4	109	-45.95
22.4	110	-43.44	56.0	120	-9.83	70.6	103	-46.26	89.0	160	-10.05	118.8	229	52.47	150.5	300	-11.52	157.5	106	-46.11
22.5	106	-46.09	56.1	121	-5.92	70.7	100	-46.41	91.0	160	-10.11	118.9	233	53.67	152.5	300	-11.62	157.6	103	-46.26
22.6	103	-46.25	56.2	125	8.94	70.8	97	-46.56	93.0	160	-10.11	119.0	237	54.53	152.6	298	-17.57	157.7	100	-46.41
22.7	100	-46.40	56.3	129	22.61	70.9	94	-46.71	95.0	160	-10.05	119.1	241	54.81	152.7	295	-36.92	157.8	97	-46.56
22.8	97	-46.55	56.4	133	32.15	71.0	92	-46.86	95.1	161	-5.37	119.2	245	55.64	152.8	291	-51.69	157.9	94	-46.71
22.9	94	-46.70	56.5	137	38.57	71.1	89	-47.01	95.2	165	11.18	119.3	249	55.94	152.9	287	-60.71	158.0	92	-46.86
23.0	92	-46.78	56.6	141	42.94	71.2	87	-45.57	95.3	169	25.19	119.4	253	56.11	153.0	283	-66.92	158.1	89	-47.01
25.0	80	-8.93	56.7	145	45.91	71.3	84	-43.89	95.4	173	34.82	119.5	257	56.27	153.1	279	-70.74	158.2	87	-45.34
27.0	80	-9.64	56.8	149	47.85	71.4	82	-42.32	95.5	177	41.23	119.6	261	56.47	153.2	275	-73.02	158.3	85	-43.69
29.0	80	-9.72	56.9	153	49.26	71.5	80	-40.84	95.6	181	45.62	119.7	265	56.59	153.3	271	-74.49	158.4	82	-42.11
31.0	80	-9.69	57.0	157	50.28	71.6	78	-39.41	95.7	185	48.50	119.8	269	56.67	153.4	267	-75.36	158.5	80	-40.64

Time (min)	T_s (°C)	DSC (mW)	Time (min)	T_s (°C)	DSC (mW)	Time (min)	T_s (°C)	DSC (mW)	Time (min)	T_s (°C)	DSC (mW)	Time (min)	T_s (°C)	DSC (mW)	Time (min)	T_s (°C)	DSC (mW)	Time (min)	T_s (°C)	DSC (mW)
33.0	80	-9.66	57.1	161	50.96	71.7	76	-38.12	95.8	189	50.48	119.9	273	56.82	153.5	263	-75.48	158.6	78	-39.22
33.1	81	-6.55	57.2	165	51.42	71.8	75	-36.94	95.9	193	51.82	120.0	277	56.88	153.6	259	-75.87	158.7	77	-37.90
33.2	85	6.11	57.3	169	51.88	71.9	73	-35.46	96.0	197	52.74	122.0	280	-11.44	153.7	255	-75.76	158.8	75	-36.67
33.3	89	19.25	57.4	173	52.29	72.0	71	-34.38	96.1	201	53.37	124.0	280	-11.29	153.8	251	-75.80	158.9	73	-35.48
33.4	93	28.66	57.5	177	52.61	74.0	50	-19.46	96.2	205	53.89	126.0	280	-11.35	153.9	247	-75.53			
33.5	97	35.22	57.6	181	52.77	76.0	41	-13.78	96.3	209	54.27	128.0	280	-11.29	154.0	243	-75.42			

Table 3.6. Reduced Dataset of DSC Signal as a Function of Time and Temperature for the First Segment K Sample Run

Time (min)	T_s (°C)	DSC (mW)	Time (min)	T_s (°C)	DSC (mW)	Time (min)	T_s (°C)	DSC (mW)	Time (min)	T_s (°C)	DSC (mW)	Time (min)	T_s (°C)	DSC (mW)	Time (min)	T_s (°C)	DSC (mW)	Time (min)	T_s (°C)	DSC (mW)
0.0	41	-0.05	33.7	105	23.06	57.9	193	21.95	82.1	41	-1.51	96.8	229	21.77	130.5	263	-31.73	154.7	215	-30.20
2.0	41	-3.14	33.8	109	23.25	58.0	197	21.75	82.2	44	5.26	96.9	233	21.48	130.6	259	-31.87	154.8	211	-30.17
4.0	41	-3.14	33.9	113	23.30	60.0	200	-4.95	82.3	48	12.62	97.0	237	21.23	130.7	255	-31.84	154.9	207	-29.96
6.0	41	-3.14	34.0	117	23.28	62.0	200	-4.80	82.4	52	17.40	99.0	240	-5.51	130.8	251	-31.72	155.0	203	-29.85
8.0	41	-3.13	34.1	121	23.34	64.0	200	-4.68	82.5	56	20.04	101.0	240	-5.48	130.9	247	-31.66	155.1	199	-29.72
10.0	41	-3.07	34.2	125	23.33	66.0	200	-4.63	82.6	61	21.46	103.0	240	-5.54	131.0	243	-31.40	155.2	195	-29.54
10.1	41	-0.78	34.3	129	23.30	68.0	200	-4.72	82.7	65	22.09	105.0	240	-5.40	133.0	239	-4.98	155.3	191	-29.45
10.2	44	6.63	34.4	133	23.26	68.1	199	-8.18	82.8	69	22.28	107.0	240	-5.53	135.0	240	-4.97	155.4	187	-29.35
10.3	48	13.72	34.5	137	23.26	68.2	195	-18.21	82.9	73	22.47	107.1	238	-9.44	137.0	240	-5.19	155.5	183	-29.17
10.4	52	18.20	34.6	141	23.26	68.3	192	-24.47	83.0	77	22.47	107.2	235	-20.31	139.0	240	-5.06	155.6	179	-29.06
10.5	56	20.71	34.7	145	23.17	68.4	188	-27.45	83.1	81	22.39	107.3	231	-26.50	141.0	240	-4.98	155.7	175	-28.90
10.6	60	22.00	34.8	149	23.23	68.5	184	-28.68	83.2	85	22.39	107.4	227	-29.15	141.1	241	-0.61	155.8	171	-28.81
10.7	65	22.69	34.9	153	23.23	68.6	179	-29.18	83.3	89	22.33	107.5	223	-30.21	141.2	244	11.51	155.9	167	-28.67
10.8	69	22.95	35.0	157	23.19	68.7	175	-29.24	83.4	93	22.31	107.6	219	-30.52	141.3	248	17.79	156.0	163	-28.47
10.9	73	23.08	37.0	160	-4.19	68.8	171	-29.28	83.5	97	22.28	107.7	215	-30.60	141.4	252	20.30	156.1	159	-28.35
11.0	77	23.12	39.0	160	-4.13	68.9	167	-29.10	83.6	101	22.24	107.8	211	-30.54	141.5	256	21.35	156.2	155	-28.17
11.1	81	23.14	41.0	160	-4.05	69.0	163	-28.94	83.7	105	22.22	107.9	207	-30.41	141.6	261	21.67	156.3	151	-28.08
11.2	85	23.12	43.0	160	-4.07	69.1	159	-28.73	83.8	109	22.22	108.0	203	-30.10	141.7	265	21.90	156.4	147	-27.89
11.3	89	23.13	45.0	160	-4.12	69.2	155	-28.52	83.9	113	22.19	110.0	200	-4.42	141.8	269	21.95	156.5	143	-27.77
11.4	93	23.12	45.1	159	-7.04	69.3	151	-28.36	84.0	117	22.13	112.0	200	-4.45	141.9	273	21.89	156.6	139	-27.51
11.5	97	23.15	45.2	156	-16.06	69.4	147	-28.16	84.1	121	22.16	114.0	200	-4.45	142.0	277	21.92	156.7	135	-27.35
11.6	101	23.16	45.3	152	-22.24	69.5	143	-28.08	84.2	125	22.13	116.0	200	-4.47	142.1	281	21.92	156.8	132	-27.14
11.7	105	23.16	45.4	148	-25.47	69.6	140	-27.76	84.3	129	22.17	118.0	200	-4.39	142.2	285	21.91	156.9	128	-27.00

Time (min)	T_s (^oC)	DSC (mW)	Time (min)	T_s (^oC)	DSC (mW)	Time (min)	T_s (^oC)	DSC (mW)	Time (min)	T_s (^oC)	DSC (mW)	Time (min)	T_s (^oC)	DSC (mW)	Time (min)	T_s (^oC)	DSC (mW)	Time (min)	T_s (^oC)	DSC (mW)
11.8	109	23.11	45.5	144	-26.98	69.7	136	-27.55	84.4	133	22.07	118.1	201	-0.25	142.3	289	22.03	157.0	124	-27.36
11.9	113	23.10	45.6	140	-27.56	69.8	132	-27.37	84.5	137	22.08	118.2	204	11.11	142.4	293	22.04	157.1	120	-26.35
12.0	117	23.06	45.7	136	-27.75	69.9	128	-27.12	84.6	141	22.10	118.3	208	17.51	142.5	297	21.87	157.2	116	-25.81
14.0	120	-3.06	45.8	132	-27.68	70.0	124	-27.28	84.7	145	22.05	118.4	212	20.36	144.5	300	-6.74	157.3	112	-26.49
16.0	120	-2.94	45.9	128	-27.48	70.1	120	-26.56	84.8	149	22.04	118.5	216	21.47	146.5	300	-6.62	157.4	109	-25.75
18.0	120	-2.89	46.0	124	-27.67	70.2	116	-25.91	84.9	153	22.13	118.6	221	21.92	148.5	300	-6.48	157.5	105	-24.80
20.0	120	-2.97	48.0	120	-3.34	70.3	112	-26.68	85.0	157	22.00	118.7	225	21.98	150.5	300	-6.47	157.6	102	-23.78
22.0	120	-3.02	50.0	120	-3.49	70.4	109	-25.96	87.0	160	-4.08	118.8	229	22.14	152.5	300	-6.55	157.7	99	-22.82
22.1	119	-5.86	52.0	120	-3.48	70.5	105	-24.99	89.0	160	-4.12	118.9	233	22.15	152.6	298	-11.37	157.8	96	-21.87
22.2	117	-13.41	54.0	120	-3.48	70.6	102	-24.00	91.0	160	-3.97	119.0	237	21.73	152.7	295	-23.14	157.9	93	-20.98
22.3	113	-18.35	56.0	120	-3.43	70.7	99	-22.99	93.0	160	-4.02	119.1	241	21.79	152.8	291	-29.17	158.0	90	-20.15
22.4	110	-22.54	56.1	121	-0.27	70.8	96	-22.04	95.0	160	-3.90	119.2	245	21.92	152.9	287	-31.35	158.1	88	-19.37
22.5	106	-23.52	56.2	125	9.60	70.9	93	-21.17	95.1	161	-0.26	119.3	249	22.06	153.0	283	-32.22	158.2	86	-18.62
22.6	103	-23.37	56.3	129	16.49	71.0	90	-20.32	95.2	165	10.43	119.4	253	21.98	153.1	279	-32.61	158.3	83	-17.95
22.7	100	-22.74	56.4	133	19.74	71.1	88	-19.53	95.3	169	17.10	119.5	257	21.87	153.2	275	-32.52	158.4	81	-17.30
22.8	97	-21.95	56.5	137	21.32	71.2	85	-18.81	95.4	173	20.13	119.6	261	21.89	153.3	271	-32.34	158.5	79	-16.69
22.9	94	-21.12	56.6	141	21.99	71.3	83	-18.09	95.5	177	21.47	119.7	265	21.82	153.4	267	-32.29	158.6	77	-16.14
23.0	91	-20.25	56.7	145	22.35	71.4	81	-17.44	95.6	181	22.10	119.8	269	21.64	153.5	263	-32.06	158.7	75	-15.60
25.0	80	-2.54	56.8	149	22.36	71.5	79	-16.83	95.7	185	22.33	119.9	273	21.54	153.6	259	-31.93	158.8	73	-15.11
27.0	80	-2.86	56.9	153	22.37	71.6	77	-16.25	95.8	189	22.32	120.0	277	21.36	153.7	255	-31.73	158.9	72	-14.65
29.0	80	-2.89	57.0	157	22.23	71.7	75	-15.69	95.9	193	22.32	122.0	280	-6.68	153.8	251	-31.65			
31.0	80	-2.90	57.1	161	22.34	71.8	73	-15.22	96.0	197	22.29	124.0	280	-6.34	153.9	247	-31.49			
33.0	80	-2.82	57.2	165	22.32	71.9	71	-14.73	96.1	201	22.29	126.0	280	-6.24	154.0	243	-31.45			
33.1	81	0.44	57.3	169	22.25	72.0	70	-14.24	96.2	205	22.23	128.0	280	-6.14	154.1	239	-31.21			
33.2	85	9.63	57.4	173	22.21	74.0	49	-7.45	96.3	209	22.15	130.0	280	-6.20	154.2	235	-30.95			
33.3	89	16.31	57.5	177	22.18	76.0	41	-4.95	96.4	213	22.10	130.1	278	-10.51	154.3	231	-30.84			
33.4	93	19.96	57.6	181	22.15	78.0	41	-3.23	96.5	217	22.09	130.2	275	-22.17	154.4	227	-30.70			
33.5	97	21.77	57.7	185	22.11	80.0	41	-3.26	96.6	221	21.92	130.3	271	-28.21	154.5	223	-30.63			
33.6	101	22.64	57.8	189	21.96	82.0	41	-3.18	96.7	225	21.88	130.4	267	-30.71	154.6	219	-30.46			

Table 3.7. Reduced Dataset of DSC Signal as a Function of Time and Temperature for the Second Segment K Sample Run

Time (min)	T_s (^oC)	DSC (mW)	Time (min)	T_s (^oC)	DSC (mW)	Time (min)	T_s (^oC)	DSC (mW)	Time (min)	T_s (^oC)	DSC (mW)	Time (min)	T_s (^oC)	DSC (mW)	Time (min)	T_s (^oC)	DSC (mW)	Time (min)	T_s (^oC)	DSC (mW)
159.0	70	-14.13	192.7	105	22.18	216.9	193	22.02	241.1	41	-1.53	255.8	229	21.87	289.5	263	-31.48	313.7	215	-30.33
161.0	49	-7.45	192.8	109	22.33	217.0	197	21.97	241.2	44	5.26	255.9	233	21.84	289.6	259	-31.75	313.8	211	-30.10
163.0	41	-4.90	192.9	113	22.37	219.0	200	-4.67	241.3	48	12.63	256.0	237	21.57	289.7	255	-31.66	313.9	207	-29.98
165.0	41	-3.19	193.0	117	22.38	221.0	200	-4.62	241.4	52	17.36	258.0	240	-5.21	289.8	251	-31.54	314.0	203	-29.82
167.0	41	-3.26	193.1	121	22.40	223.0	200	-4.63	241.5	56	19.94	260.0	240	-5.28	289.9	247	-31.48	314.1	199	-29.73
169.0	41	-3.19	193.2	125	22.35	225.0	200	-4.66	241.6	61	21.38	262.0	240	-5.23	290.0	243	-31.28	314.2	195	-29.58
169.1	41	-1.53	193.3	129	22.34	227.0	200	-4.70	241.7	65	22.08	264.0	240	-5.31	292.0	239	-5.12	314.3	191	-29.45
169.2	44	5.22	193.4	133	22.28	227.1	199	-8.19	241.8	69	22.32	266.0	240	-5.23	294.0	240	-5.12	314.4	187	-29.31
169.3	48	12.66	193.5	137	22.16	227.2	195	-18.25	241.9	73	22.44	266.1	238	-9.35	296.0	240	-5.10	314.5	183	-29.17
169.4	52	17.39	193.6	141	22.25	227.3	192	-24.44	242.0	77	22.40	266.2	235	-20.18	298.0	240	-5.14	314.6	179	-29.07
169.5	56	19.96	193.7	145	22.25	227.4	188	-27.39	242.1	81	22.36	266.3	231	-26.45	300.0	240	-5.01	314.7	175	-28.94
169.6	61	21.36	193.8	149	22.13	227.5	184	-28.60	242.2	85	22.33	266.4	227	-29.08	300.1	241	-0.14	314.8	171	-28.83
169.7	65	21.98	193.9	153	21.92	227.6	179	-29.13	242.3	89	22.27	266.5	223	-30.08	300.2	244	11.49	314.9	167	-28.64
169.8	69	22.23	194.0	157	21.98	227.7	175	-29.17	242.4	93	22.25	266.6	219	-30.40	300.3	248	17.72	315.0	163	-28.47
169.9	73	22.40	196.0	160	-4.13	227.8	171	-29.12	242.5	97	22.19	266.7	215	-30.49	300.4	252	20.26	315.1	159	-28.33
170.0	77	22.39	198.0	160	-4.08	227.9	167	-29.00	242.6	101	22.20	266.8	211	-30.37	300.5	256	21.25	315.2	155	-28.22
170.1	81	22.35	200.0	160	-4.03	228.0	163	-28.83	242.7	105	22.17	266.9	207	-30.25	300.6	261	21.63	315.3	151	-28.04
170.2	85	22.35	202.0	160	-4.02	228.1	159	-28.64	242.8	109	22.17	267.0	203	-30.02	300.7	265	21.76	315.4	147	-27.90
170.3	89	22.30	204.0	160	-4.09	228.2	155	-28.42	242.9	113	22.13	269.0	200	-4.42	300.8	269	21.77	315.5	143	-27.70
170.4	93	22.24	204.1	159	-7.06	228.3	151	-28.28	243.0	117	22.16	271.0	200	-4.45	300.9	273	21.75	315.6	139	-27.58
170.5	97	22.22	204.2	156	-15.89	228.4	147	-28.12	243.1	121	22.07	273.0	200	-4.46	301.0	277	21.75	315.7	135	-27.37
170.6	101	22.21	204.3	152	-22.13	228.5	143	-27.88	243.2	125	22.10	275.0	200	-4.53	301.1	281	21.78	315.8	132	-27.13
170.7	105	22.18	204.4	148	-25.30	228.6	140	-27.70	243.3	129	22.06	277.0	200	-4.42	301.2	285	21.86	315.9	128	-27.01
170.8	109	22.17	204.5	144	-26.86	228.7	136	-27.49	243.4	133	22.07	277.1	201	-0.22	301.3	289	21.84	316.0	124	-27.44
170.9	113	22.15	204.6	140	-27.42	228.8	132	-27.30	243.5	137	22.03	277.2	204	11.21	301.4	293	21.83	316.1	120	-26.32
171.0	117	22.10	204.7	136	-27.60	228.9	128	-27.10	243.6	141	22.10	277.3	208	17.56	301.5	297	21.80	316.2	116	-25.86
173.0	120	-3.68	204.8	132	-27.66	229.0	124	-27.29	243.7	145	22.06	277.4	212	20.29	303.5	300	-6.43	316.3	112	-26.47
175.0	120	-3.55	204.9	128	-27.43	229.1	120	-26.48	243.8	149	22.01	277.5	217	21.38	305.5	300	-6.43	316.4	109	-25.73
177.0	120	-3.55	205.0	124	-27.70	229.2	116	-25.86	243.9	153	21.96	277.6	221	21.86	307.5	300	-6.42	316.5	105	-24.78
179.0	120	-3.55	207.0	120	-3.27	229.3	112	-26.63	244.0	157	21.86	277.7	225	21.94	309.5	300	-6.38	316.6	102	-23.77
181.0	120	-3.62	209.0	120	-3.47	229.4	109	-25.89	246.0	160	-4.10	277.8	229	22.05	311.5	300	-6.46	316.7	99	-22.79
181.1	119	-5.89	211.0	120	-3.52	229.5	105	-24.94	248.0	160	-3.99	277.9	233	21.97	311.6	298	-11.31	316.8	96	-21.86
181.2	117	-13.02	213.0	120	-3.48	229.6	102	-23.94	250.0	160	-4.17	278.0	237	21.83	311.7	295	-23.11	316.9	93	-20.95
181.3	113	-18.26	215.0	120	-3.43	229.7	99	-22.94	252.0	160	-4.08	278.1	241	21.87	311.8	291	-29.06	317.0	91	-20.14

Time (min)	T_s (°C)	DSC (mW)	Time (min)	T_s (°C)	DSC (mW)	Time (min)	T_s (°C)	DSC (mW)	Time (min)	T_s (°C)	DSC (mW)	Time (min)	T_s (°C)	DSC (mW)	Time (min)	T_s (°C)	DSC (mW)	Time (min)	T_s (°C)	DSC (mW)
181.4	110	-22.49	215.1	121	-0.27	229.8	96	-22.01	254.0	160	-3.96	278.2	245	21.85	311.9	287	-30.97	317.1	88	-19.35
181.5	106	-23.66	215.2	125	9.59	229.9	93	-21.11	254.1	161	-0.36	278.3	249	21.92	312.0	283	-31.81	317.2	86	-18.61
181.6	103	-23.58	215.3	129	16.45	230.0	90	-20.27	254.2	165	10.54	278.4	253	21.83	312.1	279	-32.43	317.3	83	-17.92
181.7	100	-23.02	215.4	133	19.81	230.1	88	-19.49	254.3	169	17.07	278.5	257	21.76	312.2	275	-32.32	317.4	81	-17.29
181.8	97	-22.15	215.5	137	21.28	230.2	85	-18.73	254.4	173	20.12	278.6	261	21.79	312.3	271	-32.26	317.5	79	-16.67
181.9	94	-21.29	215.6	141	21.95	230.3	83	-18.05	254.5	177	21.50	278.7	265	21.79	312.4	267	-32.08	317.6	77	-16.12
182.0	91	-20.44	215.7	145	22.23	230.4	81	-17.40	254.6	181	22.01	278.8	269	21.73	312.5	263	-31.96	317.7	75	-15.59
184.0	80	-2.91	215.8	149	22.32	230.5	79	-16.79	254.7	185	22.11	278.9	273	21.72	312.6	259	-31.85	317.8	73	-15.09
186.0	80	-3.21	215.9	153	22.42	230.6	77	-16.22	254.8	189	22.21	279.0	277	21.65	312.7	255	-31.73	317.9	72	-14.64
188.0	80	-3.24	216.0	157	22.20	230.7	75	-15.67	254.9	193	22.17	281.0	280	-5.97	312.8	251	-31.59			
190.0	80	-3.23	216.1	161	22.26	230.8	73	-15.18	255.0	197	22.18	283.0	280	-6.06	312.9	247	-31.40			
192.0	80	-3.16	216.2	165	22.30	230.9	71	-14.71	255.1	201	22.20	285.0	280	-5.96	313.0	243	-31.23			
192.1	81	-0.63	216.3	169	22.23	231.0	70	-14.20	255.2	205	22.12	287.0	280	-5.98	313.1	239	-31.12			
192.2	85	8.12	216.4	173	22.33	233.0	49	-7.47	255.3	209	22.06	289.0	280	-6.02	313.2	235	-30.98			
192.3	89	15.17	216.5	177	22.16	235.0	41	-4.94	255.4	213	22.04	289.1	278	-9.64	313.3	231	-30.89			
192.4	93	19.04	216.6	181	22.09	237.0	41	-3.22	255.5	217	21.95	289.2	275	-22.08	313.4	227	-30.68			
192.5	97	20.89	216.7	185	22.06	239.0	41	-3.27	255.6	221	21.98	289.3	271	-28.13	313.5	223	-30.57			
192.6	101	21.79	216.8	189	22.03	241.0	41	-3.20	255.7	225	21.81	289.4	267	-30.61	313.6	219	-30.37			

Table 3.8. Reduced Dataset of DSC Signal as a Function of Time and Temperature for the Third Segment K Sample Run

Time (min)	T_s (°C)	DSC (mW)	Time (min)	T_s (°C)	DSC (mW)	Time (min)	T_s (°C)	DSC (mW)	Time (min)	T_s (°C)	DSC (mW)	Time (min)	T_s (°C)	DSC (mW)	Time (min)	T_s (°C)	DSC (mW)	Time (min)	T_s (°C)	DSC (mW)
318.0	70	-14.13	351.7	105	22.16	375.9	193	21.97	400.1	41	-1.54	414.8	229	21.75	448.5	263	-31.44	472.7	215	-30.23
320.0	49	-7.44	351.8	109	22.33	376.0	197	21.98	400.2	44	5.27	414.9	233	21.84	448.6	259	-31.66	472.8	211	-30.09
322.0	41	-4.91	351.9	113	22.35	378.0	200	-4.67	400.3	48	12.71	415.0	237	21.67	448.7	255	-31.72	472.9	207	-29.94
324.0	41	-3.20	352.0	117	22.37	380.0	200	-4.62	400.4	52	17.42	417.0	240	-5.38	448.8	251	-31.58	473.0	203	-29.82
326.0	41	-3.26	352.1	121	22.34	382.0	200	-4.60	400.5	56	20.07	419.0	240	-5.20	448.9	247	-31.45	473.1	199	-29.71
328.0	41	-3.20	352.2	125	22.33	384.0	200	-4.58	400.6	61	21.33	421.0	240	-5.30	449.0	243	-31.13	473.2	195	-29.56
328.1	41	-1.56	352.3	129	22.33	386.0	200	-4.71	400.7	65	22.03	423.0	240	-5.20	451.0	239	-5.00	473.3	191	-29.43
328.2	44	5.24	352.4	133	22.27	386.1	199	-8.20	400.8	69	22.32	425.0	240	-5.34	453.0	240	-5.13	473.4	187	-29.32
328.3	48	12.62	352.5	137	22.21	386.2	195	-18.24	400.9	73	22.38	425.1	238	-9.39	455.0	240	-5.13	473.5	183	-29.13
328.4	52	17.40	352.6	141	22.31	386.3	192	-24.49	401.0	77	22.43	425.2	235	-20.25	457.0	240	-5.04	473.6	179	-29.05
328.5	56	19.99	352.7	145	22.41	386.4	188	-27.46	401.1	81	22.35	425.3	231	-26.37	459.0	240	-5.03	473.7	175	-28.87

Time (min)	T_s (°C)	DSC (mW)	Time (min)	T_s (°C)	DSC (mW)	Time (min)	T_s (°C)	DSC (mW)	Time (min)	T_s (°C)	DSC (mW)	Time (min)	T_s (°C)	DSC (mW)	Time (min)	T_s (°C)	DSC (mW)	Time (min)	T_s (°C)	DSC (mW)
328.6	61	21.35	352.8	149	21.94	386.5	183	-28.69	401.2	85	22.31	425.4	227	-29.14	459.1	241	-0.39	473.8	171	-28.79
328.7	65	22.04	352.9	153	22.48	386.6	179	-29.09	401.3	89	22.26	425.5	223	-30.09	459.2	244	11.56	473.9	167	-28.65
328.8	69	22.33	353.0	157	21.90	386.7	175	-29.15	401.4	93	22.23	425.6	219	-30.41	459.3	248	17.60	474.0	163	-28.44
328.9	73	22.40	355.0	160	-4.06	386.8	171	-29.10	401.5	97	22.21	425.7	215	-30.37	459.4	252	20.20	474.1	159	-28.36
329.0	77	22.38	357.0	160	-3.98	386.9	167	-29.02	401.6	101	22.16	425.8	211	-30.40	459.5	257	21.23	474.2	155	-28.21
329.1	81	22.34	359.0	160	-3.97	387.0	163	-28.84	401.7	105	22.17	425.9	207	-30.23	459.6	261	21.59	474.3	151	-28.06
329.2	85	22.31	361.0	160	-4.02	387.1	159	-28.63	401.8	109	22.15	426.0	203	-29.98	459.7	265	21.76	474.4	147	-27.94
329.3	89	22.29	363.0	160	-4.08	387.2	155	-28.50	401.9	113	22.12	428.0	200	-4.39	459.8	269	21.75	474.5	143	-27.72
329.4	93	22.22	363.1	159	-7.02	387.3	151	-28.30	402.0	117	22.12	430.0	200	-4.47	459.9	273	21.73	474.6	139	-27.57
329.5	97	22.21	363.2	156	-15.93	387.4	147	-28.13	402.1	121	22.09	432.0	200	-4.48	460.0	277	21.67	474.7	135	-27.39
329.6	101	22.22	363.3	152	-22.15	387.5	143	-27.93	402.2	125	22.05	434.0	200	-4.43	460.1	281	21.71	474.8	132	-27.20
329.7	105	22.15	363.4	148	-25.36	387.6	140	-27.74	402.3	129	22.06	436.0	200	-4.40	460.2	285	21.74	474.9	128	-27.01
329.8	109	22.13	363.5	144	-26.89	387.7	136	-27.51	402.4	133	21.91	436.1	201	-0.16	460.3	289	21.71	475.0	124	-27.58
329.9	113	22.15	363.6	140	-27.47	387.8	132	-27.27	402.5	137	21.92	436.2	204	11.19	460.4	293	21.65	475.1	120	-26.32
330.0	117	22.05	363.7	136	-27.63	387.9	128	-27.13	402.6	141	21.94	436.3	208	17.58	460.5	297	21.54	475.2	116	-25.94
332.0	120	-3.60	363.8	132	-27.61	388.0	124	-27.40	402.7	145	22.00	436.4	212	20.33	462.5	300	-6.37	475.3	112	-26.48
334.0	120	-3.56	363.9	128	-27.46	388.1	120	-26.47	402.8	149	21.92	436.5	217	21.37	464.5	300	-6.40	475.4	109	-25.72
336.0	120	-3.56	364.0	124	-27.81	388.2	116	-25.85	402.9	153	21.98	436.6	221	21.81	466.5	300	-6.38	475.5	105	-24.74
338.0	120	-3.51	366.0	120	-3.35	388.3	112	-26.61	403.0	157	21.93	436.7	225	21.97	468.5	300	-6.35	475.6	102	-23.75
340.0	120	-3.54	368.0	120	-3.49	388.4	109	-25.87	405.0	160	-4.13	436.8	229	21.96	470.5	300	-6.33	475.7	99	-22.77
340.1	119	-5.84	370.0	120	-3.48	388.5	105	-24.91	407.0	160	-4.06	436.9	233	21.83	470.6	298	-11.34	475.8	96	-21.82
340.2	117	-13.16	372.0	120	-3.51	388.6	102	-23.91	409.0	160	-4.06	437.0	237	21.89	470.7	295	-23.12	475.9	93	-20.94
340.3	113	-18.26	374.0	120	-3.41	388.7	99	-22.92	411.0	160	-4.05	437.1	241	21.69	470.8	291	-28.78	476.0	91	-20.13
340.4	110	-22.57	374.1	121	-0.25	388.8	96	-21.98	413.0	160	-3.97	437.2	245	21.68	470.9	287	-31.10	476.1	88	-19.33
340.5	106	-23.66	374.2	125	9.57	388.9	93	-21.09	413.1	161	-0.18	437.3	249	21.75	471.0	283	-32.15	476.2	86	-18.62
340.6	103	-23.55	374.3	129	16.39	389.0	90	-20.25	413.2	165	10.59	437.4	253	21.77	471.1	279	-32.30	476.3	83	-17.91
340.7	100	-22.92	374.4	133	19.76	389.1	88	-19.48	413.3	169	17.07	437.5	257	21.69	471.2	275	-32.28	476.4	81	-17.28
340.8	97	-22.14	374.5	137	21.39	389.2	85	-18.72	413.4	173	20.15	437.6	261	21.76	471.3	271	-32.15	476.5	79	-16.67
340.9	94	-21.32	374.6	141	21.89	389.3	83	-18.04	413.5	177	21.45	437.7	265	21.69	471.4	267	-32.09	476.6	77	-16.09
341.0	91	-20.42	374.7	145	22.22	389.4	81	-17.38	413.6	181	21.97	437.8	269	21.65	471.5	263	-32.01	476.7	75	-15.58
343.0	80	-2.93	374.8	149	22.29	389.5	79	-16.78	413.7	185	22.13	437.9	273	21.65	471.6	259	-31.74	476.8	73	-15.08
345.0	80	-3.21	374.9	153	22.39	389.6	77	-16.20	413.8	189	22.20	438.0	277	21.56	471.7	255	-31.61	476.9	72	-14.61
347.0	80	-3.32	375.0	157	22.29	389.7	75	-15.66	413.9	193	22.21	440.0	280	-6.00	471.8	251	-31.45			
349.0	80	-3.37	375.1	161	22.29	389.8	73	-15.18	414.0	197	22.17	442.0	280	-5.99	471.9	247	-31.30			
351.0	80	-3.17	375.2	165	22.27	389.9	71	-14.70	414.1	201	22.17	444.0	280	-6.04	472.0	243	-31.24			

Time (min)	T_s (°C)	DSC (mW)	Time (min)	T_s (°C)	DSC (mW)	Time (min)	T_s (°C)	DSC (mW)	Time (min)	T_s (°C)	DSC (mW)	Time (min)	T_s (°C)	DSC (mW)	Time (min)	T_s (°C)	DSC (mW)	Time (min)	T_s (°C)	DSC (mW)
351.1	81	-0.59	375.3	169	22.24	390.0	70	-14.19	414.2	205	22.13	446.0	280	-5.97	472.1	239	-31.06			
351.2	85	8.15	375.4	173	22.18	392.0	49	-7.45	414.3	209	22.06	448.0	280	-6.04	472.2	235	-30.90			
351.3	89	15.22	375.5	177	22.10	394.0	41	-4.93	414.4	213	22.02	448.1	278	-9.78	472.3	231	-30.73			
351.4	93	19.04	375.6	181	22.02	396.0	41	-3.22	414.5	217	22.01	448.2	275	-22.09	472.4	227	-30.63			
351.5	97	20.89	375.7	185	22.09	398.0	41	-3.27	414.6	221	21.96	448.3	271	-28.11	472.5	223	-30.45			
351.6	101	21.77	375.8	189	22.05	400.0	41	-3.21	414.7	225	21.85	448.4	267	-30.62	472.6	219	-30.36			

Table 3.9. Reduced Dataset of DSC Signal as a Function of Time and Temperature for the Fourth Segment K Sample Run

Time (min)	T_s (°C)	DSC (mW)	Time (min)	T_s (°C)	DSC (mW)	Time (min)	T_s (°C)	DSC (mW)	Time (min)	T_s (°C)	DSC (mW)	Time (min)	T_s (°C)	DSC (mW)	Time (min)	T_s (°C)	DSC (mW)	Time (min)	T_s (°C)	DSC (mW)
477.0	70	-14.12	510.7	105	22.14	534.9	193	21.97	559.1	41	-1.48	573.8	229	21.81	607.5	263	-31.48	631.7	215	-30.20
479.0	50	-7.44	510.8	109	22.32	535.0	197	21.87	559.2	44	5.37	573.9	233	21.90	607.6	259	-31.70	631.8	211	-30.11
481.0	41	-4.91	510.9	113	22.34	537.0	200	-4.68	559.3	48	12.82	574.0	237	21.54	607.7	255	-31.68	631.9	207	-29.95
483.0	41	-3.23	511.0	117	22.36	539.0	200	-4.63	559.4	52	17.54	576.0	240	-5.31	607.8	251	-31.60	632.0	203	-29.76
485.0	41	-3.27	511.1	121	22.29	541.0	200	-4.60	559.5	56	20.10	578.0	240	-5.41	607.9	247	-31.48	632.1	199	-29.66
487.0	41	-3.20	511.2	125	22.29	543.0	200	-4.59	559.6	61	21.42	580.0	240	-5.24	608.0	243	-31.23	632.2	195	-29.50
487.1	41	-1.51	511.3	129	22.20	545.0	200	-4.64	559.7	65	22.05	582.0	240	-5.29	610.0	239	-5.04	632.3	191	-29.39
487.2	44	5.30	511.4	133	22.13	545.1	199	-8.22	559.8	69	22.34	584.0	240	-5.26	612.0	240	-5.09	632.4	187	-29.33
487.3	48	12.77	511.5	137	22.13	545.2	195	-18.31	559.9	73	22.40	584.1	238	-9.48	614.0	240	-5.12	632.5	183	-29.20
487.4	52	17.53	511.6	141	22.13	545.3	192	-24.54	560.0	77	22.39	584.2	235	-20.48	616.0	240	-5.06	632.6	179	-29.03
487.5	56	20.09	511.7	145	22.08	545.4	188	-27.42	560.1	81	22.39	584.3	231	-26.41	618.0	240	-4.98	632.7	175	-28.93
487.6	61	21.43	511.8	149	22.10	545.5	183	-28.66	560.2	85	22.33	584.4	227	-29.10	618.1	241	-0.29	632.8	171	-28.68
487.7	65	22.08	511.9	153	22.05	545.6	179	-29.08	560.3	89	22.29	584.5	223	-30.14	618.2	244	11.59	632.9	167	-28.62
487.8	69	22.31	512.0	157	21.95	545.7	175	-29.19	560.4	93	22.23	584.6	219	-30.38	618.3	248	17.80	633.0	163	-28.53
487.9	73	22.43	514.0	160	-4.13	545.8	171	-29.17	560.5	97	22.21	584.7	215	-30.46	618.4	252	20.29	633.1	159	-28.27
488.0	77	22.39	516.0	160	-4.00	545.9	167	-29.06	560.6	101	22.18	584.8	211	-30.38	618.5	257	21.30	633.2	155	-28.24
488.1	81	22.38	518.0	160	-4.00	546.0	163	-28.89	560.7	105	22.18	584.9	207	-30.26	618.6	261	21.61	633.3	151	-28.09
488.2	85	22.33	520.0	160	-4.01	546.1	159	-28.67	560.8	109	22.15	585.0	203	-30.05	618.7	265	21.69	633.4	147	-27.82
488.3	89	22.30	522.0	160	-3.94	546.2	155	-28.46	560.9	113	22.13	587.0	200	-4.43	618.8	269	21.73	633.5	143	-27.77
488.4	93	22.23	522.1	159	-7.02	546.3	151	-28.30	561.0	117	22.10	589.0	200	-4.50	618.9	273	21.72	633.6	139	-27.55
488.5	97	22.21	522.2	156	-16.11	546.4	147	-28.14	561.1	121	22.08	591.0	200	-4.48	619.0	277	21.69	633.7	135	-27.38
488.6	101	22.17	522.3	152	-22.23	546.5	143	-27.88	561.2	125	22.07	593.0	200	-4.47	619.1	281	21.68	633.8	132	-27.15
488.7	105	22.17	522.4	148	-25.38	546.6	140	-27.71	561.3	129	22.08	595.0	200	-4.45	619.2	285	21.74	633.9	128	-26.99

Time (min)	T_s (°C)	DSC (mW)	Time (min)	T_s (°C)	DSC (mW)	Time (min)	T_s (°C)	DSC (mW)	Time (min)	T_s (°C)	DSC (mW)	Time (min)	T_s (°C)	DSC (mW)	Time (min)	T_s (°C)	DSC (mW)	Time (min)	T_s (°C)	DSC (mW)
488.8	109	22.12	522.5	144	-26.80	546.7	136	-27.53	561.4	133	21.97	595.1	201	-0.17	619.3	289	21.67	634.0	124	-27.46
488.9	113	22.11	522.6	140	-27.50	546.8	132	-27.30	561.5	137	22.02	595.2	204	11.26	619.4	293	21.64	634.1	120	-26.32
489.0	117	22.02	522.7	136	-27.66	546.9	128	-27.12	561.6	141	22.01	595.3	208	17.64	619.5	297	21.57	634.2	116	-25.91
491.0	120	-3.65	522.8	132	-27.59	547.0	124	-27.38	561.7	145	21.92	595.4	212	20.31	621.5	300	-6.38	634.3	112	-26.49
493.0	120	-3.53	522.9	128	-27.44	547.1	120	-26.48	561.8	149	21.87	595.5	217	21.39	623.5	300	-6.33	634.4	109	-25.73
495.0	120	-3.57	523.0	124	-27.82	547.2	116	-25.88	561.9	153	21.93	595.6	221	21.80	625.5	300	-6.30	634.5	105	-24.76
497.0	120	-3.56	525.0	120	-3.38	547.3	112	-26.61	562.0	157	21.89	595.7	225	21.98	627.5	300	-6.33	634.6	102	-23.75
499.0	120	-3.64	527.0	120	-3.50	547.4	109	-25.88	564.0	160	-4.16	595.8	229	21.87	629.5	300	-6.38	634.7	99	-22.77
499.1	119	-5.90	529.0	120	-3.51	547.5	105	-24.93	566.0	160	-4.04	595.9	233	21.91	629.6	298	-11.36	634.8	96	-21.83
499.2	117	-13.24	531.0	120	-3.44	547.6	102	-23.91	568.0	160	-4.08	596.0	237	21.90	629.7	295	-23.15	634.9	93	-20.94
499.3	113	-18.31	533.0	120	-3.48	547.7	99	-22.92	570.0	160	-4.02	596.1	241	21.92	629.8	291	-28.98	635.0	91	-20.11
499.4	110	-22.61	533.1	121	-0.23	547.8	96	-21.98	572.0	160	-3.95	596.2	245	21.77	629.9	287	-31.25	635.1	88	-19.33
499.5	106	-23.67	533.2	125	9.57	547.9	93	-21.08	572.1	161	-0.25	596.3	249	21.83	630.0	283	-32.10	635.2	86	-18.61
499.6	103	-23.54	533.3	129	16.44	548.0	90	-20.26	572.2	165	10.58	596.4	253	21.80	630.1	279	-32.29	635.3	83	-17.91
499.7	100	-22.91	533.4	133	19.75	548.1	88	-19.46	572.3	169	17.15	596.5	257	21.77	630.2	275	-32.23	635.4	81	-17.27
499.8	97	-22.12	533.5	137	21.17	548.2	85	-18.72	572.4	173	20.09	596.6	261	21.73	630.3	271	-32.16	635.5	79	-16.68
499.9	94	-21.29	533.6	141	21.89	548.3	83	-18.02	572.5	177	21.48	596.7	265	21.72	630.4	267	-32.13	635.6	77	-16.10
500.0	91	-20.38	533.7	145	22.21	548.4	81	-17.37	572.6	181	21.91	596.8	269	21.71	630.5	263	-31.98	635.7	75	-15.58
502.0	80	-2.94	533.8	149	22.22	548.5	79	-16.77	572.7	185	22.10	596.9	273	21.67	630.6	259	-31.66	635.8	73	-15.07
504.0	80	-3.24	533.9	153	22.29	548.6	77	-16.20	572.8	189	22.20	597.0	277	21.58	630.7	255	-31.57	635.9	72	-14.62
506.0	80	-3.24	534.0	157	22.34	548.7	75	-15.68	572.9	193	22.21	599.0	280	-6.05	630.8	251	-31.36			
508.0	80	-3.24	534.1	161	22.21	548.8	73	-15.16	573.0	197	22.16	601.0	280	-5.95	630.9	247	-31.30			
510.0	80	-3.18	534.2	165	22.22	548.9	71	-14.71	573.1	201	22.13	603.0	280	-6.02	631.0	243	-31.20			
510.1	81	-0.56	534.3	169	22.17	549.0	70	-14.17	573.2	205	22.08	605.0	280	-6.02	631.1	239	-31.09			
510.2	85	8.22	534.4	173	22.14	551.0	49	-7.45	573.3	209	22.04	607.0	280	-6.04	631.2	235	-30.82			
510.3	89	15.25	534.5	177	22.11	553.0	41	-4.93	573.4	213	21.99	607.1	278	-9.25	631.3	231	-30.79			
510.4	93	19.05	534.6	181	22.08	555.0	41	-3.22	573.5	217	21.97	607.2	275	-22.11	631.4	227	-30.57			
510.5	97	20.90	534.7	185	22.09	557.0	41	-3.25	573.6	221	21.94	607.3	271	-28.24	631.5	223	-30.47			
510.6	101	21.76	534.8	189	21.99	559.0	41	-3.19	573.7	225	21.83	607.4	267	-30.51	631.6	219	-30.29			

Table 3.10. Reduced Dataset of DSC Signal as a Function of Time and Temperature for the Fifth Segment K Sample Run

Time (min)	T_s (°C)	DSC (mW)	Time (min)	T_s (°C)	DSC (mW)	Time (min)	T_s (°C)	DSC (mW)	Time (min)	T_s (°C)	DSC (mW)	Time (min)	T_s (°C)	DSC (mW)	Time (min)	T_s (°C)	DSC (mW)	Time (min)	T_s (°C)	DSC (mW)
636.0	70	-14.13	669.7	105	22.18	693.9	193	22.03	718.1	41	-1.50	732.8	229	21.85	766.5	263	-31.38	790.7	215	-30.24
638.0	49	-7.43	669.8	109	22.31	694.0	197	21.86	718.2	44	5.33	732.9	233	21.85	766.6	259	-31.70	790.8	211	-30.11
640.0	41	-4.90	669.9	113	22.38	696.0	200	-4.65	718.3	48	12.77	733.0	237	21.56	766.7	255	-31.64	790.9	207	-29.93
642.0	41	-3.21	670.0	117	22.36	698.0	200	-4.59	718.4	52	17.46	735.0	240	-5.29	766.8	251	-31.45	791.0	203	-29.87
644.0	41	-3.27	670.1	121	22.36	700.0	200	-4.65	718.5	56	20.06	737.0	240	-5.27	766.9	247	-31.45	791.1	199	-29.68
646.0	41	-3.20	670.2	125	22.33	702.0	200	-4.59	718.6	61	21.40	739.0	240	-5.25	767.0	243	-31.29	791.2	195	-29.52
646.1	41	-1.55	670.3	129	22.29	704.0	200	-4.68	718.7	65	22.01	741.0	240	-5.28	769.0	239	-5.01	791.3	191	-29.43
646.2	44	5.29	670.4	133	22.27	704.1	199	-8.25	718.8	69	22.31	743.0	240	-5.29	771.0	240	-5.06	791.4	187	-29.29
646.3	48	12.77	670.5	137	22.15	704.2	195	-18.39	718.9	73	22.40	743.1	238	-9.41	773.0	240	-5.05	791.5	183	-29.19
646.4	52	17.53	670.6	141	22.12	704.3	192	-24.62	719.0	77	22.38	743.2	235	-20.45	775.0	240	-5.09	791.6	179	-29.06
646.5	56	20.12	670.7	145	22.08	704.4	188	-27.46	719.1	81	22.38	743.3	231	-26.54	777.0	240	-5.03	791.7	175	-28.93
646.6	61	21.42	670.8	149	22.08	704.5	183	-28.69	719.2	85	22.33	743.4	227	-29.06	777.1	241	-0.40	791.8	171	-28.74
646.7	65	22.03	670.9	153	22.11	704.6	179	-29.10	719.3	89	22.27	743.5	223	-30.11	777.2	244	11.65	791.9	167	-28.63
646.8	69	22.31	671.0	157	22.07	704.7	175	-29.21	719.4	93	22.26	743.6	219	-30.43	777.3	248	17.83	792.0	163	-28.50
646.9	73	22.36	673.0	160	-4.12	704.8	171	-29.02	719.5	97	22.21	743.7	215	-30.33	777.4	252	20.37	792.1	159	-28.32
647.0	77	22.38	675.0	160	-4.04	704.9	167	-28.97	719.6	101	22.17	743.8	211	-30.34	777.5	257	21.24	792.2	155	-28.20
647.1	81	22.35	677.0	160	-4.05	705.0	163	-28.84	719.7	105	22.17	743.9	207	-30.20	777.6	261	21.64	792.3	151	-28.05
647.2	85	22.30	679.0	160	-4.04	705.1	159	-28.68	719.8	109	22.15	744.0	203	-30.03	777.7	265	21.77	792.4	147	-27.93
647.3	89	22.29	681.0	160	-4.06	705.2	155	-28.47	719.9	113	22.14	746.0	200	-4.42	777.8	269	21.77	792.5	143	-27.64
647.4	93	22.23	681.1	159	-7.00	705.3	151	-28.25	720.0	117	22.17	748.0	200	-4.44	777.9	273	21.76	792.6	139	-27.52
647.5	97	22.22	681.2	156	-15.99	705.4	147	-28.15	720.1	121	22.14	750.0	200	-4.51	778.0	277	21.72	792.7	135	-27.32
647.6	101	22.21	681.3	152	-22.16	705.5	143	-27.84	720.2	125	22.11	752.0	200	-4.49	778.1	281	21.75	792.8	132	-27.19
647.7	105	22.14	681.4	148	-25.50	705.6	140	-27.72	720.3	129	22.02	754.0	200	-4.43	778.2	285	21.72	792.9	128	-27.00
647.8	109	22.12	681.5	144	-26.91	705.7	136	-27.46	720.4	133	22.07	754.1	201	-0.17	778.3	289	21.74	793.0	124	-27.44
647.9	113	22.12	681.6	140	-27.57	705.8	132	-27.28	720.5	137	22.10	754.2	204	11.34	778.4	293	21.68	793.1	120	-26.29
648.0	117	22.03	681.7	136	-27.69	705.9	128	-27.11	720.6	141	22.02	754.3	208	17.62	778.5	297	21.56	793.2	116	-25.95
650.0	120	-3.63	681.8	132	-27.53	706.0	124	-27.35	720.7	145	21.99	754.4	212	20.32	780.5	300	-6.33	793.3	112	-26.48
652.0	120	-3.58	681.9	128	-27.45	706.1	120	-26.47	720.8	149	21.95	754.5	217	21.40	782.5	300	-6.27	793.4	109	-25.70
654.0	120	-3.51	682.0	124	-27.77	706.2	116	-25.82	720.9	153	22.03	754.6	221	21.85	784.5	300	-6.28	793.5	105	-24.73
656.0	120	-3.52	684.0	120	-3.29	706.3	112	-26.58	721.0	157	21.87	754.7	225	21.97	786.5	300	-6.25	793.6	102	-23.74
658.0	120	-3.63	686.0	120	-3.50	706.4	109	-25.87	723.0	160	-4.06	754.8	229	21.97	788.5	300	-6.37	793.7	99	-22.75
658.1	119	-5.92	688.0	120	-3.54	706.5	105	-24.90	725.0	160	-4.02	754.9	233	21.97	788.6	298	-11.42	793.8	96	-21.82
658.2	117	-13.28	690.0	120	-3.51	706.6	102	-23.91	727.0	160	-4.03	755.0	237	21.96	788.7	295	-23.26	793.9	93	-20.93
658.3	113	-18.34	692.0	120	-3.39	706.7	99	-22.89	729.0	160	-4.05	755.1	241	21.66	788.8	291	-29.03	794.0	91	-20.10

Time (min)	T_s (^oC)	DSC (mW)	Time (min)	T_s (^oC)	DSC (mW)	Time (min)	T_s (^oC)	DSC (mW)	Time (min)	T_s (^oC)	DSC (mW)	Time (min)	T_s (^oC)	DSC (mW)	Time (min)	T_s (^oC)	DSC (mW)	Time (min)	T_s (^oC)	DSC (mW)
658.4	109	-22.66	692.1	121	-0.21	706.8	96	-21.96	731.0	160	-3.94	755.2	245	21.62	788.9	287	-31.07	794.1	88	-19.33
658.5	106	-23.69	692.2	125	9.77	706.9	93	-21.08	731.1	161	-0.14	755.3	249	21.82	789.0	283	-32.04	794.2	86	-18.58
658.6	103	-23.54	692.3	129	16.49	707.0	90	-20.23	731.2	165	10.72	755.4	253	21.79	789.1	279	-32.30	794.3	83	-17.90
658.7	100	-22.91	692.4	133	19.83	707.1	88	-19.45	731.3	169	17.20	755.5	257	21.78	789.2	275	-32.34	794.4	81	-17.26
658.8	97	-22.12	692.5	137	21.33	707.2	85	-18.71	731.4	173	20.12	755.6	261	21.72	789.3	271	-32.18	794.5	79	-16.66
658.9	94	-21.30	692.6	141	21.94	707.3	83	-18.02	731.5	177	21.45	755.7	265	21.67	789.4	267	-32.08	794.6	77	-16.10
659.0	91	-20.39	692.7	145	22.16	707.4	81	-17.37	731.6	181	22.00	755.8	269	21.69	789.5	263	-31.89	794.7	75	-15.57
661.0	80	-2.93	692.8	149	22.36	707.5	79	-16.75	731.7	185	22.19	755.9	273	21.62	789.6	259	-31.76	794.8	73	-15.08
663.0	80	-3.21	692.9	153	22.31	707.6	77	-16.19	731.8	189	22.21	756.0	277	21.56	789.7	255	-31.66	794.9	72	-14.62
665.0	80	-3.24	693.0	157	22.33	707.7	75	-15.67	731.9	193	22.15	758.0	280	-6.01	789.8	251	-31.43			
667.0	80	-3.24	693.1	161	22.24	707.8	73	-15.16	732.0	197	22.17	760.0	280	-5.97	789.9	247	-31.33			
669.0	80	-3.16	693.2	165	22.24	707.9	71	-14.70	732.1	201	22.13	762.0	280	-5.94	790.0	243	-31.26			
669.1	81	-0.52	693.3	169	22.19	708.0	70	-14.18	732.2	205	22.12	764.0	280	-5.95	790.1	239	-31.09			
669.2	85	8.24	693.4	173	22.14	710.0	49	-7.45	732.3	209	22.06	766.0	280	-5.98	790.2	235	-30.89			
669.3	89	15.31	693.5	177	22.04	712.0	41	-4.91	732.4	213	22.02	766.1	278	-9.27	790.3	231	-30.80			
669.4	93	19.12	693.6	181	22.07	714.0	41	-3.23	732.5	217	21.99	766.2	275	-22.16	790.4	227	-30.68			
669.5	97	20.95	693.7	185	22.02	716.0	41	-3.28	732.6	221	21.95	766.3	271	-28.17	790.5	223	-30.49			
669.6	101	21.78	693.8	189	22.00	718.0	41	-3.21	732.7	225	21.85	766.4	267	-30.44	790.6	219	-30.34			

3.3.2 Segment L

The DSC sample obtained from Segment L measured approximately 3.0 mm long by 4.25 mm wide, 1.392 mm thick, and weighed 105.1 mg. A baseline of the DSC instrument was obtained by running both the sample and reference pans empty over a single thermal cycle defined in Table 2.2. A graphical representation of the baseline run as a function of temperature is provided in Figure 3.12 both before and after the sample measurement. A reduced data set of the DSC signal as a function of time and temperature is provided in Table 3.11 for the pre-sample baseline run. The reference run was obtained by placing a 101.37 mg NIST traceable sapphire into the sample pan of the instrument over a single thermal cycle defined in Table 2.2. A graphical representation of the DSC signal as a function of temperature is provided in Figure 3.13 both before and after the sample measurement. A reduced data set of the DSC signal as a function of time and temperature is provided in Table 3.12 for the pre-sample reference run. Finally, the sample runs were obtained by placing the DSC sample into the sample pan of the instrument. The sample was subjected to five thermal cycles, as defined in Table 2.2, run in series. A graphical representation of the DSC signal as a function of temperature is provided in Figure 3.14, and a reduced data set of the DSC signal as a function of time and temperature is provided in Table 3.13 through Table 3.17 for each measurement cycle. Observation of Figure 3.14 shows the very repeatable behavior of the segment L sample over each measurement cycle.

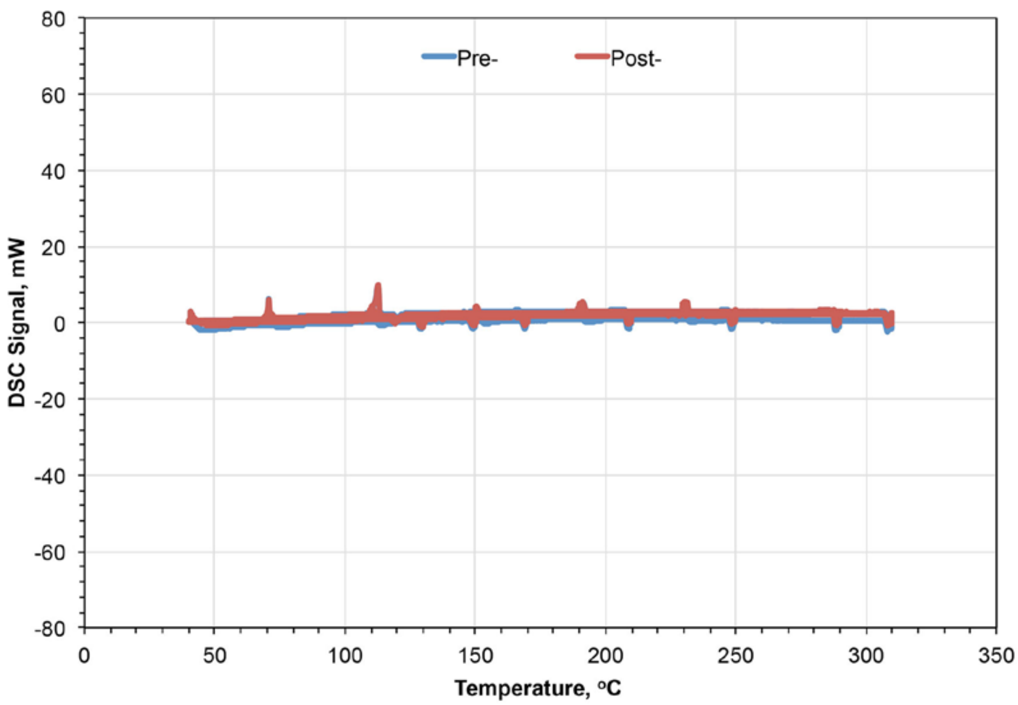

Figure 3.12. DSC Signal as a Function of Temperature for the Baseline Run of Segment L Before and After the Sample Measurement

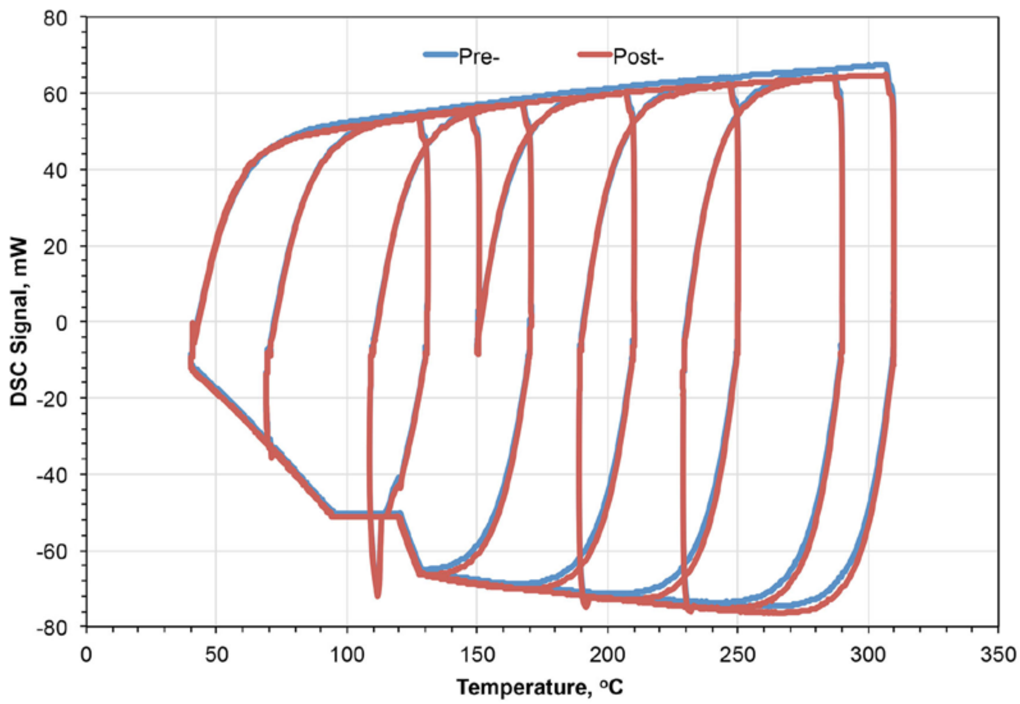

Figure 3.13. DSC Signal as a Function of Temperature for the Reference Run of Segment L Before and After the Sample Measurement

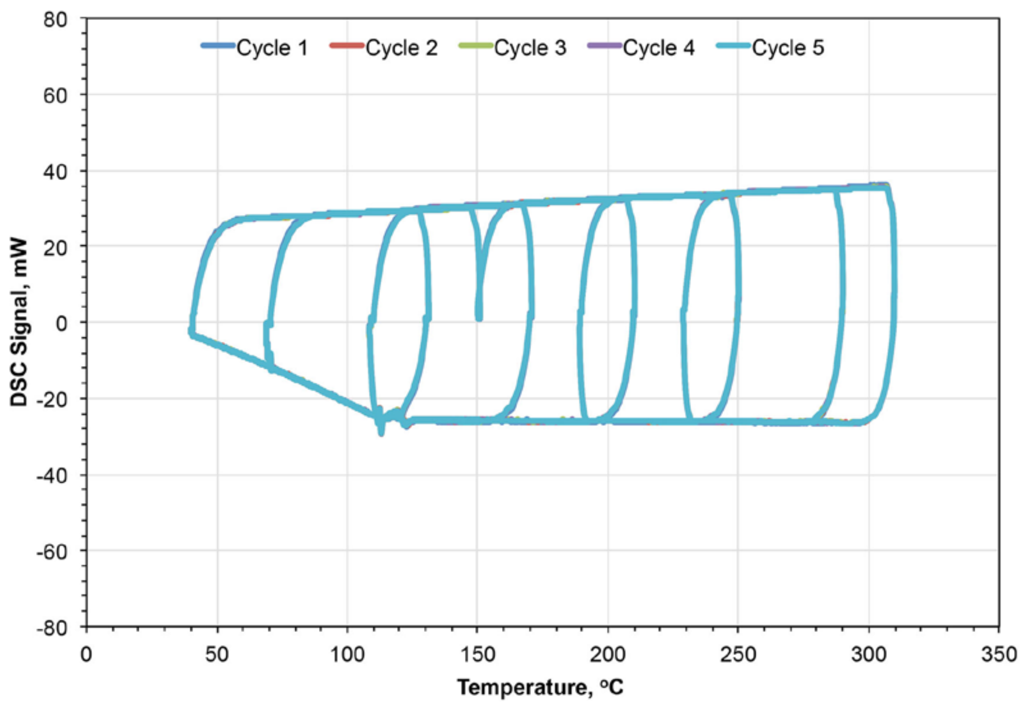

Figure 3.14. DSC Signal as a Function of Temperature for the Sample Run of Segment L for Each Thermal Cycle

Table 3.11. Reduced Dataset of DSC Signal as a Function of Time and Temperature for Segment L Baseline Run (Pre-Sample)

Time (min)	T_s (°C)	DSC (mW)	Time (min)	T_s (°C)	DSC (mW)	Time (min)	T_s (°C)	DSC (mW)	Time (min)	T_s (°C)	DSC (mW)	Time (min)	T_s (°C)	DSC (mW)	Time (min)	T_s (°C)	DSC (mW)	Time (min)	T_s (°C)	DSC (mW)	Time (min)	T_s (°C)	DSC (mW)
0.0	41	-0.01	29.8	70	0.70	55.8	110	1.34	72.3	132	2.60	86.9	133	0.39	111.0	203	2.99	135.1	239	2.92	159.2	235	2.94
2.0	41	0.07	31.8	70	0.66	57.8	110	3.49	72.4	128	2.51	87.0	137	0.46	111.1	199	2.98	135.2	235	2.95	159.3	231	2.96
4.0	41	0.08	33.8	71	2.82	57.9	113	-0.16	72.5	124	2.29	87.1	141	0.43	111.2	195	2.98	135.3	233	2.95	159.4	227	2.97
6.0	41	0.09	33.9	73	-0.42	58.0	117	-0.16	72.6	120	0.77	87.2	145	0.52	111.3	193	2.98	137.3	230	2.03	159.5	223	2.98
8.0	41	0.06	34.0	76	-1.15	58.1	121	0.11	72.7	116	2.27	87.3	147	0.58	113.3	190	2.03	139.3	230	2.07	159.6	219	2.98
10.0	41	0.08	34.1	81	-0.70	58.2	125	0.32	72.8	112	2.47	89.3	150	1.67	115.3	190	2.01	141.3	230	2.01	159.7	215	2.98
10.1	41	1.31	34.2	85	-0.44	58.3	129	0.28	72.9	108	2.38	91.3	150	1.66	117.3	190	1.99	143.3	230	2.06	159.8	211	3.00
10.2	44	-1.65	34.3	89	-0.30	58.4	133	0.34	73.0	105	2.25	93.3	150	1.69	119.3	190	2.02	145.3	230	4.26	159.9	207	2.98
10.3	48	-1.94	34.4	93	-0.25	58.5	137	0.41	73.1	101	2.15	95.3	150	1.72	121.3	190	4.31	145.4	232	0.20	160.0	203	2.98
10.4	52	-1.53	34.5	97	-0.16	58.6	141	0.49	73.2	98	2.05	97.3	150	3.90	121.4	193	0.21	145.5	236	0.69	160.1	199	2.99
10.5	56	-1.27	34.6	101	-0.08	58.7	145	0.29	73.3	95	1.96	97.4	153	0.15	121.5	197	0.54	145.6	240	0.64	160.2	195	2.99
10.6	60	-0.87	34.7	105	0.02	58.8	149	0.61	73.4	92	1.87	97.5	157	0.14	121.6	201	0.85	145.7	245	0.61	160.3	191	2.99
10.7	65	-0.77	34.8	109	0.07	58.9	153	0.56	73.5	90	1.79	97.6	161	0.57	121.7	205	0.90	145.8	249	0.83	160.4	187	2.96
10.8	69	-0.69	34.9	113	0.16	59.0	157	0.56	73.6	87	1.72	97.7	165	0.63	121.8	209	0.88	145.9	253	0.79	160.5	183	2.96
10.9	73	-0.54	35.0	117	0.26	59.1	161	0.64	73.7	85	1.63	97.8	169	0.75	121.9	213	0.95	146.0	257	0.79	160.6	179	2.94
11.0	77	-0.46	35.1	121	0.25	59.2	165	0.66	73.8	82	1.56	97.9	173	0.78	122.0	217	0.95	146.1	261	0.78	160.7	175	2.92
11.1	81	-0.42	35.2	125	0.28	59.3	169	0.58	73.9	80	1.49	98.0	177	0.76	122.1	221	0.97	146.2	265	0.78	160.8	171	2.92
11.2	85	-0.32	35.3	129	0.36	59.4	173	0.80	74.0	78	1.43	98.1	181	0.79	122.2	225	0.89	146.3	269	0.75	160.9	167	2.91
11.3	89	-0.26	35.4	133	0.48	59.5	177	0.88	74.1	76	1.37	98.2	185	0.83	122.3	229	0.91	146.4	273	0.71	161.0	163	2.86
11.4	93	-0.17	35.5	137	0.35	59.6	181	0.85	74.2	74	1.31	98.3	189	0.91	122.4	233	0.95	146.5	277	0.69	161.1	159	2.88
11.5	97	-0.12	35.6	141	0.53	59.7	185	0.87	74.3	72	1.25	98.4	193	0.88	122.5	237	0.64	146.6	281	0.65	161.2	155	2.80
11.6	101	-0.05	35.7	145	0.61	59.8	189	0.89	74.4	71	1.20	98.5	197	0.90	122.6	241	0.61	146.7	285	0.59	161.3	151	2.78
11.7	105	0.00	35.8	149	0.60	59.9	193	0.89	74.5	69	1.13	98.6	201	0.92	122.7	245	0.79	146.8	289	0.59	161.4	147	2.77
11.8	109	0.09	35.9	153	0.62	60.0	197	0.89	76.5	49	0.45	98.7	205	0.98	122.8	249	0.81	146.9	293	0.57	161.5	143	2.71
11.9	113	0.21	36.0	157	0.75	60.1	201	0.95	78.5	41	0.27	98.8	209	0.95	122.9	253	0.81	147.0	297	0.57	161.6	139	2.67
12.0	117	0.27	36.1	161	0.68	60.2	205	0.96	80.5	41	0.07	98.9	213	1.02	123.0	257	0.92	147.1	301	0.47	161.7	135	2.60
12.1	121	0.35	36.2	165	0.72	60.3	207	0.97	82.5	41	0.08	99.0	217	0.98	123.1	261	0.84	147.2	305	0.42	161.8	131	2.54
12.2	125	0.26	36.3	167	0.72	62.3	210	1.96	84.5	41	0.08	99.1	221	0.94	123.2	265	0.83	147.3	307	0.46	161.9	128	2.45
12.3	127	0.46	38.3	170	1.81	64.3	210	1.94	84.6	41	1.18	99.2	225	0.93	123.3	269	0.82	149.3	310	1.20	162.0	124	2.16
14.3	130	1.55	40.3	170	1.83	66.3	210	1.95	84.7	44	-1.72	99.3	229	1.02	123.4	273	0.79	151.3	310	1.30	162.1	120	0.87
16.3	130	1.54	42.3	170	1.83	68.3	210	1.96	84.8	48	-1.87	99.4	233	0.92	123.5	277	0.74	153.3	310	1.22	162.2	116	2.24
18.3	130	1.51	44.3	170	1.87	70.3	210	-0.12	84.9	52	-1.37	99.5	237	0.77	123.6	281	0.71	155.3	310	1.17	162.3	112	2.46
20.3	130	1.58	46.3	170	-0.12	70.4	207	3.37	85.0	56	-1.17	99.6	241	0.82	123.7	285	0.72	157.3	310	-1.02	162.4	108	2.34
22.3	130	-0.28	46.4	167	3.14	70.5	203	3.31	85.1	61	-0.90	99.7	245	0.94	123.8	287	0.62	157.4	307	2.83	162.5	105	2.22
22.4	128	2.43	46.5	164	3.18	70.6	199	3.11	85.2	65	-0.72	99.8	247	0.92	125.8	290	1.46	157.5	303	2.48	162.6	101	2.11
22.5	125	2.58	46.6	160	2.98	70.7	195	3.06	85.3	69	-0.66	101.8	250	1.78	127.8	290	1.52	157.6	299	2.37	162.7	98	2.03
22.6	121	1.85	46.7	156	2.89	70.8	191	3.02	85.4	73	-0.56	103.8	250	1.80	129.8	290	1.45	157.7	295	2.44	162.8	95	1.94
22.7	117	2.29	46.8	152	2.86	70.9	187	3.01	85.5	77	-0.49	105.8	250	1.79	131.8	290	1.50	157.8	291	2.42	162.9	93	1.86

Time (min)	T_s (°C)	DSC (mW)	Time (min)	T_s (°C)	DSC (mW)	Time (min)	T_s (°C)	DSC (mW)	Time (min)	T_s (°C)	DSC (mW)	Time (min)	T_s (°C)	DSC (mW)	Time (min)	T_s (°C)	DSC (mW)	Time (min)	T_s (°C)	DSC (mW)	Time (min)	T_s (°C)	DSC (mW)
22.8	113	2.57	46.9	148	2.85	71.0	183	3.00	85.6	81	-0.42	107.8	250	1.82	133.8	289	-0.82	157.9	287	2.59	163.0	90	1.78
22.9	109	2.45	47.0	144	2.82	71.1	179	2.99	85.7	85	-0.34	109.8	249	0.76	133.9	287	3.07	158.0	283	2.94	163.1	87	1.70
23.0	106	2.31	47.1	140	2.73	71.2	175	2.95	85.8	89	-0.28	109.9	247	3.38	134.0	283	2.98	158.1	279	2.58	163.2	85	1.63
23.1	102	2.20	47.2	136	2.66	71.3	171	2.95	85.9	93	-0.19	110.0	243	3.17	134.1	279	2.67	158.2	275	2.69	163.3	83	1.55
23.2	99	2.11	47.3	132	2.62	71.4	167	2.92	86.0	97	-0.13	110.1	239	2.97	134.2	275	2.72	158.3	271	2.78	163.4	80	1.48
23.3	96	2.02	47.4	128	2.53	71.5	163	2.93	86.1	101	-0.07	110.2	235	2.98	134.3	271	2.84	158.4	267	2.73	163.5	78	1.42
23.4	93	1.93	47.5	124	2.33	71.6	159	2.88	86.2	105	0.01	110.3	231	2.96	134.4	267	2.75	158.5	263	2.80	163.6	76	1.35
23.5	90	1.84	47.6	120	0.82	71.7	155	2.82	86.3	109	0.11	110.4	227	2.95	134.5	263	2.73	158.6	259	2.80	163.7	74	1.30
23.6	88	1.76	47.7	116	2.30	71.8	151	2.87	86.4	113	0.14	110.5	223	3.00	134.6	259	2.81	158.7	255	2.83	163.8	73	1.24
23.7	85	1.67	47.8	114	2.26	71.9	147	2.79	86.5	117	0.19	110.6	219	3.00	134.7	255	2.85	158.8	251	2.88	163.9	71	1.18
23.8	84	1.64	49.8	110	1.31	72.0	143	2.76	86.6	121	0.33	110.7	215	3.01	134.8	251	2.86	158.9	247	2.90			
25.8	70	0.67	51.8	110	1.36	72.1	139	2.73	86.7	125	0.32	110.8	211	3.02	134.9	247	2.88	159.0	243	2.90			
27.8	70	0.71	53.8	110	1.34	72.2	135	2.65	86.8	129	0.36	110.9	207	3.00	135.0	243	2.90	159.1	239	2.93			

Table 3.12. Reduced Dataset of DSC Signal as a Function of Time and Temperature for Segment L Reference Run (Pre-Sample)

Time (min)	T_s (°C)	DSC (mW)	Time (min)	T_s (°C)	DSC (mW)	Time (min)	T_s (°C)	DSC (mW)	Time (min)	T_s (°C)	DSC (mW)	Time (min)	T_s (°C)	DSC (mW)	Time (min)	T_s (°C)	DSC (mW)	Time (min)	T_s (°C)	DSC (mW)	Time (min)	T_s (°C)	DSC (mW)
0.0	41	-0.16	29.8	70	-7.87	55.8	110	-7.14	73.3	97	-50.46	97.9	173	51.61	122.5	237	63.32	146.6	281	65.88	161.2	155	-68.17
2.0	41	-8.58	31.8	70	-7.84	57.8	110	-4.46	73.4	94	-50.50	98.0	177	54.47	122.6	241	63.65	146.7	285	66.25	161.3	151	-67.94
4.0	41	-8.51	33.8	71	-5.36	57.9	113	5.03	73.5	92	-48.61	98.1	181	56.59	122.7	245	63.66	146.8	289	66.47	161.4	147	-67.47
6.0	41	-8.51	33.9	73	2.49	58.0	117	18.92	73.6	89	-46.67	98.2	185	58.11	122.8	249	64.13	146.9	293	66.77	161.5	143	-67.01
8.0	41	-8.50	34.0	76	14.97	58.1	121	30.23	73.7	87	-44.81	98.3	189	59.20	122.9	253	64.62	147.0	297	67.00	161.6	139	-66.70
10.0	41	-8.50	34.1	80	25.95	58.2	125	38.39	73.8	85	-43.05	98.4	193	60.07	123.0	257	64.83	147.1	301	67.15	161.7	136	-66.11
10.1	41	-4.22	34.2	85	34.04	58.3	129	44.15	73.9	83	-41.37	98.5	197	60.64	123.1	261	65.02	147.2	305	67.38	161.8	132	-65.64
10.2	44	4.58	34.3	89	39.88	58.4	133	48.27	74.0	81	-39.79	98.6	201	61.16	123.2	265	65.23	147.3	307	67.32	161.9	128	-64.18
10.3	48	15.86	34.4	93	44.11	58.5	137	51.24	74.1	79	-38.26	98.7	205	61.59	123.3	269	65.42	149.3	310	-5.95	162.0	124	-57.34
10.4	52	25.48	34.5	97	47.10	58.6	141	53.32	74.2	77	-36.83	98.8	209	61.90	123.4	273	65.63	151.3	310	-5.89	162.1	120	-50.20
10.5	56	32.72	34.6	101	49.24	58.7	145	54.84	74.3	75	-35.47	98.9	213	62.19	123.5	277	65.84	153.3	310	-5.87	162.2	116	-50.23
10.6	60	38.02	34.7	105	50.80	58.8	149	56.01	74.4	73	-34.18	99.0	217	62.51	123.6	281	66.03	155.3	310	-5.84	162.3	113	-50.27
10.7	65	41.81	34.8	109	51.96	58.9	153	56.78	74.5	72	-32.96	99.1	221	62.79	123.7	285	66.20	157.3	310	-9.03	162.4	109	-50.31
10.8	69	44.58	34.9	113	52.86	59.0	157	57.46	76.5	51	-18.17	99.2	225	63.00	123.8	287	66.34	157.4	307	-23.25	162.5	106	-50.35
10.9	73	46.52	35.0	117	53.58	59.1	161	57.98	78.5	42	-12.58	99.3	229	63.16	125.8	290	-6.05	157.5	303	-40.18	162.6	103	-50.39
11.0	77	47.98	35.1	121	54.22	59.2	165	58.37	80.5	41	-8.29	99.4	233	63.42	127.8	290	-5.92	157.6	299	-52.33	162.7	100	-50.43
11.1	81	49.37	35.2	125	54.72	59.3	169	58.83	82.5	41	-8.47	99.5	237	63.68	129.8	290	-5.93	157.7	295	-60.35	162.8	97	-50.46
11.2	85	50.34	35.3	129	55.18	59.4	173	59.17	84.5	41	-8.49	99.6	241	63.84	131.8	290	-5.93	157.8	291	-65.46	162.9	94	-50.40
11.3	89	51.09	35.4	133	55.52	59.5	177	59.56	84.7	44	4.38	99.7	245	63.85	133.8	289	-8.99	157.9	287	-68.92	163.0	92	-48.39
11.4	93	51.65	35.5	137	55.93	59.6	181	59.79	84.9	52	25.18	99.8	247	63.95	133.9	287	-22.45	158.0	283	-71.50	163.1	90	-46.45
11.5	97	52.09	35.6	141	56.34	59.7	185	60.14	85.1	60	37.77	101.8	250	-6.24	134.0	283	-38.95	158.1	279	-72.95	163.2	87	-44.63

Time (min)	T_s (°C)	DSC (mW)	Time (min)	T_s (°C)	DSC (mW)	Time (min)	T_s (°C)	DSC (mW)	Time (min)	T_s (°C)	DSC (mW)	Time (min)	T_s (°C)	DSC (mW)	Time (min)	T_s (°C)	DSC (mW)	Time (min)	T_s (°C)	DSC (mW)	Time (min)	T_s (°C)	DSC (mW)
11.6	101	52.51	35.7	145	56.67	59.8	189	60.43	85.3	69	44.41	103.8	250	-6.08	134.1	279	-51.14	158.2	275	-73.78	163.3	85	-42.87
11.7	105	52.90	35.8	149	56.96	59.9	193	60.75	85.5	77	47.90	105.8	250	-6.03	134.2	275	-58.96	158.3	271	-74.35	163.4	83	-41.20
11.8	109	53.31	35.9	153	57.37	60.0	197	61.03	85.6	81	49.01	107.8	250	-6.01	134.3	271	-64.54	158.4	267	-74.59	163.5	81	-39.62
11.9	113	53.71	36.0	157	57.66	60.1	201	61.27	85.7	85	49.95	109.8	249	-8.11	134.4	267	-68.06	158.5	263	-74.66	163.6	79	-38.13
12.0	117	54.04	36.1	161	58.04	60.2	205	61.54	85.8	89	50.69	109.9	247	-21.34	134.5	263	-70.50	158.6	259	-74.69	163.7	77	-36.70
12.1	121	54.43	36.2	165	58.36	60.3	207	61.68	85.9	93	51.25	110.0	243	-37.08	134.6	259	-71.86	158.7	255	-74.59	163.8	75	-35.34
12.2	125	54.83	36.3	167	58.60	68.3	210	-6.16	86.0	97	51.78	110.1	239	-48.90	134.7	255	-72.75	158.8	251	-74.39	163.9	74	-34.06
12.3	127	54.99	38.3	170	-6.74	70.6	199	-46.32	86.1	101	52.29	110.2	235	-56.91	134.8	251	-73.23	158.9	247	-74.29			
14.3	130	-7.23	40.3	170	-6.59	70.9	187	-63.33	86.2	105	52.74	110.3	231	-62.28	134.9	247	-73.59	159.0	243	-73.96			
16.3	130	-6.93	42.3	170	-6.50	71.1	179	-67.05	86.3	109	53.17	110.4	227	-65.82	135.0	243	-73.53	159.1	239	-73.85			
18.3	130	-6.95	44.3	170	-6.45	71.3	171	-68.53	86.4	113	53.57	110.5	223	-68.09	135.1	239	-73.70	159.2	235	-73.61			
20.3	130	-6.94	46.3	170	-8.98	71.4	167	-68.70	86.5	117	53.99	110.6	219	-69.61	135.2	235	-73.58	159.3	231	-73.32			
22.3	130	-9.16	46.4	168	-18.81	71.5	163	-68.70	86.6	121	54.35	110.7	215	-70.56	135.3	233	-73.39	159.4	227	-73.15			
22.4	128	-17.22	46.5	164	-32.39	71.6	159	-68.64	86.7	125	54.75	110.8	211	-71.01	137.3	230	-5.71	159.5	223	-72.79			
22.5	125	-28.72	46.6	160	-43.35	71.7	155	-68.37	86.8	129	55.13	110.9	207	-71.42	139.3	230	-5.94	159.6	219	-72.80			
22.6	121	-40.80	46.7	156	-51.13	71.8	151	-68.13	86.9	133	55.53	111.0	203	-71.40	141.3	230	-5.95	159.7	215	-72.36			
22.7	117	-44.86	46.8	152	-56.60	71.9	147	-67.77	87.0	137	55.85	111.1	199	-71.23	143.3	230	-5.96	159.8	211	-72.17			
22.8	113	-50.26	46.9	148	-60.14	72.0	144	-67.38	87.1	141	56.19	111.2	195	-71.27	145.3	230	-2.80	159.9	207	-71.91			
22.9	110	-50.30	47.0	144	-62.42	72.1	140	-66.87	87.2	145	56.53	111.3	193	-71.06	145.4	232	10.33	160.0	203	-71.66			
23.0	107	-50.34	47.1	140	-63.82	72.2	136	-66.38	87.3	147	56.78	115.3	190	-6.19	145.5	236	26.88	160.1	199	-71.33			
23.1	103	-50.38	47.2	136	-64.53	72.3	132	-65.91	89.3	150	-6.95	119.3	190	-6.18	145.6	240	38.91	160.2	195	-71.12			
23.2	100	-50.41	47.3	132	-64.81	72.4	128	-64.69	91.3	150	-6.70	121.4	193	8.77	145.7	244	47.29	160.3	191	-70.69			
23.3	98	-50.45	47.4	128	-64.36	72.5	124	-57.92	93.3	150	-6.68	121.6	200	36.34	145.8	248	53.11	160.4	187	-70.64			
23.4	95	-49.97	47.5	124	-57.52	72.6	120	-50.33	95.3	150	-6.72	121.8	209	50.55	145.9	253	57.07	160.5	183	-70.31			
23.5	92	-48.25	47.6	120	-50.20	72.7	116	-50.23	97.3	150	-3.83	121.9	213	54.60	146.0	257	59.93	160.6	179	-70.02			
23.6	90	-46.50	47.7	116	-50.22	72.8	113	-50.27	97.4	153	7.09	122.0	217	57.47	146.1	261	61.92	160.7	175	-69.71			
23.7	87	-44.76	47.8	115	-50.24	72.9	109	-50.31	97.5	157	21.86	122.1	221	59.53	146.2	265	63.28	160.8	171	-69.44			
23.8	86	-43.92	49.8	110	-6.52	73.0	106	-50.35	97.6	161	33.41	122.2	225	60.96	146.3	269	64.20	160.9	167	-69.15			
25.8	70	-7.12	51.8	110	-7.07	73.1	103	-50.39	97.7	165	41.70	122.3	229	61.99	146.4	273	64.91	161.0	163	-68.84			
27.8	70	-7.78	53.8	110	-7.13	73.2	100	-50.43	97.8	169	47.53	122.4	233	62.69	146.5	277	65.46	161.1	159	-68.50			

Table 3.13. Reduced Dataset of DSC Signal as a Function of Time and Temperature for the First Segment L Sample Run

Time (min)	T_s (°C)	DSC (mW)	Time (min)	T_s (°C)	DSC (mW)	Time (min)	T_s (°C)	DSC (mW)	Time (min)	T_s (°C)	DSC (mW)	Time (min)	T_s (°C)	DSC (mW)	Time (min)	T_s (°C)	DSC (mW)	Time (min)	T_s (°C)	DSC (mW)	Time (min)	T_s (°C)	DSC (mW)
0.0	41	-0.07	34.1	80	26.25	58.2	125	29.70	72.8	112	-24.98	89.3	150	1.40	115.3	190	2.49	141.3	230	3.29	159.7	215	-25.82
2.0	41	-1.84	34.2	85	27.82	58.3	129	30.08	72.9	109	-23.99	91.3	150	1.49	117.3	190	2.51	143.3	230	3.27	159.8	211	-25.80
4.0	41	-1.81	34.3	89	28.41	58.4	133	30.29	73.0	105	-22.88	93.3	150	1.27	119.3	190	2.53	145.3	230	7.19	159.9	207	-25.76
6.0	41	-1.81	34.4	93	28.62	58.5	137	30.41	73.1	102	-21.80	95.3	150	1.55	121.3	190	6.34	145.4	232	22.12	160.0	203	-25.75
8.0	41	-1.80	34.5	97	28.74	58.6	141	30.49	73.2	99	-20.78	97.3	150	4.92	121.4	193	20.59	145.5	236	30.72	160.1	199	-25.76
10.0	41	-1.81	34.6	101	28.86	58.7	145	30.67	73.3	96	-19.81	97.4	153	18.47	121.5	196	29.16	145.6	240	33.11	160.2	195	-25.71
10.1	41	3.98	34.7	105	28.99	58.8	149	30.78	73.4	93	-18.89	97.5	157	27.14	121.6	200	31.96	145.7	244	33.66	160.3	191	-25.71
10.2	44	14.14	34.8	109	29.11	58.9	153	30.88	73.5	90	-18.04	97.6	161	30.26	121.7	205	32.73	145.8	249	34.06	160.4	187	-25.75
10.3	48	21.67	34.9	113	29.19	59.0	157	30.95	73.6	88	-17.22	97.7	165	31.26	121.8	209	33.00	145.9	253	34.33	160.5	183	-25.75
10.4	52	25.27	35.0	117	29.34	59.1	161	31.10	73.7	86	-16.46	97.8	169	31.56	121.9	213	33.18	146.0	257	34.46	160.6	179	-25.71
10.5	56	26.73	35.1	121	29.46	59.2	165	31.22	73.8	83	-15.73	97.9	173	31.78	122.0	217	33.30	146.1	261	34.61	160.7	175	-25.71
10.6	60	27.29	35.2	125	29.58	59.3	169	31.35	73.9	81	-15.06	98.0	177	31.97	122.1	221	33.39	146.2	265	34.66	160.8	171	-25.71
10.7	65	27.58	35.3	129	29.72	59.4	173	31.52	74.0	79	-14.40	98.1	181	32.00	122.2	225	33.47	146.3	269	34.83	160.9	167	-25.75
10.8	69	27.72	35.4	133	29.89	59.5	177	31.63	74.1	77	-13.80	98.2	185	32.09	122.3	229	33.43	146.4	273	34.91	161.0	163	-25.64
10.9	73	27.80	35.5	137	30.07	59.6	181	31.76	74.2	75	-13.22	98.3	189	32.25	122.4	233	33.68	146.5	277	35.12	161.1	159	-25.67
11.0	77	27.89	35.6	141	30.14	59.7	185	31.88	74.3	73	-12.67	98.4	193	32.39	122.5	237	33.79	146.6	281	35.24	161.2	155	-25.65
11.1	81	28.00	35.7	145	30.36	59.8	189	31.96	74.4	72	-12.15	98.5	197	32.48	122.6	241	33.79	146.7	285	35.28	161.3	151	-25.58
11.2	85	28.11	35.8	149	30.43	59.9	193	32.07	74.5	70	-11.67	98.6	201	32.56	122.7	245	33.66	146.8	289	35.49	161.4	147	-25.53
11.3	89	28.23	35.9	153	30.58	60.0	197	32.17	76.5	49	-5.74	98.7	205	32.68	122.8	249	34.07	146.9	293	35.80	161.5	143	-25.57
11.4	93	28.35	36.0	157	30.72	60.1	201	32.23	78.5	41	-3.51	98.8	209	32.82	122.9	253	34.20	147.0	297	35.82	161.6	139	-25.52
11.5	97	28.47	36.1	161	30.95	60.2	205	32.30	80.5	41	-1.71	98.9	213	32.95	123.0	257	34.37	147.1	301	36.05	161.7	135	-25.47
11.6	101	28.61	36.2	165	30.99	60.3	207	32.31	82.5	41	-1.77	99.0	217	33.05	123.1	261	34.49	147.2	305	36.01	161.8	132	-25.45
11.7	105	28.78	36.3	167	31.00	62.3	210	2.41	84.5	41	-1.78	99.1	221	33.15	123.2	265	34.59	147.3	307	36.13	161.9	128	-25.39
11.8	109	28.94	38.3	170	1.76	64.3	210	2.58	84.6	41	3.75	99.2	225	33.21	123.3	269	34.69	149.3	310	3.53	162.0	124	-26.43
11.9	113	29.11	40.3	170	1.88	66.3	210	2.65	84.7	44	13.81	99.3	229	33.27	123.4	273	34.80	151.3	310	3.78	162.1	120	-24.93
12.0	117	29.22	42.3	170	1.90	68.3	210	2.67	84.8	48	21.40	99.4	233	33.44	123.5	277	34.83	153.3	310	3.87	162.2	116	-25.04
12.1	121	29.36	44.3	170	1.78	70.3	210	-0.65	84.9	52	25.07	99.5	237	33.42	123.6	281	34.95	155.3	310	3.75	162.3	112	-24.83
12.2	125	29.51	46.3	170	-1.12	70.4	207	-13.84	85.0	56	26.59	99.6	241	33.27	123.7	285	34.90	157.3	310	-0.12	162.4	109	-23.85
12.3	127	29.63	46.4	168	-13.02	70.5	203	-22.13	85.1	60	27.26	99.7	245	33.45	123.8	287	34.84	157.4	307	-15.36	162.5	105	-22.76
16.3	130	0.98	46.5	164	-21.18	70.6	199	-25.12	85.2	65	27.56	99.8	247	33.45	125.8	290	3.21	157.5	303	-23.55	162.6	102	-21.69
20.3	130	0.97	46.6	160	-24.58	70.7	195	-26.07	85.3	69	27.69	101.8	250	2.81	127.8	290	3.46	157.6	299	-25.99	162.7	99	-20.66
22.4	128	-11.73	46.7	156	-25.88	70.8	191	-26.30	85.4	73	27.77	103.8	250	3.08	129.8	290	3.59	157.7	295	-26.57	162.8	96	-19.70
22.6	121	-25.02	46.8	152	-26.17	70.9	187	-26.32	85.5	77	27.84	105.8	250	3.18	131.8	290	3.65	157.8	291	-26.64	162.9	93	-18.80
22.8	113	-25.11	46.9	148	-26.29	71.0	183	-26.26	85.6	81	27.97	107.8	250	3.20	133.8	289	-0.18	157.9	287	-26.38	163.0	91	-17.95
22.9	110	-24.34	47.0	144	-26.31	71.1	179	-26.23	85.7	85	28.06	109.8	249	0.54	133.9	287	-15.11	158.0	283	-26.45	163.1	88	-17.14
23.0	106	-23.25	47.1	140	-26.15	71.2	175	-26.17	85.8	89	28.16	109.9	247	-14.65	134.0	283	-23.10	158.1	279	-26.43	163.2	86	-16.38
23.1	103	-22.16	47.2	136	-26.04	71.3	171	-26.05	85.9	93	28.29	110.0	243	-22.85	134.1	279	-25.87	158.2	275	-26.32	163.3	83	-15.67
23.2	100	-21.10	47.3	132	-25.95	71.4	167	-26.06	86.0	97	28.41	110.1	239	-25.56	134.2	275	-26.52	158.3	271	-26.27	163.4	81	-14.99
23.3	97	-20.11	47.4	128	-25.91	71.5	163	-25.92	86.1	101	28.56	110.2	235	-26.23	134.3	271	-26.54	158.4	267	-26.29	163.5	79	-14.34
23.4	94	-19.18	47.5	124	-26.57	71.6	159	-26.06	86.2	105	28.72	110.3	231	-26.31	134.4	267	-26.54	158.5	263	-26.21	163.6	77	-13.73

Time (min)	T_s (°C)	DSC (mW)	Time (min)	T_s (°C)	DSC (mW)	Time (min)	T_s (°C)	DSC (mW)	Time (min)	T_s (°C)	DSC (mW)	Time (min)	T_s (°C)	DSC (mW)	Time (min)	T_s (°C)	DSC (mW)	Time (min)	T_s (°C)	DSC (mW)	Time (min)	T_s (°C)	DSC (mW)
23.5	91	-18.30	47.6	120	-25.35	71.7	155	-25.89	86.3	109	28.86	110.4	227	-26.34	134.5	263	-26.48	158.6	259	-26.14	163.7	75	-13.17
23.6	89	-17.48	47.7	116	-25.27	71.8	151	-25.84	86.4	113	28.99	110.5	223	-26.28	134.6	259	-26.37	158.7	255	-26.18	163.8	74	-12.63
23.7	86	-16.70	47.8	114	-25.51	71.9	147	-25.80	86.5	117	29.16	110.6	219	-26.21	134.7	255	-26.32	158.8	251	-26.03	163.9	72	-12.10
23.8	85	-16.33	49.8	110	0.72	72.0	143	-25.77	86.6	121	29.30	110.7	215	-26.18	134.8	251	-26.26	158.9	247	-25.98	164.0	70	-11.64
25.8	70	-0.29	51.8	110	0.54	72.1	139	-25.72	86.7	125	29.43	110.8	211	-26.08	134.9	247	-26.19	159.0	243	-25.99	166.0	50	-5.73
27.8	70	-0.71	53.8	110	0.52	72.2	136	-25.66	86.8	129	29.66	110.9	207	-26.06	135.0	243	-26.23	159.1	239	-25.99			
29.8	70	-0.75	55.8	110	0.51	72.3	132	-25.56	86.9	133	29.80	111.0	203	-26.05	135.1	239	-26.07	159.2	235	-25.91			
31.8	70	-0.76	57.8	110	3.65	72.4	128	-25.50	87.0	137	29.93	111.1	199	-25.97	135.2	235	-26.03	159.3	231	-25.85			
33.8	71	2.03	57.9	113	15.90	72.5	124	-26.10	87.1	141	30.06	111.2	195	-26.00	135.3	233	-26.04	159.4	227	-25.88			
33.9	73	12.67	58.0	117	24.95	72.6	120	-25.10	87.2	145	30.32	111.3	193	-25.97	137.3	230	3.30	159.5	223	-25.83			
34.0	76	21.97	58.1	121	28.48	72.7	116	-24.86	87.3	147	30.36	113.3	190	2.64	139.3	230	3.30	159.6	219	-25.82			

Table 3.14. Reduced Dataset of DSC Signal as a Function of Time and Temperature for the Second Segment L Sample Run

Time (min)	T_s (°C)	DSC (mW)	Time (min)	T_s (°C)	DSC (mW)	Time (min)	T_s (°C)	DSC (mW)	Time (min)	T_s (°C)	DSC (mW)	Time (min)	T_s (°C)	DSC (mW)	Time (min)	T_s (°C)	DSC (mW)	Time (min)	T_s (°C)	DSC (mW)	Time (min)	T_s (°C)	DSC (mW)
168.0	41	-3.52	198.4	93	28.53	222.6	141	30.44	237.3	96	-19.82	261.5	157	26.57	285.7	205	32.63	309.9	253	34.17	324.6	179	-25.74
170.0	41	-1.73	198.5	97	28.67	222.7	145	30.50	237.4	93	-18.90	261.6	161	29.94	285.8	209	32.92	310.0	257	34.34	324.7	175	-25.70
172.0	41	-1.79	198.6	101	28.80	222.8	149	30.56	237.5	90	-18.05	261.7	165	31.20	285.9	213	33.12	310.1	261	34.47	324.8	171	-25.73
174.0	41	-1.79	198.7	105	28.94	222.9	153	30.77	237.6	88	-17.24	261.8	169	31.47	286.0	217	33.21	310.2	265	34.53	324.9	167	-25.71
174.1	41	3.48	198.8	109	29.06	223.0	157	30.79	237.7	86	-16.47	261.9	173	31.68	286.1	221	33.30	310.3	269	34.66	325.0	163	-25.62
174.2	44	13.03	198.9	113	29.20	223.1	161	30.95	237.8	83	-15.76	262.0	177	31.78	286.2	225	33.41	310.4	273	34.77	325.1	159	-25.65
174.3	48	20.74	199.0	117	29.32	223.2	165	31.01	237.9	81	-15.06	262.1	181	31.94	286.3	229	33.47	310.5	277	34.81	325.2	155	-25.68
174.4	52	24.67	199.1	121	29.41	223.3	169	31.25	238.0	79	-14.43	262.2	185	32.02	286.4	233	33.53	310.6	281	34.85	325.3	151	-25.60
174.5	56	26.35	199.2	125	29.56	223.4	173	31.31	238.1	77	-13.80	262.3	189	32.16	286.5	237	33.73	310.7	285	35.01	325.4	147	-25.61
174.6	60	27.11	199.3	129	29.70	223.5	177	31.57	238.2	75	-13.23	262.4	193	32.25	286.6	241	33.70	310.8	289	35.01	325.5	143	-25.57
174.7	65	27.49	199.4	133	29.91	223.6	181	31.67	238.3	73	-12.70	262.5	197	32.41	286.7	245	33.79	310.9	293	35.24	325.6	139	-25.55
174.8	69	27.62	199.5	137	30.00	223.7	185	31.78	238.4	72	-12.17	262.6	201	32.48	286.8	249	33.76	311.0	297	35.46	325.7	135	-25.50
174.9	73	27.70	199.6	141	30.11	223.8	189	31.97	238.5	70	-11.67	262.7	205	32.61	286.9	253	34.08	311.1	301	35.53	325.8	132	-25.45
175.0	77	27.79	199.7	145	30.27	223.9	193	32.06	240.5	49	-5.74	262.8	209	32.72	287.0	257	34.24	311.2	305	35.61	325.9	128	-25.46
175.1	81	27.89	199.8	149	30.39	224.0	197	32.19	242.5	41	-3.51	262.9	213	32.87	287.1	261	34.32	311.3	307	35.68	326.0	124	-26.43
175.2	85	28.01	199.9	153	30.51	224.1	201	32.35	244.5	41	-1.72	263.0	217	33.01	287.2	265	34.45	313.3	310	4.06	326.1	120	-24.94
175.3	89	28.11	200.0	157	30.63	224.2	205	32.48	246.5	41	-1.78	263.1	221	33.13	287.3	269	34.48	315.3	310	4.00	326.2	116	-25.02
175.4	93	28.21	200.1	161	30.77	224.3	207	32.55	248.5	41	-1.77	263.2	225	33.24	287.4	273	34.62	317.3	310	4.03	326.3	112	-24.83
175.5	97	28.34	200.2	165	31.01	226.3	210	2.76	248.6	41	3.53	263.3	229	33.25	287.5	277	34.78	319.3	310	3.99	326.4	109	-23.86
175.6	101	28.49	200.3	167	31.03	228.3	210	2.79	248.7	44	13.15	263.4	233	33.46	287.6	281	34.93	321.3	310	0.12	326.5	105	-22.76
175.7	105	28.65	202.3	170	1.92	230.3	210	2.80	248.8	48	20.85	263.5	237	33.61	287.7	285	35.09	321.4	307	-15.12	326.6	102	-21.70
175.8	109	28.81	204.3	170	1.98	232.3	210	2.80	248.9	52	24.78	263.6	241	33.46	287.8	287	35.12	321.5	303	-23.37	326.7	99	-20.68
175.9	113	28.95	206.3	170	1.96	234.3	210	-0.54	249.0	56	26.46	263.7	245	33.51	289.8	290	3.80	321.6	299	-25.82	326.8	96	-19.72

Time (min)	T_s (^oC)	DSC (mW)	Time (min)	T_s (^oC)	DSC (mW)	Time (min)	T_s (^oC)	DSC (mW)	Time (min)	T_s (^oC)	DSC (mW)	Time (min)	T_s (^oC)	DSC (mW)	Time (min)	T_s (^oC)	DSC (mW)	Time (min)	T_s (^oC)	DSC (mW)	Time (min)	T_s (^oC)	DSC (mW)
176.0	117	29.07	208.3	170	1.98	234.4	207	-13.04	249.1	60	27.18	263.8	247	33.76	291.8	290	3.93	321.7	295	-26.40	326.9	93	-18.80
176.1	121	29.25	210.3	170	-1.00	234.5	203	-21.50	249.2	65	27.51	265.8	250	3.33	293.8	290	3.89	321.8	291	-26.40	327.0	91	-17.95
176.2	125	29.42	210.4	168	-12.10	234.6	199	-24.72	249.3	69	27.67	267.8	250	3.36	295.8	290	3.89	321.9	287	-26.33	327.1	88	-17.15
176.3	127	29.52	210.5	164	-20.38	234.7	195	-25.78	249.4	73	27.73	269.8	250	3.49	297.8	289	0.03	322.0	283	-26.25	327.2	86	-16.38
178.3	130	0.96	210.6	160	-24.10	234.8	191	-26.03	249.5	77	27.83	271.8	250	3.41	297.9	287	-14.60	322.1	279	-26.27	327.3	83	-15.67
180.3	130	1.02	210.7	156	-25.48	234.9	187	-26.13	249.6	81	27.95	273.8	249	0.29	298.0	283	-22.86	322.2	275	-26.11	327.4	81	-14.98
182.3	130	1.03	210.8	152	-25.98	235.0	183	-26.10	249.7	85	28.03	273.9	247	-13.91	298.1	279	-25.54	322.3	271	-26.11	327.5	79	-14.35
184.3	130	1.02	210.9	148	-26.10	235.1	179	-26.06	249.8	89	28.15	274.0	243	-22.29	298.2	275	-26.03	322.4	267	-26.10	327.6	77	-13.75
186.3	130	-1.64	211.0	144	-26.01	235.2	175	-26.03	249.9	93	28.27	274.1	239	-25.04	298.3	271	-26.26	322.5	263	-26.09	327.7	75	-13.16
186.4	128	-10.87	211.1	140	-25.98	235.3	171	-26.00	250.0	97	28.39	274.2	235	-25.95	298.4	267	-26.25	322.6	259	-25.95	327.8	74	-12.62
186.5	125	-18.54	211.2	136	-25.88	235.4	167	-25.91	250.1	101	28.54	274.3	231	-26.12	298.5	263	-26.20	322.7	255	-26.02	327.9	72	-12.11
186.6	121	-24.50	211.3	132	-25.75	235.5	163	-25.89	250.2	105	28.66	274.4	227	-26.16	298.6	259	-26.11	322.8	251	-25.98	328.0	70	-11.62
186.7	117	-23.55	211.4	128	-25.71	235.6	159	-25.83	250.3	109	28.85	274.5	223	-26.12	298.7	255	-26.11	322.9	247	-25.94	330.0	50	-5.72
186.8	113	-24.88	211.5	124	-26.43	235.7	155	-25.84	250.4	113	28.99	274.6	219	-26.12	298.8	251	-26.03	323.0	243	-25.89			
186.9	110	-24.22	211.6	120	-25.20	235.8	151	-25.70	250.5	117	29.14	274.7	215	-26.01	298.9	247	-26.05	323.1	239	-25.89			
187.0	106	-23.22	211.7	116	-25.09	235.9	147	-25.71	250.6	121	29.28	274.8	211	-25.95	299.0	243	-26.01	323.2	235	-25.85			
187.1	103	-22.14	211.8	114	-25.40	236.0	143	-25.65	250.7	125	29.45	274.9	207	-25.94	299.1	239	-25.95	323.3	231	-25.80			
187.2	100	-21.11	213.8	110	0.73	236.1	139	-25.60	250.8	129	29.59	275.0	203	-25.86	299.2	235	-25.94	323.4	227	-25.76			
187.3	97	-20.11	215.8	110	0.52	236.2	136	-25.52	250.9	133	29.73	275.1	199	-25.85	299.3	233	-25.91	323.5	223	-25.77			
187.4	94	-19.18	217.8	110	0.54	236.3	132	-25.44	251.0	137	29.88	275.2	195	-25.86	301.3	230	3.40	323.6	219	-25.82			
187.5	91	-18.31	219.8	110	0.54	236.4	128	-25.43	251.1	141	29.98	275.3	193	-25.81	303.3	230	3.31	323.7	215	-25.71			
187.6	89	-17.49	221.8	110	3.64	236.5	124	-26.10	251.2	145	30.22	277.3	190	2.63	305.3	230	3.33	323.8	211	-25.79			
187.7	86	-16.71	221.9	113	14.98	236.6	120	-25.03	251.3	147	30.25	279.3	190	2.54	307.3	230	3.35	323.9	207	-25.75			
187.8	85	-16.33	222.0	117	24.07	236.7	116	-24.77	253.3	150	1.43	281.3	190	2.53	309.3	230	7.27	324.0	203	-25.77			
191.8	70	-0.68	222.1	121	28.00	236.8	112	-24.95	255.3	150	1.54	283.3	190	2.56	309.4	232	21.75	324.1	199	-25.72			
195.8	70	-0.71	222.2	125	29.40	236.9	109	-23.99	257.3	150	1.60	285.3	190	6.29	309.5	236	30.45	324.2	195	-25.71			
197.9	73	11.72	222.3	129	29.95	237.0	105	-22.88	259.3	150	1.55	285.4	193	19.93	309.6	240	33.18	324.3	191	-25.72			
198.1	80	25.61	222.4	133	30.14	237.1	102	-21.81	261.3	150	4.91	285.5	196	28.70	309.7	244	33.74	324.4	187	-25.71			
198.3	89	28.23	222.5	137	30.28	237.2	99	-20.79	261.4	153	17.80	285.6	200	31.72	309.8	249	33.86	324.5	183	-25.67			

Table 3.15. Reduced Dataset of DSC Signal as a Function of Time and Temperature for the Third Segment L Sample Run

Time (min)	T_s (°C)	DSC (Mw)	Time (min)	T_s (°C)	DSC (Mw)	Time (min)	T_s (°C)	DSC (Mw)	Time (min)	T_s (°C)	DSC (Mw)	Time (min)	T_s (°C)	DSC (Mw)	Time (min)	T_s (°C)	DSC (mW)	Time (min)	T_s (°C)	DSC (mW)	Time (min)	T_s (°C)	DSC (mW)
332.0	41	-3.52	361.9	73	11.71	386.1	121	28.02	400.8	112	-24.95	419.3	150	1.64	447.3	190	2.60	473.4	232	21.86	488.1	199	-25.72
334.0	41	-1.72	362.0	76	20.91	386.2	125	29.42	400.9	109	-24.00	421.3	150	1.19	449.3	190	6.31	473.5	236	30.41	488.2	195	-25.69
336.0	41	-1.78	362.1	80	25.60	386.3	129	29.95	401.0	105	-22.91	423.3	150	1.53	449.4	193	19.90	473.6	240	32.88	488.3	191	-25.68
338.0	41	-1.76	362.2	85	27.51	386.4	133	30.18	401.1	102	-21.83	425.3	150	4.94	449.5	196	28.65	473.7	244	33.62	488.4	187	-25.67
338.1	41	3.49	362.3	89	28.23	386.5	137	30.29	401.2	99	-20.80	425.4	153	17.79	449.6	200	31.67	473.8	249	34.14	488.5	183	-25.52
338.2	44	13.05	362.4	93	28.52	386.6	141	30.41	401.3	96	-19.83	425.5	157	26.63	449.7	205	32.61	473.9	253	34.28	488.6	179	-25.74
338.3	48	20.74	362.5	97	28.68	386.7	145	30.51	401.4	93	-18.92	425.6	161	29.93	449.8	209	32.95	474.0	257	34.38	488.7	175	-25.61
338.4	52	24.68	362.6	101	28.81	386.8	149	30.50	401.5	90	-18.06	425.7	165	31.15	449.9	213	33.11	474.1	261	34.49	488.8	171	-25.71
338.5	56	26.41	362.7	105	28.93	386.9	153	30.81	401.6	88	-17.24	425.8	169	31.56	450.0	217	33.20	474.2	265	34.58	488.9	167	-25.67
338.6	60	27.18	362.8	109	29.03	387.0	157	30.84	401.7	85	-16.49	425.9	173	31.74	450.1	221	33.29	474.3	269	34.61	489.0	163	-25.58
338.7	65	27.50	362.9	113	29.19	387.1	161	31.09	401.8	83	-15.76	426.0	177	31.91	450.2	225	33.35	474.4	273	34.72	489.1	159	-25.59
338.8	69	27.66	363.0	117	29.28	387.2	165	31.15	401.9	81	-15.08	426.1	181	31.93	450.3	229	33.41	474.5	277	34.86	489.2	155	-25.62
338.9	73	27.76	363.1	121	29.42	387.3	169	31.28	402.0	79	-14.44	426.2	185	32.05	450.4	233	33.58	474.6	281	34.95	489.3	151	-25.63
339.0	77	27.79	363.2	125	29.54	387.4	173	31.43	402.1	77	-13.81	426.3	189	32.20	450.5	237	33.62	474.7	285	34.93	489.4	147	-25.56
339.1	81	27.91	363.3	129	29.65	387.5	177	31.56	402.2	75	-13.24	426.4	193	32.29	450.6	241	33.34	474.8	289	35.08	489.5	143	-25.50
339.2	85	28.01	363.4	133	29.83	387.6	181	31.77	402.3	73	-12.69	426.5	197	32.40	450.7	245	33.64	474.9	293	35.33	489.6	139	-25.49
339.3	89	28.12	363.5	137	29.94	387.7	185	31.82	402.4	72	-12.17	426.6	201	32.45	450.8	249	33.93	475.0	297	35.39	489.7	135	-25.43
339.4	93	28.25	363.6	141	30.05	387.8	189	31.93	402.5	70	-11.67	426.7	205	32.61	450.9	253	34.05	475.1	301	35.49	489.8	132	-25.39
339.5	97	28.38	363.7	145	30.18	387.9	193	32.05	404.5	49	-5.74	426.8	209	32.73	451.0	257	34.21	475.2	305	35.67	489.9	128	-25.39
339.6	101	28.49	363.8	149	30.34	388.0	197	32.25	406.5	41	-3.51	426.9	213	32.89	451.1	261	34.28	475.3	307	35.64	490.0	124	-26.29
339.7	105	28.62	363.9	153	30.49	388.1	201	32.33	408.5	41	-1.70	427.0	217	32.99	451.2	265	34.37	477.3	310	4.08	490.1	120	-24.94
339.8	109	28.83	364.0	157	30.72	388.2	205	32.49	410.5	41	-1.75	427.1	221	33.13	451.3	269	34.48	479.3	310	4.05	490.2	116	-25.01
339.9	113	28.97	364.1	161	30.85	388.3	207	32.60	412.5	41	-1.74	427.2	225	33.24	451.4	273	34.61	481.3	310	3.97	490.3	112	-24.83
340.0	117	29.09	364.2	165	30.93	390.3	210	2.73	412.6	41	3.54	427.3	229	33.29	451.5	277	34.72	483.3	310	4.04	490.4	109	-23.84
340.1	121	29.23	364.3	167	31.01	392.3	210	2.81	412.7	44	13.10	427.4	233	33.52	451.6	281	34.80	485.3	309	0.16	490.5	105	-22.76
340.2	125	29.37	366.3	170	1.92	394.3	210	2.84	412.8	48	20.79	427.5	237	33.36	451.7	285	34.95	485.4	307	-15.19	490.6	102	-21.69
340.3	127	29.46	368.3	170	2.05	396.3	210	2.82	412.9	52	24.72	427.6	241	33.61	451.8	287	35.03	485.5	303	-23.31	490.7	99	-20.68
342.3	130	0.89	370.3	170	2.01	398.3	210	-0.52	413.0	56	26.37	427.7	245	33.75	453.8	290	3.92	485.6	299	-25.82	490.8	96	-19.71
344.3	130	1.05	372.3	170	2.08	398.4	207	-13.02	413.1	60	27.19	427.8	247	33.80	455.8	290	3.88	485.7	295	-26.40	490.9	93	-18.80
346.3	130	1.03	374.3	170	-1.03	398.5	203	-21.47	413.2	65	27.51	429.8	250	3.34	457.8	290	3.89	485.8	291	-26.45	491.0	91	-17.94
348.3	130	1.00	374.4	168	-12.08	398.6	199	-24.68	413.3	69	27.66	431.8	250	3.41	459.8	290	3.91	485.9	287	-26.27	491.1	88	-17.15
350.3	130	-1.65	374.5	164	-20.32	398.7	195	-25.74	413.4	73	27.73	433.8	250	3.43	461.8	289	0.02	486.0	283	-26.13	491.2	86	-16.37
350.4	128	-10.79	374.6	160	-24.08	398.8	191	-26.09	413.5	77	27.86	435.8	250	3.40	461.9	287	-14.69	486.1	279	-26.35	491.3	83	-15.66
350.5	125	-18.45	374.7	156	-25.49	398.9	187	-26.11	413.6	81	27.93	437.8	249	0.91	462.0	283	-22.58	486.2	275	-26.14	491.4	81	-14.99
350.6	121	-24.34	374.8	152	-25.91	399.0	183	-26.08	413.7	85	28.04	437.9	247	-13.81	462.1	279	-25.41	486.3	271	-26.16	491.5	79	-14.35
350.7	117	-23.55	374.9	148	-26.08	399.1	179	-26.02	413.8	89	28.14	438.0	243	-22.19	462.2	275	-26.11	486.4	267	-26.13	491.6	77	-13.75
350.8	113	-24.87	375.0	144	-26.04	399.2	175	-26.01	413.9	93	28.26	438.1	239	-25.08	462.3	271	-26.17	486.5	263	-26.09	491.7	75	-13.17
350.9	110	-24.26	375.1	140	-25.95	399.3	171	-26.03	414.0	97	28.38	438.2	235	-25.86	462.4	267	-26.24	486.6	259	-26.11	491.8	74	-12.62
351.0	106	-23.21	375.2	136	-25.82	399.4	167	-25.94	414.1	101	28.53	438.3	231	-26.04	462.5	263	-26.14	486.7	255	-25.95	491.9	72	-12.11
351.1	103	-22.15	375.3	132	-25.74	399.5	163	-25.83	414.2	105	28.66	438.4	227	-26.15	462.6	259	-26.12	486.8	251	-25.99	492.0	70	-11.62

Time (min)	T_s (°C)	DSC (Mw)	Time (min)	T_s (°C)	DSC (Mw)	Time (min)	T_s (°C)	DSC (Mw)	Time (min)	T_s (°C)	DSC (Mw)	Time (min)	T_s (°C)	DSC (Mw)	Time (min)	T_s (°C)	DSC (mW)	Time (min)	T_s (°C)	DSC (mW)	Time (min)	T_s (°C)	DSC (mW)
351.2	100	-21.12	375.4	128	-25.69	399.6	159	-25.79	414.3	109	28.81	438.5	223	-26.10	462.7	255	-26.10	486.9	247	-25.94	494.0	50	-5.74
351.3	97	-20.11	375.5	124	-26.30	399.7	155	-25.71	414.4	113	28.99	438.6	219	-26.00	462.8	251	-26.06	487.0	243	-25.92			
351.4	94	-19.19	375.6	120	-25.21	399.8	151	-25.74	414.5	117	29.11	438.7	215	-26.01	462.9	247	-26.04	487.1	239	-25.91			
351.5	91	-18.32	375.7	116	-25.02	399.9	147	-25.74	414.6	121	29.26	438.8	211	-25.96	463.0	243	-26.02	487.2	235	-25.88			
351.6	89	-17.51	375.8	114	-25.40	400.0	143	-25.68	414.7	125	29.41	438.9	207	-25.88	463.1	239	-25.93	487.3	231	-25.83			
351.7	86	-16.71	377.8	110	0.72	400.1	139	-25.56	414.8	129	29.55	439.0	203	-25.85	463.2	235	-25.95	487.4	227	-25.83			
351.8	85	-16.35	379.8	110	0.57	400.2	136	-25.50	414.9	133	29.66	439.1	199	-25.86	463.3	233	-25.89	487.5	223	-25.73			
353.8	70	-0.28	381.8	110	0.57	400.3	132	-25.49	415.0	137	29.75	439.2	195	-25.84	465.3	230	3.40	487.6	219	-25.82			
355.8	70	-0.69	383.8	110	0.57	400.4	128	-25.44	415.1	141	29.99	439.3	193	-25.83	467.3	230	3.34	487.7	215	-25.84			
357.8	70	-0.69	385.8	110	3.64	400.5	124	-25.94	415.2	145	30.15	441.3	190	2.65	469.3	230	3.35	487.8	211	-25.76			
359.8	70	-0.71	385.9	113	14.92	400.6	120	-25.04	415.3	147	30.20	443.3	190	2.58	471.3	230	3.33	487.9	207	-25.77			
361.8	71	2.08	386.0	117	24.05	400.7	116	-24.69	417.3	150	1.52	445.3	190	2.58	473.3	230	7.24	488.0	203	-25.71			

Table 3.16. Reduced Dataset of DSC Signal as a Function of Time and Temperature for the Fourth Segment L Sample Run

Time (min)	T_s (°C)	DSC (mW)	Time (min)	T_s (°C)	DSC (mW)	Time (min)	T_s (°C)	DSC (mW)	Time (min)	T_s (°C)	DSC (mW)	Time (min)	T_s (°C)	DSC (mW)	Time (min)	T_s (°C)	DSC (mW)	Time (min)	T_s (°C)	DSC (mW)	Time (min)	T_s (°C)	DSC (mW)
496.0	41	-3.52	525.9	73	11.72	550.1	121	28.04	564.8	112	-24.94	589.5	157	26.54	614.2	225	33.33	638.9	293	35.32	653.6	139	-25.52
498.0	41	-1.72	526.0	76	20.95	550.2	125	29.50	564.9	109	-23.98	589.6	161	30.01	614.3	229	33.38	639.0	297	35.38	653.7	135	-25.48
500.0	41	-1.78	526.1	80	25.60	550.3	129	29.98	565.0	105	-22.88	589.7	165	31.04	614.4	233	33.61	639.1	301	35.53	653.8	131	-25.40
502.0	41	-1.78	526.2	85	27.53	550.4	133	30.26	565.1	102	-21.81	589.8	169	31.50	614.5	237	33.46	639.2	305	35.58	653.9	128	-25.37
502.1	41	3.50	526.3	89	28.24	550.5	137	30.35	565.2	99	-20.79	589.9	173	31.70	614.6	241	33.55	639.3	307	35.57	654.0	124	-26.20
502.2	44	13.01	526.4	93	28.55	550.6	141	30.46	565.3	96	-19.83	590.0	177	31.85	614.7	245	33.78	641.3	310	4.03	654.1	120	-24.94
502.3	48	20.75	526.5	97	28.71	550.7	145	30.59	565.4	93	-18.91	590.1	181	31.94	614.8	249	33.95	643.3	310	4.07	654.2	116	-24.99
502.4	52	24.64	526.6	101	28.83	550.8	149	30.67	565.5	90	-18.05	590.2	185	32.04	614.9	253	34.09	645.3	310	3.99	654.3	112	-24.84
502.5	56	26.36	526.7	105	28.96	550.9	153	30.86	565.6	88	-17.25	590.3	189	32.20	615.0	257	34.23	647.3	310	3.99	654.4	109	-23.86
502.6	60	27.13	526.8	109	29.07	551.0	157	30.88	565.7	86	-16.48	590.4	193	32.28	615.1	261	34.30	649.3	309	0.08	654.5	105	-22.78
502.7	65	27.43	526.9	113	29.17	551.1	161	31.07	565.8	83	-15.75	590.5	197	32.40	615.2	265	34.42	649.4	307	-15.22	654.6	102	-21.70
502.8	69	27.65	527.0	117	29.31	551.2	165	31.09	565.9	81	-15.07	590.6	201	32.50	615.3	269	34.54	649.5	303	-23.34	654.7	99	-20.69
502.9	73	27.75	527.1	121	29.47	551.3	169	31.25	566.0	79	-14.43	590.7	205	32.63	615.4	273	34.70	649.6	299	-25.90	654.8	96	-19.72
503.0	77	27.82	527.2	125	29.52	551.4	173	31.38	566.1	77	-13.82	590.8	209	32.75	615.5	277	34.81	649.7	295	-26.47	654.9	93	-18.81
503.1	81	27.90	527.3	129	29.68	551.5	177	31.54	566.2	75	-13.24	590.9	213	32.89	615.6	281	34.93	649.8	291	-26.48	655.0	91	-17.95
503.2	85	28.02	527.4	133	29.80	551.6	181	31.67	566.3	73	-12.70	591.0	217	32.99	615.7	285	35.06	649.9	287	-26.03	655.1	88	-17.15
503.3	89	28.13	527.5	137	30.01	551.7	185	31.81	566.4	72	-12.18	591.1	221	33.10	615.8	287	34.99	650.0	283	-26.34	655.2	86	-16.39
503.4	93	28.26	527.6	141	30.15	551.8	189	31.95	566.5	70	-11.68	591.2	225	33.17	617.8	290	3.86	650.1	279	-26.27	655.3	83	-15.67
503.5	97	28.36	527.7	145	30.45	551.9	193	32.08	570.5	41	-3.51	591.3	229	33.43	619.8	290	3.87	650.2	275	-26.23	655.4	81	-14.99
503.6	101	28.52	527.8	149	30.40	552.0	197	32.23	574.5	41	-1.76	591.4	233	33.34	621.8	290	3.90	650.3	271	-26.03	655.5	79	-14.35
503.7	105	28.65	527.9	153	30.58	552.1	201	32.33	576.6	41	3.53	591.5	237	33.35	623.8	290	3.92	650.4	267	-26.14	655.6	77	-13.75
503.8	109	28.81	528.0	157	30.65	552.2	205	32.48	576.8	48	20.77	591.6	241	33.71	625.8	289	0.00	650.5	263	-26.10	655.7	75	-13.17

Time (min)	T_s (°C)	DSC (mW)	Time (min)	T_s (°C)	DSC (mW)	Time (min)	T_s (°C)	DSC (mW)	Time (min)	T_s (°C)	DSC (mW)	Time (min)	T_s (°C)	DSC (mW)	Time (min)	T_s (°C)	DSC (mW)	Time (min)	T_s (°C)	DSC (mW)	Time (min)	T_s (°C)	DSC (mW)
503.9	113	28.96	528.1	161	30.83	552.3	207	32.56	577.0	56	26.37	591.7	245	33.74	625.9	287	-14.76	650.6	259	-26.04	655.8	74	-12.63
504.0	117	29.11	528.2	165	30.95	554.3	210	2.73	577.1	60	27.16	591.8	247	33.82	626.0	283	-22.72	650.7	255	-26.01	655.9	72	-12.12
504.1	121	29.28	528.3	167	31.10	556.3	210	2.83	577.2	65	27.52	593.8	250	3.35	626.1	279	-25.48	650.8	251	-26.00	656.0	70	-11.63
504.2	125	29.38	530.3	170	1.97	558.3	210	2.84	577.3	69	27.69	595.8	250	3.43	626.2	275	-26.03	650.9	247	-25.96	658.0	50	-5.72
504.3	127	29.48	532.3	170	2.08	560.3	210	2.82	577.4	73	27.72	597.8	250	3.43	626.3	271	-26.14	651.0	243	-25.88			
506.3	130	1.01	534.3	170	2.05	562.3	210	-0.54	577.5	77	27.83	599.8	250	3.42	626.4	267	-26.25	651.1	239	-25.81			
508.3	130	1.04	536.3	170	1.94	562.4	207	-13.01	577.6	81	27.93	601.8	249	0.89	626.5	263	-26.18	651.2	235	-25.84			
510.3	130	0.98	538.3	170	-1.07	562.5	203	-21.43	577.7	85	28.04	601.9	247	-13.88	626.6	259	-26.15	651.3	231	-25.80			
512.3	130	1.08	538.4	167	-12.08	562.6	199	-24.65	577.8	89	28.16	602.0	243	-22.23	626.7	255	-26.11	651.4	227	-25.86			
514.3	130	-1.67	538.5	164	-20.35	562.7	195	-25.72	577.9	93	28.26	602.1	239	-25.05	626.8	251	-25.99	651.5	223	-25.83			
514.4	128	-10.84	538.6	160	-24.05	562.8	191	-26.04	578.0	97	28.39	602.2	235	-25.90	626.9	247	-26.07	651.6	219	-25.73			
514.5	125	-18.48	538.7	156	-25.48	562.9	187	-26.13	578.1	101	28.57	602.3	231	-26.04	627.0	243	-25.95	651.7	215	-25.75			
514.6	121	-24.23	538.8	152	-25.95	563.0	183	-26.05	578.2	105	28.69	602.4	227	-26.10	627.1	239	-25.94	651.8	211	-25.71			
514.7	117	-23.56	538.9	148	-26.04	563.1	179	-26.02	578.3	109	28.83	602.5	223	-26.06	627.2	235	-25.92	651.9	207	-25.70			
514.8	113	-24.89	539.0	144	-26.02	563.2	175	-26.03	578.4	113	28.98	602.6	219	-25.98	627.3	233	-25.91	652.0	203	-25.69			
514.9	110	-24.24	539.1	140	-25.95	563.3	171	-25.96	578.5	117	29.19	602.7	215	-25.95	631.3	230	3.33	652.1	199	-25.65			
515.0	106	-23.22	539.2	136	-25.88	563.4	167	-25.89	578.6	121	29.28	602.8	211	-25.92	635.3	230	3.33	652.2	195	-25.71			
515.1	103	-22.16	539.3	132	-25.77	563.5	163	-25.86	578.7	125	29.45	602.9	207	-25.88	637.4	232	21.98	652.3	191	-25.67			
515.2	100	-21.12	539.4	128	-25.73	563.6	159	-25.72	578.8	129	29.64	603.0	203	-25.87	637.6	240	32.97	652.4	187	-25.73			
515.3	97	-20.13	539.5	124	-26.27	563.7	155	-25.79	578.9	133	29.77	603.1	199	-25.83	637.8	249	34.14	652.5	183	-25.65			
515.4	94	-19.21	539.6	120	-25.22	563.8	151	-25.77	579.0	137	29.96	603.2	195	-25.82	637.9	253	34.27	652.6	179	-25.68			
515.5	91	-18.32	539.7	116	-25.05	563.9	147	-25.68	579.1	141	30.05	603.3	193	-25.83	638.0	257	34.42	652.7	175	-25.70			
515.6	89	-17.50	539.8	114	-25.40	564.0	143	-25.67	579.2	145	30.27	607.3	190	2.56	638.1	261	34.49	652.8	171	-25.63			
515.7	86	-16.72	541.8	110	0.77	564.1	139	-25.55	579.3	147	30.31	611.3	190	2.53	638.2	265	34.60	652.9	167	-25.71			
515.8	85	-16.35	543.8	110	0.57	564.2	135	-25.55	581.3	150	1.50	613.4	193	19.99	638.3	269	34.69	653.0	163	-25.55			
517.8	70	-0.28	545.8	110	0.54	564.3	132	-25.44	583.3	150	1.49	613.6	201	31.69	638.4	273	34.79	653.1	159	-25.62			
519.8	70	-0.68	547.8	110	0.56	564.4	128	-25.38	585.3	150	1.55	613.8	209	32.96	638.5	277	34.78	653.2	155	-25.55			
521.8	70	-0.73	549.8	110	3.69	564.5	124	-25.95	587.3	150	1.46	613.9	213	33.09	638.6	281	34.93	653.3	151	-25.63			
523.8	70	-0.70	549.9	113	14.97	564.6	120	-25.03	589.3	150	4.93	614.0	217	33.21	638.7	285	34.98	653.4	147	-25.59			
525.8	71	2.07	550.0	117	24.07	564.7	116	-24.71	589.4	153	17.75	614.1	221	33.33	638.8	289	35.05	653.5	143	-25.64			

Table 3.17. Reduced Dataset of DSC Signal as a Function of Time and Temperature for the Fifth Segment L Sample Run

Time (min)	T_s (°C)	DSC (mW)	Time (min)	T_s (°C)	DSC (mW)	Time (min)	T_s (°C)	DSC (mW)	Time (min)	T_s (°C)	DSC (mW)	Time (min)	T_s (°C)	DSC (mW)	Time (min)	T_s (°C)	DSC (mW)	Time (min)	T_s (°C)	DSC (mW)	Time (min)	T_s (°C)	DSC (mW)
660.0	41	-3.52	689.9	73	11.78	714.1	121	28.04	728.8	112	-24.95	747.3	150	1.60	775.3	190	2.56	801.4	232	21.95	816.1	199	-25.74
662.0	41	-1.73	690.0	76	21.00	714.2	125	29.42	728.9	109	-24.00	749.3	150	1.59	777.3	190	6.32	801.5	236	30.32	816.2	195	-25.73
664.0	41	-1.78	690.1	80	25.63	714.3	129	29.99	729.0	105	-22.91	751.3	150	1.62	777.4	193	20.02	801.6	240	32.86	816.3	191	-25.73
666.0	41	-1.77	690.2	85	27.54	714.4	133	30.16	729.1	102	-21.83	753.3	150	4.96	777.5	196	28.75	801.7	244	33.88	816.4	187	-25.76
666.1	41	3.52	690.3	89	28.25	714.5	137	30.34	729.2	99	-20.81	753.4	153	17.88	777.6	201	31.75	801.8	249	34.13	816.5	183	-25.68
666.2	44	13.06	690.4	93	28.56	714.6	141	30.42	729.3	96	-19.84	753.5	157	26.68	777.7	205	32.65	801.9	253	34.26	816.6	179	-25.72
666.3	48	20.77	690.5	97	28.71	714.7	145	30.49	729.4	93	-18.93	753.6	161	29.86	777.8	209	32.96	802.0	257	34.33	816.7	175	-25.70
666.4	52	24.73	690.6	101	28.84	714.8	149	30.62	729.5	90	-18.06	753.7	165	31.18	777.9	213	33.13	802.1	261	34.44	816.8	171	-25.72
666.5	56	26.42	690.7	105	28.95	714.9	153	30.71	729.6	88	-17.25	753.8	169	31.54	778.0	217	33.22	802.2	265	34.54	816.9	167	-25.70
666.6	60	27.17	690.8	109	29.09	715.0	157	30.92	729.7	85	-16.49	753.9	173	31.71	778.1	221	33.33	802.3	269	34.60	817.0	163	-25.64
666.7	65	27.55	690.9	113	29.18	715.1	161	31.04	729.8	83	-15.76	754.0	177	31.82	778.2	225	33.38	802.4	273	34.66	817.1	159	-25.67
666.8	69	27.64	691.0	117	29.32	715.2	165	31.05	729.9	81	-15.09	754.1	181	31.94	778.3	229	33.40	802.5	277	34.77	817.2	155	-25.62
666.9	73	27.73	691.1	121	29.45	715.3	169	31.29	730.0	79	-14.43	754.2	185	32.08	778.4	233	33.70	802.6	281	34.85	817.3	151	-25.65
667.0	77	27.82	691.2	125	29.61	715.4	173	31.40	730.1	77	-13.82	754.3	189	32.21	778.5	237	33.48	802.7	285	34.97	817.4	147	-25.55
667.1	81	27.90	691.3	129	29.71	715.5	177	31.61	730.2	75	-13.24	754.4	193	32.27	778.6	241	33.46	802.8	289	35.03	817.5	143	-25.58
667.2	85	28.05	691.4	133	29.85	715.6	181	31.69	730.3	73	-12.69	754.5	197	32.40	778.7	245	33.86	802.9	293	35.18	817.6	139	-25.56
667.3	89	28.14	691.5	137	29.90	715.7	185	31.79	730.4	72	-12.17	754.6	201	32.51	778.8	249	33.94	803.0	297	35.29	817.7	135	-25.47
667.4	93	28.27	691.6	141	30.13	715.8	189	31.94	730.5	70	-11.64	754.7	205	32.62	778.9	253	34.04	803.1	301	35.43	817.8	131	-25.43
667.5	97	28.38	691.7	145	30.26	715.9	193	32.10	732.5	49	-5.74	754.8	209	32.76	779.0	257	34.24	803.2	305	35.49	817.9	128	-25.38
667.6	101	28.52	691.8	149	30.35	716.0	197	32.23	734.5	41	-3.51	754.9	213	32.90	779.1	261	34.34	803.3	307	35.50	818.0	124	-26.10
667.7	105	28.70	691.9	153	30.46	716.1	201	32.35	736.5	41	-1.71	755.0	217	33.00	779.2	265	34.41	805.3	310	4.07	818.1	120	-24.95
667.8	109	28.83	692.0	157	30.61	716.2	205	32.45	738.5	41	-1.77	755.1	221	33.08	779.3	269	34.49	807.3	310	4.13	818.2	116	-24.94
667.9	113	28.97	692.1	161	30.82	716.3	207	32.56	740.5	41	-1.74	755.2	225	33.18	779.4	273	34.60	809.3	310	4.00	818.3	112	-24.85
668.0	117	29.17	692.2	165	31.03	718.3	210	2.77	740.6	41	3.58	755.3	229	33.31	779.5	277	34.70	811.3	310	4.06	818.4	109	-23.87
668.1	121	29.27	692.3	167	31.05	720.3	210	2.83	740.7	44	13.17	755.4	233	33.37	779.6	281	34.76	813.3	309	0.06	818.5	105	-22.79
668.2	125	29.42	694.3	170	1.87	722.3	210	2.72	740.8	48	20.86	755.5	237	33.16	779.7	285	34.89	813.4	307	-15.25	818.6	102	-21.72
668.3	127	29.50	696.3	170	2.03	724.3	210	2.84	740.9	52	24.82	755.6	241	33.57	779.8	287	35.01	813.5	303	-23.41	818.7	99	-20.70
670.3	130	0.91	698.3	170	2.04	726.3	210	-0.55	741.0	56	26.50	755.7	245	33.78	781.8	290	3.82	813.6	299	-25.82	818.8	96	-19.73
672.3	130	1.03	700.3	170	2.02	726.4	207	-13.06	741.1	60	27.21	755.8	247	33.78	783.8	290	3.94	813.7	295	-26.42	818.9	93	-18.82
674.3	130	1.09	702.3	170	-1.05	726.5	203	-21.45	741.2	65	27.51	757.8	250	3.37	785.8	290	3.89	813.8	291	-26.47	819.0	91	-17.96
676.3	130	1.09	702.4	167	-12.09	726.6	199	-24.68	741.3	69	27.59	759.8	250	3.39	787.8	290	3.87	813.9	287	-26.37	819.1	88	-17.16
678.3	130	-1.67	702.5	164	-20.41	726.7	195	-25.75	741.4	73	27.77	761.8	250	3.45	789.8	289	-0.02	814.0	283	-26.01	819.2	86	-16.39
678.4	128	-10.89	702.6	160	-24.03	726.8	191	-26.06	741.5	77	27.83	763.8	250	3.40	789.9	287	-14.81	814.1	279	-26.24	819.3	83	-15.68
678.5	125	-18.52	702.7	156	-25.40	726.9	187	-26.11	741.6	81	27.93	765.8	249	0.79	790.0	283	-22.83	814.2	275	-26.26	819.4	81	-15.01
678.6	121	-24.07	702.8	152	-25.95	727.0	183	-26.04	741.7	85	28.04	765.9	247	-13.89	790.1	279	-25.45	814.3	271	-26.05	819.5	79	-14.36
678.7	117	-23.58	702.9	148	-26.00	727.1	179	-26.04	741.8	89	28.17	766.0	243	-22.30	790.2	275	-26.03	814.4	267	-26.13	819.6	77	-13.76
678.8	113	-24.90	703.0	144	-26.01	727.2	175	-26.01	741.9	93	28.29	766.1	239	-25.05	790.3	271	-26.20	814.5	263	-26.11	819.7	75	-13.17
678.9	110	-24.25	703.1	140	-25.96	727.3	171	-25.93	742.0	97	28.42	766.2	235	-25.90	790.4	267	-26.26	814.6	259	-26.01	819.8	74	-12.63
679.0	106	-23.24	703.2	136	-25.86	727.4	167	-25.90	742.1	101	28.53	766.3	231	-26.11	790.5	263	-26.15	814.7	255	-26.00	819.9	72	-12.11
679.1	103	-22.16	703.3	132	-25.76	727.5	163	-25.83	742.2	105	28.69	766.4	227	-26.13	790.6	259	-26.16	814.8	251	-25.92			

Time (min)	T_s (°C)	DSC (mW)	Time (min)	T_s (°C)	DSC (mW)	Time (min)	T_s (°C)	DSC (mW)	Time (min)	T_s (°C)	DSC (mW)	Time (min)	T_s (°C)	DSC (mW)	Time (min)	T_s (°C)	DSC (mW)	Time (min)	T_s (°C)	DSC (mW)	Time (min)	T_s (°C)	DSC (mW)
679.2	100	-21.13	703.4	128	-25.67	727.6	159	-25.80	742.3	109	28.85	766.5	223	-26.05	790.7	255	-26.06	814.9	247	-25.94			
679.3	97	-20.13	703.5	124	-26.15	727.7	155	-25.86	742.4	113	28.98	766.6	219	-26.00	790.8	251	-26.02	815.0	243	-25.95			
679.4	94	-19.20	703.6	120	-25.21	727.8	151	-25.73	742.5	117	29.15	766.7	215	-26.01	790.9	247	-26.00	815.1	239	-25.88			
679.5	91	-18.33	703.7	116	-25.00	727.9	147	-25.63	742.6	121	29.32	766.8	211	-25.91	791.0	243	-26.00	815.2	235	-25.87			
679.6	89	-17.50	703.8	114	-25.41	728.0	143	-25.65	742.7	125	29.39	766.9	207	-25.92	791.1	239	-25.91	815.3	231	-25.87			
679.7	86	-16.72	705.8	110	0.74	728.1	139	-25.58	742.8	129	29.54	767.0	203	-25.85	791.2	235	-25.81	815.4	227	-25.81			
679.8	85	-16.35	707.8	110	0.57	728.2	135	-25.55	742.9	133	29.71	767.1	199	-25.88	791.3	233	-25.90	815.5	223	-25.76			
681.8	70	-0.29	709.8	110	0.56	728.3	132	-25.43	743.0	137	29.89	767.2	195	-25.89	793.3	230	3.41	815.6	219	-25.77			
683.8	70	-0.70	711.8	110	0.56	728.4	128	-25.42	743.1	141	30.04	767.3	193	-25.84	795.3	230	3.34	815.7	215	-25.78			
685.8	70	-0.77	713.8	110	3.68	728.5	124	-25.85	743.2	145	30.14	769.3	190	2.69	797.3	230	3.34	815.8	211	-25.76			
687.8	70	-0.76	713.9	113	15.00	728.6	120	-25.05	743.3	147	30.23	771.3	190	2.62	799.3	230	3.35	815.9	207	-25.76			
689.8	71	2.05	714.0	117	24.11	728.7	116	-24.69	745.3	150	1.54	773.3	190	2.56	801.3	230	7.17	816.0	203	-25.77			

3.4 Laser Flash Analysis

The laser flash analysis results presented in this section are organized according to fuel segment identification.

3.4.1 Segment K

The LFA sample obtained from Segment K measured approximately 9.0 mm long by 9.0 mm wide, 1.370 mm thick, and weighed 548.4 mg. Photographs of the sample before coating with graphite and being subjected to LFA and after the LFA measurements are provided in Figure 3.15. The fuel meat within the AA6061 cladding can be clearly observed in Figure 3.15. The sample did not experience any noticeable delamination as a result of LFA and the graphite coating remained intact.

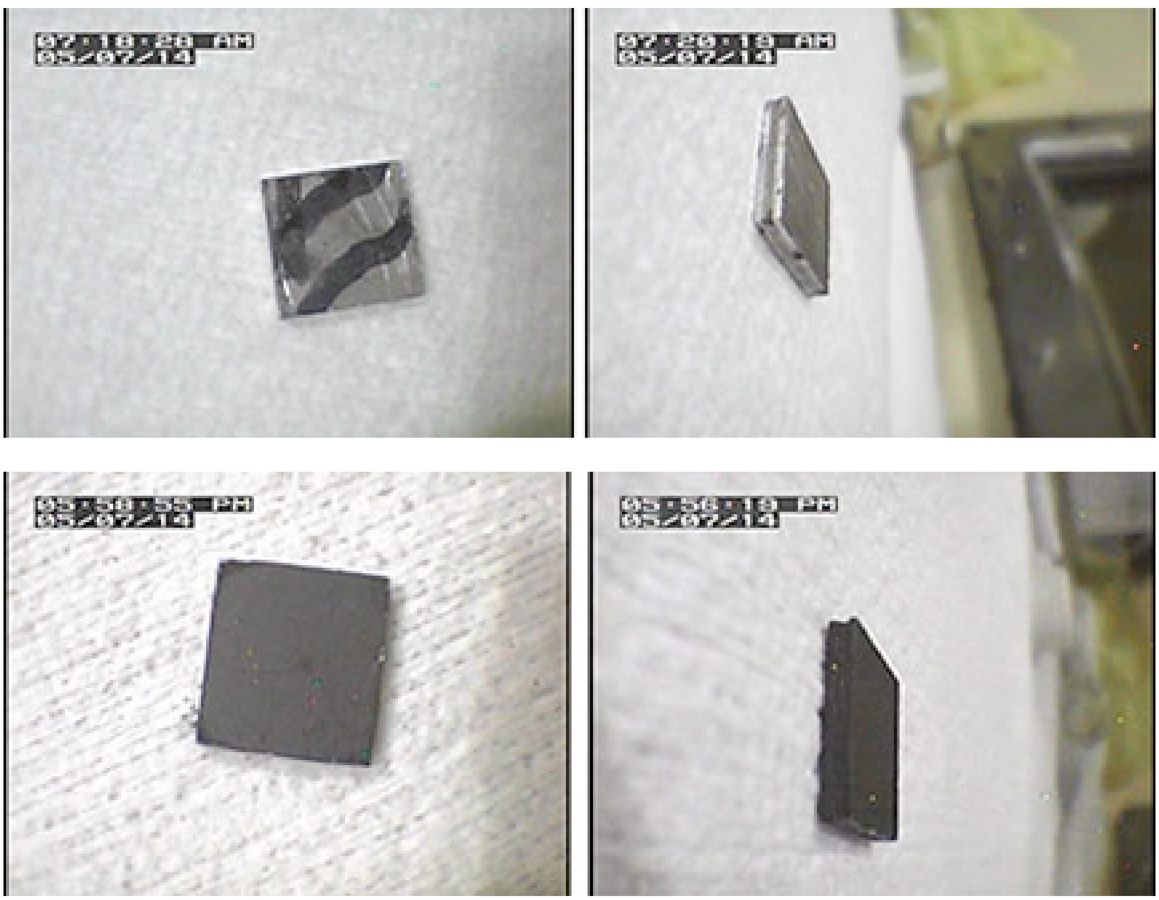

Figure 3.15. Photographs of the TK Sample for LFA Before Coating with Graphite and Being Subjected to LFA (top) and After the LFA Measurements (bottom)

The LFA sample was subjected to the thermal profile provided in Table 2.3. Results of the LFA measurements are provided in Table 3.18. The results presented in Table 3.18 have been converted using the Cape-Lehman + Pulse Correction model, and the overall sample thickness was determined using a micrometer in the hot cell (1.370 mm). Note that data highlighted with an asterisk was considered abnormal because the sample temperature deviated significantly from the program temperature.

Table 3.18. LFA Measurements for Sample TK-LFA1

Temperature (°C)	Thermal Diffusivity ($mm^2 \cdot sec^{-1}$)	Temperature (°C)	Thermal Diffusivity ($mm^2 \cdot sec^{-1}$)	Temperature (°C)	Thermal Diffusivity ($mm^2 \cdot sec^{-1}$)
25.46	5.104	99.78	5.816	250.21	7.121
25.29	5.063	99.86	5.820	250.02	7.127
25.12	5.055	99.89	5.804	250.04	7.116
24.98	5.063	99.91	5.831	250.07	7.123
24.82	5.082	73.25*	5.545*	250.05	7.125
48.17	5.358	74.19	5.577	300.44	7.448
48.39	5.302	74.64	5.520	300.31	7.426
49.31	5.367	74.76	5.557	300.14	7.422
49.49	5.391	74.84	5.600	300.06	7.403
49.78	5.352	74.90	5.558	299.99	7.390
73.90	5.534	47.28*	5.297*	299.95	7.380
73.82	5.620	49.02	5.288	299.92	7.366
74.43	5.579	49.46	5.251	299.90	7.363
74.72	5.562	49.67	5.285	299.89	7.369
74.78	5.579	49.83	5.284	299.88	7.377
99.30	5.837	49.85	5.319	249.03	6.990
99.50	5.828	28.07*	5.078*	249.48	6.984
99.80	5.829	26.82	5.059	249.70	6.980
99.90	5.846	26.47	5.129	249.83	6.967
99.92	5.851	26.13	5.140	249.88	6.976
125.14	6.068	25.86	5.034	199.14	6.581
125.07	6.065	25.58	4.986	199.57	6.574
125.01	6.048	149.49	6.430	199.77	6.579
124.96	6.055	149.71	6.287	199.86	6.556
124.94	6.058	149.84	6.285	199.89	6.585
124.92	6.048	149.90	6.282	148.99	6.153
124.90	6.055	149.93	6.296	149.50	6.140
124.91	6.057	199.71	6.719	149.73	6.159
124.90	6.055	199.95	6.720	149.83	6.149
124.88	6.049	200.02	6.723	149.89	6.154
98.98	5.817	200.03	6.733		
99.52	5.806	200.03	6.729		

*Data not included in calculations due to deviation from ideal temperature during measurement

3.4.2 Segment L

The LFA sample obtained from Segment L measured approximately 9.0 mm long by 9.0 mm wide, 1.367 mm thick, and weighed 592.9 mg. Photographs of the sample before coating with graphite and being subjected to LFA and after the LFA measurements are provided in Figure 3.16. The fuel meat within the AA6061 cladding can be clearly observed in Figure 3.16. The sample did not experience any noticeable delamination as a result of LFA.

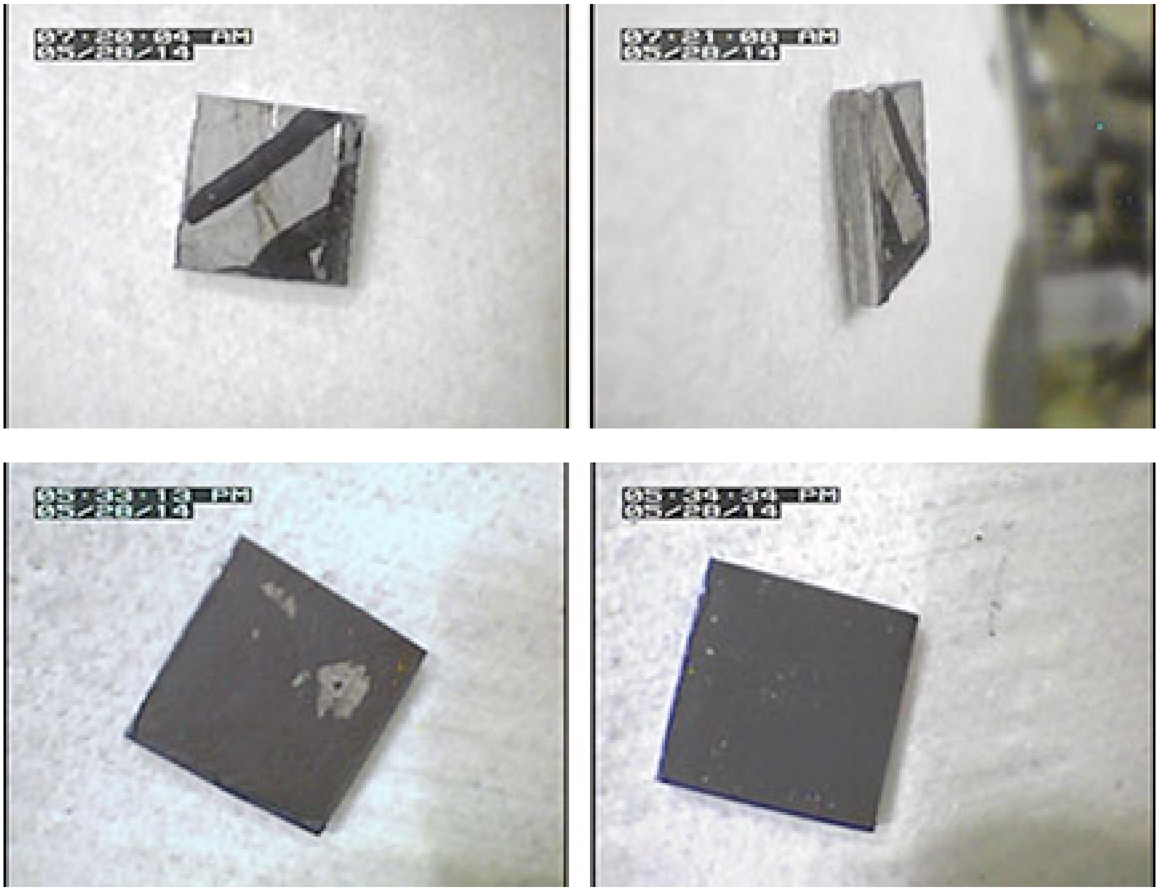

Figure 3.16. Photographs of the TL Sample for LFA Before Coating with Graphite and Being Subjected to LFA (top) and After the LFA Measurements (bottom). Note that the graphite coating was intact at the end of the measurement but spalled off when the vacuum tool was used to remove the sample from the sample holder (bottom left).

The LFA sample was subjected to the thermal profile provided in Table 2.3. The results presented in Table 3.19 have been converted using the Cape-Lehman + Pulse Correction model and the sample thickness determined using a micrometer in the hot cell (1.367 mm). Note that data highlighted with an asterisk was considered abnormal because the sample temperature deviated significantly from the program temperature.

Table 3.19. LFA Measurements for Sample TL-LFA1

Temperature (°C)	Thermal Diffusivity (mm^2•sec^{-1})	Temperature (°C)	Thermal Diffusivity (mm^2•sec^{-1})	Temperature (°C)	Thermal Diffusivity (mm^2•sec^{-1})
25.31	9.244	99.74	10.380	250.35	12.072
25.12	9.116	99.84	10.364	250.22	12.075
24.97	8.983	99.88	10.345	250.09	12.079
24.83	8.963	99.91	10.376	250.10	12.069
24.69	9.013	73.38*	9.994*	250.06	12.078
48.12	9.576	74.16	10.001	300.48	12.291
48.36	9.371	74.62	9.903	300.33	12.302
49.27	9.402	74.76	10.016	300.16	12.278
49.53	9.589	74.85	10.005	300.08	12.263
49.75	9.571	74.90	9.904	300.00	12.240
73.95	9.858	47.30*	9.511*	299.96	12.240
73.78	9.980	48.97	9.655	299.93	12.271
74.43	9.947	49.40	9.407	299.91	12.250
74.69	9.977	49.66	9.471	299.90	12.212
74.78	9.994	49.79	9.496	299.88	12.199
99.59	10.369	49.85	9.641	249.02	11.736
99.43	10.356	28.08*	9.079*	249.46	11.719
99.53	10.400	26.83	8.991	249.68	11.725
99.75	10.354	26.49	9.206	249.82	11.720
99.90	10.382	26.17	9.005	249.88	11.710
126.37	10.750	25.89	9.091	199.04	11.158
125.62	10.742	25.65	9.309	199.52	11.168
125.21	10.727	149.56	11.108	199.74	11.165
125.03	10.723	149.77	11.077	199.85	11.176
124.94	10.728	149.87	11.069	199.88	11.149
124.92	10.742	149.90	11.080	148.93	10.542
124.91	10.737	149.93	11.090	149.43	10.530
124.90	10.747	199.37	11.656	149.69	10.536
124.89	10.734	199.56	11.621	149.83	10.528
124.88	10.729	199.87	11.656	149.89	10.575
98.95	10.356	199.98	11.669		
99.50	10.368	200.01	11.652		

*Data not included in calculations due to deviation from ideal temperature during measurement

As observed in Table 3.19, the thermal diffusivity was observed to decrease more dramatically than expected upon cooling from 300°C. The graphite coating remained intact during the measurement, but small bubbles were observed upon completion of the measurement for both TL- and TK-LFA samples. At the request of the customer, the TL-LFA sample was removed from the LFA instrument followed by removal of the graphite coating. Sample TL-LFA was recoated with graphite and a second series of measurements was performed according to the thermal profile provided in Table 2.3. Photographs of the sample before LFA measurement and after the LFA measurement are provided in Figure 3.17.

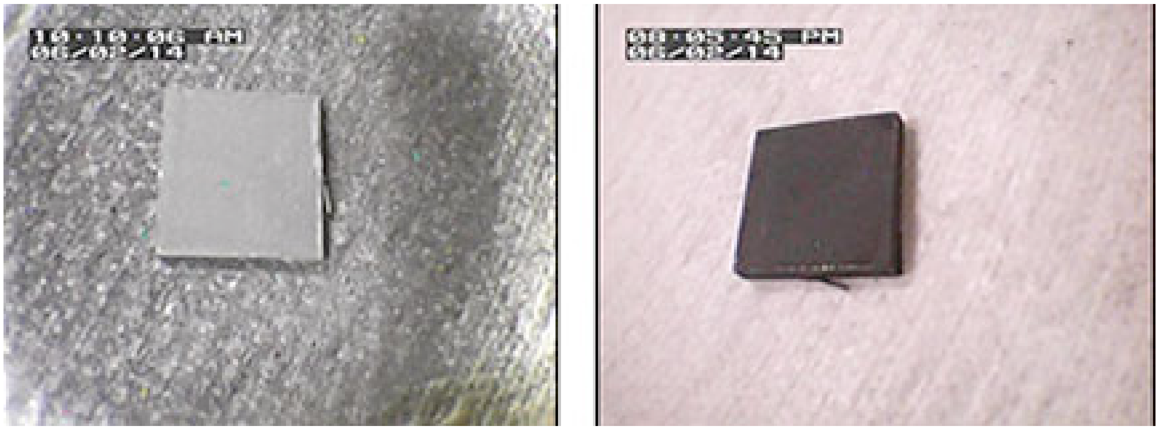

Figure 3.17. Photographs of the TL Sample for LFA with Graphite Coating Before Measurement (left) and with Graphite Coating After the LFA Measurements (right)

Results of the LFA measurements are provided in Table 3.20. The results presented in Table 3.20 have been converted using the Cape-Lehman + Pulse Correction model and the sample thickness determined using a micrometer in the hot cell (1.367 mm). Note that data highlighted with an asterisk was considered abnormal because the sample temperature deviated significantly from the program temperature.

Table 3.20. LFA Measurements for Sample TL-LFA1 Re-Run

Temperature (^oC)	Thermal Diffusivity ($mm^2 \bullet sec^{-1}$)	Temperature (^oC)	Thermal Diffusivity ($mm^2 \bullet sec^{-1}$)	Temperature (^oC)	Thermal Diffusivity ($mm^2 \bullet sec^{-1}$)
25.54	8.740	99.75	9.960	250.30	11.513
25.35	8.698	99.85	9.991	250.19	11.549
25.20	8.946	99.89	9.967	250.05	11.563
25.06	8.889	99.90	9.943	250.09	11.570
24.95	8.845	73.22*	9.614*	250.06	11.592
51.42	9.170	74.19	9.697	300.80	11.939
49.10	9.143	74.61	9.662	300.58	11.968
49.17	9.203	74.75	9.643	300.33	11.996
49.63	9.141	74.85	9.664	300.19	12.018
49.74	9.237	74.89	9.575	300.09	12.020
73.76	9.510	47.30*	9.127*	300.02	12.014
73.78	9.680	49.02	9.286	299.97	12.005
74.45	9.590	49.45	9.139	299.93	12.019
74.72	9.620	49.67	9.106	299.91	11.994
74.78	9.630	49.81	9.151	299.90	12.019
99.47	9.969	49.86	9.212	249.00	11.563
99.54	10.001	28.28*	8.833*	249.46	11.574

Temperature (^oC)	Thermal Diffusivity ($mm^2 \bullet sec^{-1}$)	Temperature (^oC)	Thermal Diffusivity ($mm^2 \bullet sec^{-1}$)	Temperature (^oC)	Thermal Diffusivity ($mm^2 \bullet sec^{-1}$)
99.62	9.994	26.86	8.841	249.69	11.572
99.76	9.949	26.54	8.803	249.81	11.561
99.88	9.957	26.25	8.769	249.88	11.545
126.34	10.296	25.96	8.880	199.07	11.068
125.57	10.305	25.73	8.724	199.53	11.070
125.18	10.323	149.19	10.775	199.75	11.063
125.01	10.294	149.56	10.595	199.85	11.066
124.95	10.317	149.77	10.583	199.89	11.069
124.93	10.328	149.87	10.605	148.94	10.489
124.91	10.317	149.91	10.601	149.43	10.503
124.91	10.321	199.62	11.059	149.69	10.499
124.90	10.315	199.89	11.101	149.82	10.478
124.89	10.320	199.98	11.112	149.88	10.478
98.98	9.934	200.00	11.106	250.30	11.513
99.53	10.009	200.01	11.140	250.19	11.549

*Data not included in calculations due to deviation from ideal temperature during measurement

The data obtained from the TL-LFA re-run is very consistent and repeatable, even upon cooling from 300^oC. A comparison between the initial series of measurements and the second series of measurements for the TL-LFA sample is provided in Figure 3.18. The thermal diffusivity of the TL-LFA sample was lower than that obtained during the initial series of measurements and in fact tracks the thermal diffusivity upon cooling from 300^oC for the initial series of measurements. This observation indicates that the lower thermal diffusivity observed during cooling from 300^oC from the initial series of measurements is associated with some change within the sample itself and not necessarily a result of the graphite coating detachment during the measurement. Without further analysis, it is not possible to identify either the cause of the sample change or the degree to which it changed; however, it appears that the change is not the result of graphite coating integrity based on the consistency of measurements upon both heating and cooling during the second series of measurements.

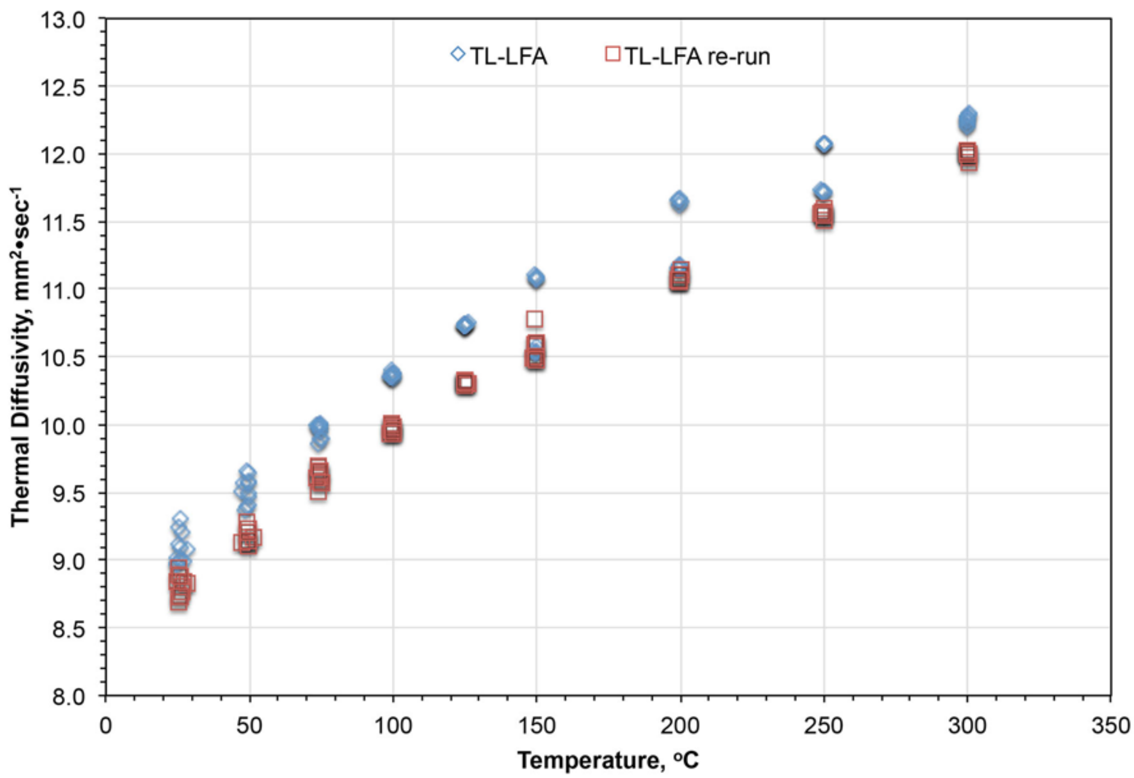

Figure 3.18. Comparison of Thermal Diffusivity of the TL-LFA Sample as a Function of Temperature for the Initial Series of LFA Measurements and the Second Series of LFA Measurements After Re-Application of the Graphite Coating

4.0 Observations

TUM requested that PNNL perform thermal-physical property measurement services for determining thermal conductivity of irradiated U-Mo dispersion fuel samples. Two dispersion fuel segments containing U-7Mo dispersion fuel in an Al-2wt% Si matrix harvested from the AFIP-1 irradiation experiment were provided to PNNL for this effort. The segments were sectioned into samples for pycnometry (density) and laser flash analysis (thermal diffusivity), differential scanning calorimetry (specific heat capacity), and optical metallography (thickness, image analysis). This report summarizes the findings of the analysis performed at TUM's request. In particular, the following observations were made:

- OM indicated that the average diameter of the U-7Mo fuel particles was consistent for both segments, approximately 45 µm. The fuel meat was thicker for Segment K than for Segment L, consistent with the higher burnup experienced by this segment. In addition, the Al-2wt% Si matrix was completely consumed, resulting in an interaction product for Segment K, while Segment L retained a modest portion of the original Al-2wt% Si matrix, again consistent with the higher burnup experienced by Segment K.
- Room temperature composite density was slightly higher for Segment L than for Segment K, indicating a slight decrease in density with increasing burnup.
- Differential scanning calorimetry measurements performed on both fuel segments produced stable, reproducible results. The data obtained from these measurements can be used to calculate specific heat capacity of the fuel segments.
- Laser flash analysis measurements conducted on both fuel segments produced stable, reproducible results. Composite thermal diffusivity increased with increasing temperature for both Segment L and Segment K. Composite thermal diffusivity was higher for Segment L than for Segment K, indicating that thermal diffusivity of the composite decreases with increasing burnup. The sample prepared from Segment L experienced a material change during the high-temperature measurement cycle, confirmed by a re-run of the sample.

5.0 References

ASTM. 2011. *ASTM E1461-11, Standard Test Method for Thermal Diffusivity by the Flash Method,* ASTM International, West Conshohocken, Pennsylvania.

Cape JA and GW Lehman. 1963. "Temperature and Finite Pulse-Time Effects in the Flash Method for Measuring Thermal Diffusivity." *Journal of Applied Physics*, 34(7):1909-1913.

Cowan RD. 1963. "Pulse Method of Measuring Thermal Diffusivity at High Temperatures." *Journal of Applied Physics*, 34(4):926-927.

Huber TK, MK Fig, D Garrett, JR Kennedy, AB Robinson, and DM Wachs. 2012. *First Results of Scanning Thermal Diffusivity Microscope (STDM) Measurements on Irradiated Monolithic and Dispersion Fuel*. INL/EXT-12-26708, Idaho National Laboratory, Idaho Falls, Idaho.

Lowell S, JE Shields, MA Thomas, and M Thommes. 2004. *Characterization of Porous Solids and Powders: Surface Area, Pore Size and Density*. Kluwer Academic Publishers, Norwell, Massachusetts.

Perez DM, MA Lillo, GS Chang, GA Roth, NE Woolstenhulme, and DM Wachs. 2011. *AFIP-1 Irradiation Summary Report.* INL/EXT-11-22045, Idaho National Laboratory, Idaho Falls, Idaho.

Petry, W. 2013. E-mail to D. Burkes (PNNL) from W. Petry (TUM), "Statement of Work Thermal Conductivity of Irradiated U-Mo Dispersion Fuel," Nov. 25, 2013.

Robinson, AB, FJ Rice, DM Wachs, and DM Perez. 2012. *RERTR-12 Insertion 1 PIE Report*. INL/LTD-12-25756, Idaho National Laboratory, Idaho Falls, Idaho.

Sheindlin M, D Halton, M Musella, and C Ronchi. 1998. "Advances in the Use of Laser-Flash Techniques for Thermal Diffusivity Measurement." *Review of Scientific Instruments*, 69(3):1426-1436.

Distribution

No. of Copies	
1	Technische Universität München Forschungs-Neutronenquelle Heniz Maier-Leibnitz (FRM-II) Lichtenbergstr.1 85747 Garching/Germany Prof. Dr. Winfried Petry Dr. Harald Breitkreutz (PDF) Ms. Tanja Huber (PDF)

No. of Copies		
1	**Local Distribution**	
	Pacific Northwest National Laboratory	
	Douglas Burkes	K8-34
	Andrew Casella	(PDF)
	Edgar Buck	(PDF)
	Amanda Casella	(PDF)
	Matthew Edwards	(PDF)
	Paul MacFarlan	(PDF)
	Karl Pool	(PDF)
	Frances Smith	(PDF)
	Franciska Steen	(PDF)

Pacific Northwest
NATIONAL LABORATORY

Proudly Operated by **Battelle** *Since 1965*

U.S. DEPARTMENT OF
ENERGY

902 Battelle Boulevard
P.O. Box 999
Richland, WA 99352
1-888-375-PNNL (7665)
www.pnnl.gov